


8-2017

MECHANISMS UNDERLYING THE SENSITIVITY AND RESISTANCE OF GASTRIC CANCER CELLS TO MET INHIBITORS

Rebecca Schroeder

Follow this and additional works at: http://digitalcommons.library.tmc.edu/utgsbs_dissertations

 Part of the [Biology Commons](#), [Cancer Biology Commons](#), [Cell Biology Commons](#), and the [Medicine and Health Sciences Commons](#)

Recommended Citation

Schroeder, Rebecca, "MECHANISMS UNDERLYING THE SENSITIVITY AND RESISTANCE OF GASTRIC CANCER CELLS TO MET INHIBITORS" (2017). *UT GSBS Dissertations and Theses (Open Access)*. 795.
http://digitalcommons.library.tmc.edu/utgsbs_dissertations/795

This Dissertation (PhD) is brought to you for free and open access by the Graduate School of Biomedical Sciences at DigitalCommons@TMC. It has been accepted for inclusion in UT GSBS Dissertations and Theses (Open Access) by an authorized administrator of DigitalCommons@TMC. For more information, please contact laurel.sanders@library.tmc.edu.

**MECHANISMS UNDERLYING THE SENSITIVITY AND RESISTANCE OF
GASTRIC CANCER CELLS TO MET INHIBITORS**

by

Rebecca Dunbar Schroeder, B.S.

APPROVED:

David J. McConkey, Ph.D.
Advisory Professor

David Hong, M.D.
Advisory Professor

Joseph Alcorn, Ph.D.

Varsha Gandhi, Ph.D.

Gary Gallick, Ph.D.

Approved:

Dean, The University of Texas

MD Anderson Cancer Center UTHealth Graduate School of Biomedical Sciences

**MECHANISMS UNDERLYING THE SENSITIVITY AND RESISTANCE OF GASTRIC CANCER CELLS
TO MET INHIBITORS**

A DISSERTATION

Presented to the Faculty of

The University of Texas

MD Anderson Cancer Center UTHealth

Graduate School of Biomedical Sciences

in Partial Fulfillment

of the Requirements

for the Degree of

DOCTOR of PHILOSOPHY

By

Rebecca Lynette Schroeder, B.S.

Houston, Texas

August, 2017

DEDICATION

To my amazing husband, who has supported and loved me over the course of this entire educational mission. Thank you for your encouragement, understanding, friendship, support, and most of all love. You are an amazing person and you have been my rock through this entire journey. To my sweet Abby blue eyes, you have brought me so much joy and have given me the motivation to accomplish this work. To my mother, who instilled in me my Christian faith and my desire for higher education and to my mother in-law for reinforcing these values and providing so much support over the years. Thank you all for supporting me in my moments of weakness and for always providing so much love. Finally, I want to thank God for giving me the strength and conviction to complete the task He put in front of me. Thank you all for being part of my life; this thesis and my doctorate are dedicated to you.



ACKNOWLEDGEMENTS

There are many people who have contributed to the successful completion of this work. First of all, I would like to thank Dr. David McConkey for training me in his laboratory and dedicating so much time to mold me into a successful scientist. You have been an exceptional role model and have provided the foundation for me to understand the importance of high-quality scientific research with rigorous technical standards, scholarship, and integrity all while demonstrating that work-life balance is crucial for a successful and joyful life. You have been an excellent mentor.

I would also like to thank Dr. David Hong for being my co-advisor and providing me with a strong foundation in clinical research. You have supported me over the years and taught me so much about the clinical aspects of world-class scientific research. The MET working group meetings have given me such an excellent forum to discuss topics relevant to MET and provided me with the opportunity to improve upon my communication skills; for this, I cannot thank you enough. I wish to thank my other committee members who were more than generous with their expertise and precious time. Your countless hours of reading, reflecting, encouraging, and most of all patience throughout my entire graduate career has resulted in the achievement of my graduate training; thank you, Dr. Gary Gallick, Dr. Varsha Gandhi, and Dr. Joseph Alcorn.

Thank you to all of my fellow students and lab-mates for making this journey so enjoyable and providing me with so much support and friendship over the years. I

developed many great technical skills that are due in large part to your training and expertise, thank you for your patience and encouragement.

Lastly, I would like to thank my family and friends. Joshua thank you for being my rock, my best friend, and my biggest supporter over the many years of this journey. Also, thank you for agreeing to “following me anywhere” all of those years ago. We finally finished the mission! Abigail, you are my greatest accomplishment, and I hope that my achievement inspires you to reach for the stars and that I provide you with the support to follow your dreams as my parents have for me. Mom, Ashley, and Lexi thank you for being there for me every step of the way and for giving me so much love and support over the years. Dad, thank you for teaching me at ten years old the importance of looking someone in the eye and giving them a good firm handshake, you will never understand the importance of this in shaping my work ethic and integrity. Shane and Julie, I have had the rare privilege of growing up with two sets of parents, and for this, I want to thank you both. Thank you for helping mold me into the person I have become and for all of the love and support you have given not only me but also Joshua and Abigail. To all of my friends and extended family, you have all played a part in me achieving this dream, and I want to thank you all. My faith and trust in my Christian beliefs have given me the clarity and willpower to finish this educational journey and I want to thank God for all of his great blessings.



MECHANISMS UNDERLYING THE SENSITIVITY AND RESISTANCE OF GASTRIC CANCER CELLS TO MET INHIBITORS

Rebecca Lynette Schroeder, B.S.

Advisory Professors: David McConkey, Ph.D.

David Hong, M.D.

MET amplification has been clinically credentialed as a therapeutic target in gastric cancer, but the molecular mechanisms underlying sensitivity and resistance to MET inhibitors are still not well understood. Using whole-genome mRNA expression profiling, we identified autophagy as a top molecular pathway that was activated by the MET inhibitor crizotinib in drug-sensitive human gastric cancer cells, and functional studies confirmed that crizotinib increased autophagy levels in the drug sensitive cells in a concentration-dependent manner. We then used chemical and molecular approaches to inhibit autophagy in order to define its role in cell death. The clinically available inhibitor of autophagy, chloroquine, or RNAi-mediated knockdown of two obligate components of the autophagy pathway (ATG5 and ATG7) blocked cell death induced by crizotinib or RNAi-mediated knockdown of MET, and mechanistic studies localized the effects of autophagy to cytochrome c release from the mitochondria. Overall, the data reveal a novel relationship between autophagy and apoptosis in gastric cancer cells exposed to MET inhibitors. The observations suggest that autophagy inhibitors should not be used to enhance the effects of MET inhibitors in gastric cancer patients.

TABLE OF CONTENTS

DEDICATION	iii
ACKNOWLEDGEMENTS.....	iv
ABSTRACT.....	vi
TABLE OF CONTENTS.....	vii
LIST OF FIGURES.....	xi
LIST OF TABLES.....	xiv
Chapter 1. INTRODUCTION	1
1.1 Gastric Cancer	2
1.2 Genomic alterations in gastric cancer.....	6
1.3 MET in gastric cancer	8
1.4 MET-targeted therapy in gastric cancer.....	12
1.5 Apoptosis.....	15
1.6 Autophagy	18
1.7 Summary and scope of dissertation.....	21
Chapter 2. MATERIALS AND METHODS.....	22
2.1 Materials and Methods for Chapter 3	23
2.1.1 Cell lines and culture:	23
2.1.2 Chemicals and antibodies:.....	23
2.1.3. CCLE Methods:.....	24
2.1.3 Cell proliferation assay:	24

2.1.4 Copy number assay:	24
2.1.5 Cell death assay (apoptosis):	25
2.1.6 Immunoblotting:.....	25
2.2 Materials and Methods for Chapter 4	26
2.2.1 Cell lines and culture:	26
2.2.2 Chemicals and antibodies:.....	27
2.2.3 Gene expression profiling:.....	27
2.2.4 Pathway Analysis:	28
2.2.5 mRNA extraction, reverse transcription and quantitative real-time PCR:.....	28
2.2.6 Immunoblotting Analysis:.....	28
2.3 Materials and Methods for Chapter 5	29
2.3.1 Cell lines and culture:	29
2.3.2 Chemicals and antibodies:.....	29
2.3.3 Acridine orange autophagy detection:.....	29
2.3.4 Cyto-ID autophagy detection:	30
2.3.5 Immunoblotting Analysis:.....	30
2.3.6 Cell death assay (apoptosis):	31
2.3.7 Cell viability assay:	31
2.3.8 ATP quantification:	31
2.3.9 Cytochrome c release:	32
Chapter 3. SENSITIVITY TO CRIZOTINIB IN GASTRIC CANCER CELLS IS ASSOCIATED WITH MET AMPLIFICATION.....	33
3.1 Introduction.....	34

3.2 Results	34
3.2.1 Effects of crizotinib on cell proliferation	34
3.2.2 MET gene expression and copy number variation in panel of gastric cancer cell lines.....	38
3.2.3 Validation of effects of crizotinib on cell proliferation	40
3.2.4 Effects of crizotinib on cell death in gastric cancer cells.....	44
3.3 Discussion	48
Chapter 4.EFFECTS OF CRIZOTINIB ON GLOBAL GENE EXPRESSION IN GASTRIC CANCER CELLS	51
4.1 Introduction.....	52
4.2 Results	54
4.2.1 Effects on gene expression of the MET inhibitor crizotinib on MET amplified human gastric cancer cells.	54
4.2.2 Ingenuity Pathway Analysis.	57
4.2.3 Gene set enrichment analyses.	66
4.2.4 MET inhibition stimulates an autophagy gene expression signature.	71
4.3 Discussion	76
Chapter 5. CHARACTERIZATION OF AUTOPHAGYS INVOLVEMENT IN RESPONSE TO MET ANTAGONIST	80
5.1 Introduction.....	81
5.2 Results	81
5.2.1 Induction of autophagy in response to MET inhibition in MET-amplified gastric cancer	81

5.2.2 Effects of autophagy inhibition on apoptosis.....	85
5.2.3 Anti-apoptotic effects of chloroquine are due autophagy inhibition	89
5.2.4 MET and Autophagy antagonists modulate metabolic pathways in MET-amplified gastric cancer cells.....	92
5.2.4 Metabolic antagonists do not confer resistance to MET inhibitors.....	97
5.2.5 Molecular mechanism behind anti-apoptotic effects of autophagy inhibition	98
5.2.3 Autophagy inhibition does not confer resistance to other therapeutic agents	98
5.3 Discussion	102
Chapter 6. DISCUSSION, CONCLUSIONS AND FUTURE DIRECTIONS	104
6.1 Conclusions.....	105
6.1.1 Chapter 3 Conclusions:	105
6.1.2 Chapter 4 Conclusions:	106
6.1.3 Chapter 5 Conclusions:	107
6.2 Future Directions:.....	109
6.2.1 Chapter 3 Future Directions	109
6.2.2 Chapter 4 Future Directions	111
6.2.3 Chapter 5 Future Directions	112
6.3 Final Discussion:	114
Chapter 7. BIBLIOGRAPHY	116
VITA.....	146

LIST OF FIGURES

Chapter 1

Figure 1.1 Risk factors associated with gastric cancer.	3
Figure 1.2 Gastric cancer subtypes.	7
Figure 1.3 MET signaling pathways.....	9
Figure 1.5 Therapeutic inhibitors targeting MET.....	14
Figure 1.6 Extrinsic and intrinsic apoptotic pathways.....	17
Figure 1.7 Autophagy.....	20

Chapter 2 (No figures)

Chapter 3

Figure 3.1 Crizotinib.....	35
Figure 3.2 Drug sensitivity profiles of gastric human cancer cell lines treated with Crizotinib or PHA-665752.....	36
Figure 3.3 Drug sensitivity profiles of gastric human cancer cell lines treated with Crizotinib.	37
Figure 3.4 MET gene expression and copy number profile of gastric human cancer cell lines.	39
Figure 3.5 Crizotinib sensitivity correlates with MET phosphorylation in human gastric cancer cells.....	41

Figure 3.6 Drug sensitivity profile of gastric human cancer cell lines treated with Crizotinib.	43
Figure 3.7 Effects on apoptosis of the MET inhibitor crizotinib on human gastric cancer cells.	46
Figure 3.8 Effects on apoptosis related proteins of the MET inhibitor crizotinib on human gastric cancer cells.	47
Figure 3.9 Receptor tyrosine kinase molecular domains.	50

Chapter 4

Figure 4.1 Acquired resistance mechanisms to TK inhibitors.....	53
Figure 4.2 MET inhibition results in significant changes in gene expression in MET-amplified gastric cancer cell lines.	55
Figure 4.3 Effects on gene expression of the MET inhibitor crizotinib on MET amplified human gastric cancer cells.....	56
Figure 4.4 Quantitative RT-PCR was used to evaluate the accuracy of the gene expression profiling results.	58
Figure 4.5 IPA core analysis results.....	59
Figure 4.6 Pathway analyses of crizotinib-induced changes in gene expression.	62
Figure 4.7 Additional IPA analysis results	63
Figure 4.8 Transcriptional analyses of crizotinib-induced changes in gene expression.....	64
Figure 4.9 Transcriptional analyses of crizotinib-induced changes in gene expression.....	65
Figure 4.10. GSEA analyses of crizotinib-induced changes in gene expression.	69

Figure 4.11. GSEA analyses of crizotinib-induced changes in gene expression.	70
Figure 4.12. MET inhibition stimulates an autophagy gene expression signature.	74
Figure 4.13. MET inhibition stimulates an autophagy gene expression signature.	75

Chapter 5

Figure 5.1 MET inhibition induces autophagy in the crizotinib-sensitive cells.....	82
Figure 5.2 MET inhibition induces autophagy in the crizotinib-sensitive cells.....	84
Figure 5.3 Autophagy is required for crizotinib-induced apoptosis.	86
Figure 5.4 Autophagy inhibition effects on cell death and proliferation.	87
Figure 5.5 Effects of chloroquine at 72 and 96 hours.....	88
Figure 5.6 Autophagy is required for crizotinib-induced apoptosis.....	90
Figure 5.7 Chloroquine directly modulates autophagy.	91
Figure 5.8 MET antagonist decrease metabolic pathways.....	93
Figure 5.9 MET inhibition lowers ATP levels.....	94
Figure 5.10 MET and autophagy antagonist lower ATP levels.	95
Figure 5.11 MET and metabolic antagonist lower ATP levels	96
Figure 5.12 Figure 5.12 Metabolic antagonists do not confer resistance to MET inhibition.	97
Figure 5.13 Autophagy is required for crizotinib-induced cytochrome c release.	99
Figure 5.14 Autophagy is not required for apoptosis induced by other agents.....	101

Chapter 6

Figure 6.1 TCGA comprehensive gastric cancer molecular characterizations	113
--	-----

LIST OF TABLES

Chapter 1

Table 1.1 Advanced gastric cancer treatment regimens when chemoradiation is not recommended.....	5
Table 1.2 Therapeutic strategies aimed at targeting MET.	13

Chapter 3

Table 3.1 Crizotinib kinase selectivity profile.	35
---	----

Chapter 4

Table 4.1 Overall IPA analysis results.	60
Table 4.2 GSEA molecular signature database hallmarks gene sets.	67
Table 4.3 GSEA molecular signature database hallmarks gene sets.	68
Table 4.4 GSEA molecular signature database GO:BP gene sets.....	72
Table 4.5 Autophagy gene sets enriched in the GO:BP gene sets.....	73

Chapter 1. INTRODUCTION

1. Introduction

1.1 Gastric Cancer

The International Agency for Research on Cancer (IARC) and the World Health Organization (WHO) identify cancer as the second leading cause of death worldwide, contributing to 8.8 million deaths in 2015 (1). Cancers of the lung, liver, colon, stomach and breast are the most common disease sites contributing to this high mortality rate, with these five cancer types comprising more than half of the total cancer-related deaths for 2015. Of these disease sites, stomach cancer was credited with 800,000 deaths in 2015(1).

Although our understanding of significant risk factors and screening methods for gastric cancer has improved over the last decade, it remains the fifth most prevalent cancer and third leading cause of cancer-related death worldwide (1-4). Stomach cancer cases occur at a higher incidence rate (71%) in less developed regions with more than half of all gastric cancer cases occurring in eastern Asia. This variable distribution correlates with the increase incidence of biologic and environmental risk factors occurring in these populations as opposed to regions with more developed populations (i.e. North America and Europe) which have experienced substantial declines in gastric cancer incidence since the 1970's (5). Gastric cancer is a slowly occurring process with exposure to chemical carcinogens through alcohol and tobacco use, consumption of foods preserved by salting, family history, obesity, and exposure to the infectious agents bacterium *Helicobacter pylori* (*H. pylori*) and Epstein–Barr virus (EBV) being the primary etiological determinants [Figure 1.1] (6, 7). Gastric cancer incidence is twice as high in men as compared to women, and this is

attributed to the protective effect of female sex hormones, at least in tumors initiated by *H. pylori* infection. In women, estrogen levels are sufficient to decrease oncogenic signaling and attenuate the chronic inflammatory response in reaction to the chronic inflammatory state caused by *H. pylori* infection (8).

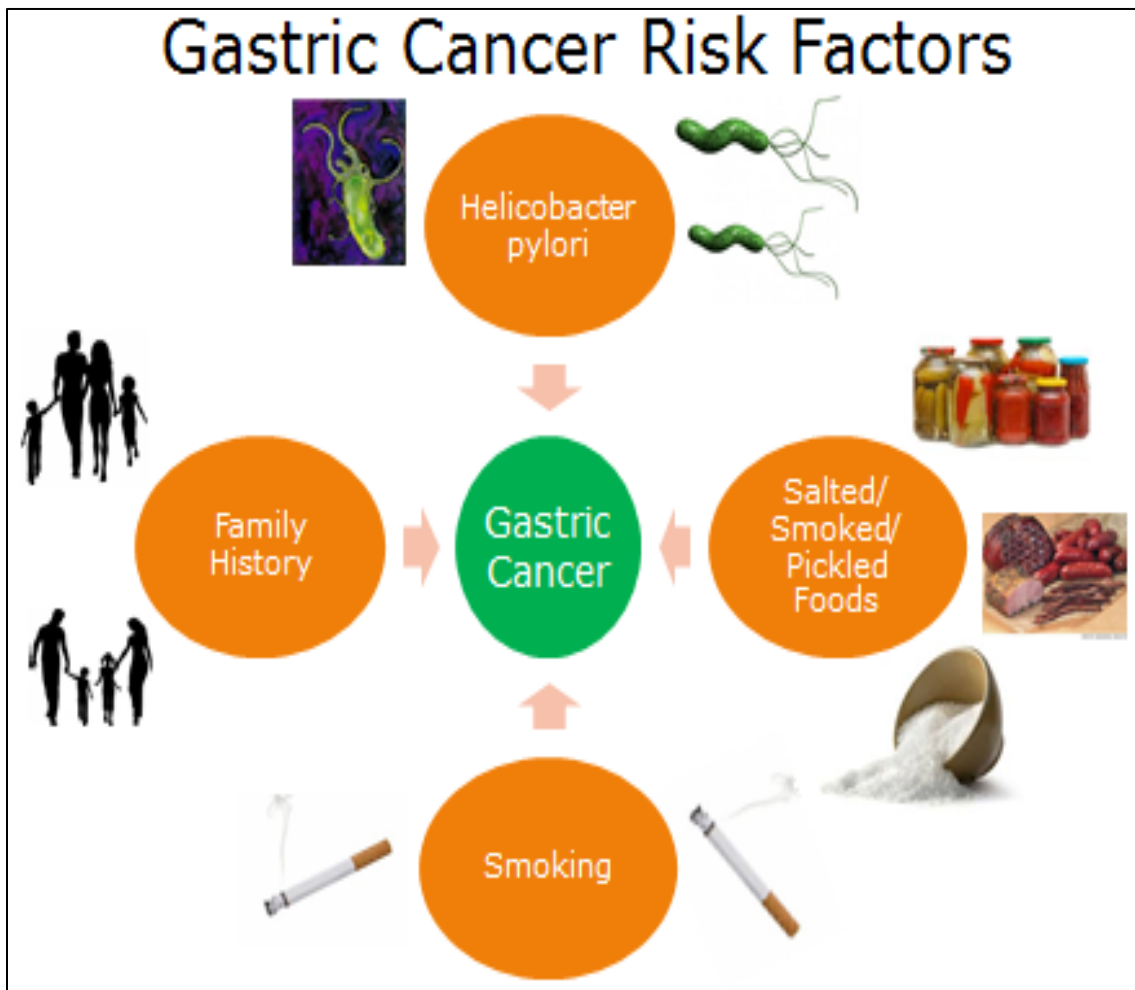



Figure 1.1 Risk factors associated with gastric cancer. Genetic and environmental risk factors are associated with the development of gastric cancer and include a family history of certain inherited disease, infection with *H. pylori*, ethnicity, sex, and exposure to toxins through ingestion of certain foods and tobacco use (6).

Gastric cancers are overwhelmingly classified as adenocarcinomas, which can be further histologically classified based on Lauren classification as intestinal and diffuse (9, 10). The development of gastric cancer is a multifactorial/multistep process, and the majority of intestinal type gastric cancers are initiated by environmental factors and the majority of diffuse gastric cancers are derived from genetic factors (6, 9). Symptoms of gastric cancer in the early stages of the disease mimic other common gastric issues including epigastric pain, bloating and nausea. Because of this most patients do not present with clinical signs specific to gastric cancer such as weight loss, jaundice, ascites, and hepatic enlargement until they have advanced disease with local or distant metastasis (6). The National Cancer Institute identifies the liver, lung, and peritoneum as the primary metastatic sites for gastric cancer. Patients with early stage gastric cancer have a high overall survival rate, but unfortunately, only 20% of all cases are early stage. The survival rate for advanced stage cases is much lower overall and is highly dependent on anatomical location and histological variant. Patients with localized distal disease have a 50% survival rate compared to a much lower survival rate of 10% for patients with localized proximal gastric cancer (11).

The frontline treatment strategies for gastric cancer are surgical resection, chemotherapy and radiation therapy with mitomycin, fluorouracil, cisplatin, paclitaxel and docetaxel being the primary chemotherapeutic agents (6). Although chemotherapy and radiation correlate with prolonged survival in early stage disease, most patients, unfortunately, present with advanced stage tumors where the only curative option currently available is surgical resection (12). Patients with nonresectable disease have few

therapeutic options and are primarily treated with chemotherapy regimens using combinations of the previously mentioned agents, where the median survival is only 10 months [Table 1.1] (13). Because of this lack of effective therapeutic options the need to identify alternative ways to treat gastric cancer of the utmost importance.



National
Comprehensive
Cancer
Network®

NCCN Guidelines Version 2.2017

Gastric Cancer

[NCCN Guidelines Index](#)
[Table of Contents](#)
[Discussion](#)

PRINCIPLES OF SYSTEMIC THERAPY

Systemic Therapy for Unresectable Locally Advanced, Recurrent or Metastatic Disease (where local therapy is not indicated)

- Trastuzumab should be added to first-line chemotherapy for HER2 overexpressing metastatic adenocarcinoma (See Principles of Pathologic Review and HER2 Testing [GAST-B])
 - › Combination with fluoropyrimidine and cisplatin (category 1)¹³
 - › Combination with other chemotherapy agents (category 2B)
 - › Trastuzumab is not recommended for use with anthracyclines

First-Line Therapy

Two-drug cytotoxic regimens are preferred because of lower toxicity. Three-drug cytotoxic regimens should be reserved for medically fit patients with good PS and access to frequent toxicity evaluation.

- Preferred Regimens:
 - › Fluoropyrimidine (fluorouracil[†] or capecitabine) and cisplatin¹⁴⁻¹⁷ (category 1)
 - › Fluoropyrimidine (fluorouracil[†] or capecitabine) and oxaliplatin^{15,18,19}
- Other Regimens:
 - › Paclitaxel with cisplatin or carboplatin²⁰⁻²²
 - › Docetaxel with cisplatin^{23,24}
 - › Fluoropyrimidine^{16,25,26} (fluorouracil[†] or capecitabine)
 - › Docetaxel^{27,28}
 - › Paclitaxel^{29,30}
 - › Fluorouracil^{†,*} and irinotecan³¹
 - › DCF modifications
 - ◊ Docetaxel, cisplatin, and fluorouracil^{†,32}
 - ◊ Docetaxel, oxaliplatin, and fluorouracil³³
 - ◊ Docetaxel, carboplatin, and fluorouracil (category 2B)³⁴
 - › ECF (epirubicin, cisplatin, and fluorouracil) (category 2B)³⁵
 - › ECF modifications (category 2B)^{3,4}
 - ◊ Epirubicin, oxaliplatin, and fluorouracil
 - ◊ Epirubicin, cisplatin, and capecitabine
 - ◊ Epirubicin, oxaliplatin, and capecitabine

Second-Line Therapy

Dependent on prior therapy and PS:

- Preferred Regimens:
 - › Ramucirumab and paclitaxel (category 1)³⁶
 - › Docetaxel (category 1)^{27,28}
 - › Paclitaxel (category 1)^{29,30,37}
 - › Irinotecan (category 1)³⁷⁻⁴⁰
 - › Ramucirumab (category 1)⁴¹
 - › Fluorouracil^{†,*} and irinotecan^{38,42,43} (if not not previously used in first-line therapy)
- Other Regimens:
 - › Irinotecan and cisplatin^{18,44}
 - › Docetaxel and irinotecan⁴⁵ (category 2B)

*Capecitabine may not be used interchangeably with fluorouracil in regimens containing irinotecan.
[†]Leucovorin is indicated with certain fluorouracil-based regimens. For important information regarding the leucovorin shortage, please see [Discussion](#).

Note: All recommendations are category 2A unless otherwise indicated.
 Clinical Trials: NCCN believes that the best management of any patient with cancer is in a clinical trial. Participation in clinical trials is especially encouraged.

Version 2.2017, 07/26/17 © National Comprehensive Cancer Network, Inc. 2017. All rights reserved. The NCCN Guidelines® and this illustration may not be reproduced in any form without the express written permission of NCCN®.

Continued

GAST-F
3 OF 11

Table 1.1 Advanced gastric cancer treatment regimens when chemoradiation is not recommended.

*Reprinted with permission from NCCN Guidelines® & Clinical Resources (14)

1.2 Genomic alterations in gastric cancer

One aspect of tumor biology that has emerged as an attractive therapeutic target in multiple cancer types is the alteration of a family of cell surface receptors, receptor tyrosine kinases (RTKs) (15). RTKs mediate important signaling pathways involved in the control of many essential processes including cell proliferation/growth, differentiation, migration, and survival through ligand-induced activation by binding various extracellular signaling molecules (i.e. growth factors, hormones, and cytokines) (12, 16). When alterations occur through mutation, amplification or chromosomal translocation these RTKs display aberrant and constitutive activation leading to increased proliferation, migration and survival (17).

Deng, *et. al.* identified the most predominant molecular alterations in a panel of 233 gastric cancers and RTK alterations were among the most frequent alterations occurring in a third of the samples (18). This group specifically identified the RTK MET as one of the top genomic alterations in their cohort of gastric cancers (18). Other groups have been able to correlate molecular targets (FGFR, PI3K, MET, HER2, VEGF, and EGFR) with anatomical location and histological classification (proximal non-diffuse, distal non-diffuse, and diffuse) in gastric cancer [Figure 1.2] (10). Specifically, MET amplification was correlated with higher incidence in the proximal non-diffuse subtype. This correlation is serving as a valuable tool to aid in the selection of patient populations for targeted molecular therapies and the identification of more effective predictive biomarkers (10).

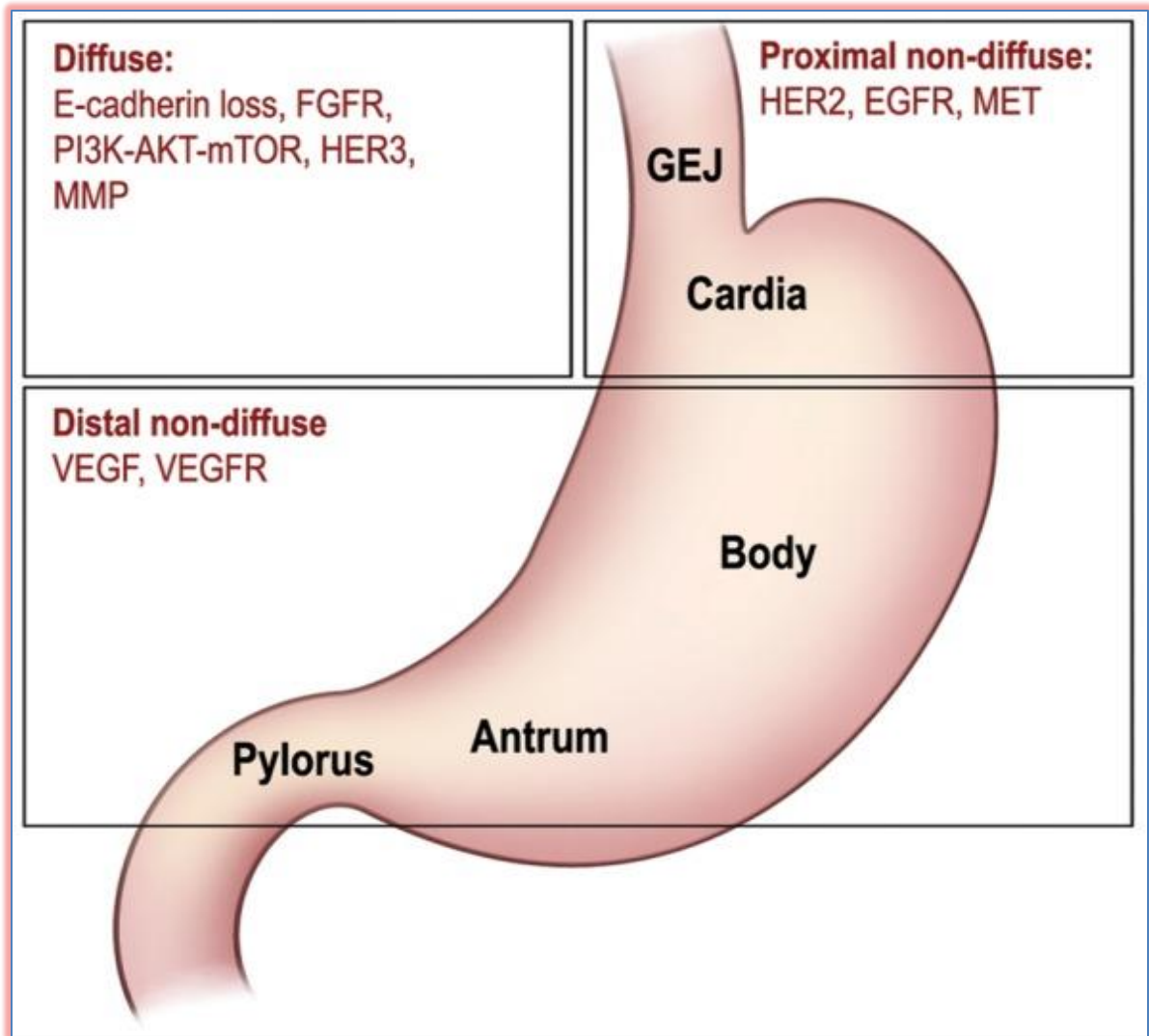


Figure 1.2 Gastric cancer subtypes. Correlation between molecular targets, anatomical location, and histological classification for each gastric cancer subtype (10). Subtypes of gastric cancer based on anatomical and histological classification, and important molecular targets implicated in each subtype.

*Reprinted with permission of Therapeutic Advances in Gastroenterology. Hilda Wong, Thomas Yau, Molecular targeted therapies in advanced gastric cancer: does tumor histology matter? SAGE Publications 01/01/2013 (10).

1.3 MET in gastric cancer

MET, also known as hepatocyte growth factor receptor (HGFR), is a transmembrane cell surface receptor expressed in epithelial cells of organs such as the liver, kidneys and bone marrow (19). MET is comprised of two subunits (glycosylated extracellular α -subunit and a transmembrane β -subunit) that are linked by a disulfide bridge (20). MET forms a heterodimer upon binding with its ligand hepatocyte growth factor (HGF) resulting in autophosphorylation of two tyrosine residues (Y1234 and Y1235) on the catalytic domain and phosphorylation of two tyrosine residues (Y1349 and Y1356) on the carboxy-terminal tail (21).

Phosphorylation of the tyrosine residues allows for the engagement of various signal transducers and adaptor proteins that activate and signal through two main oncogenic signaling pathways: the mitogen-activated protein kinase (MAPK) cascade and the PI3K/Akt signaling axis as well as several other signal transduction pathways (STAT, NOTCH, and beta-catenin) (19, 22). Signaling through these pathways allows for the regulation of multiple biologic processes (i.e. cellular metabolism, cell cycle progression, migration/motility/invasion, autophagy, proliferation and cell survival/protection from apoptosis) that are essential for tissue homeostasis (Figure 1.3).

Therefore, deregulation of MET signaling plays a crucial role in cancer development. To date, numerous different cancer types (lung, gastric, ovary, colon, breast, kidney, thyroid, and liver) have been associated with deregulation of MET signaling (23). MET signaling is modulated and deregulated through mutation, chromosomal translocation,

amplification or other mechanisms in these cancers. MET is of particular interest because multiple studies annotated the frequency of MET amplification in gastric cancers and reported rates of 9-30% (24-26), with high-level MET amplification in about 4% (12/287) of tumors (27). Additionally, in multiple studies MET amplification was associated with poor patient outcomes (25, 28) (Figure 1.2).

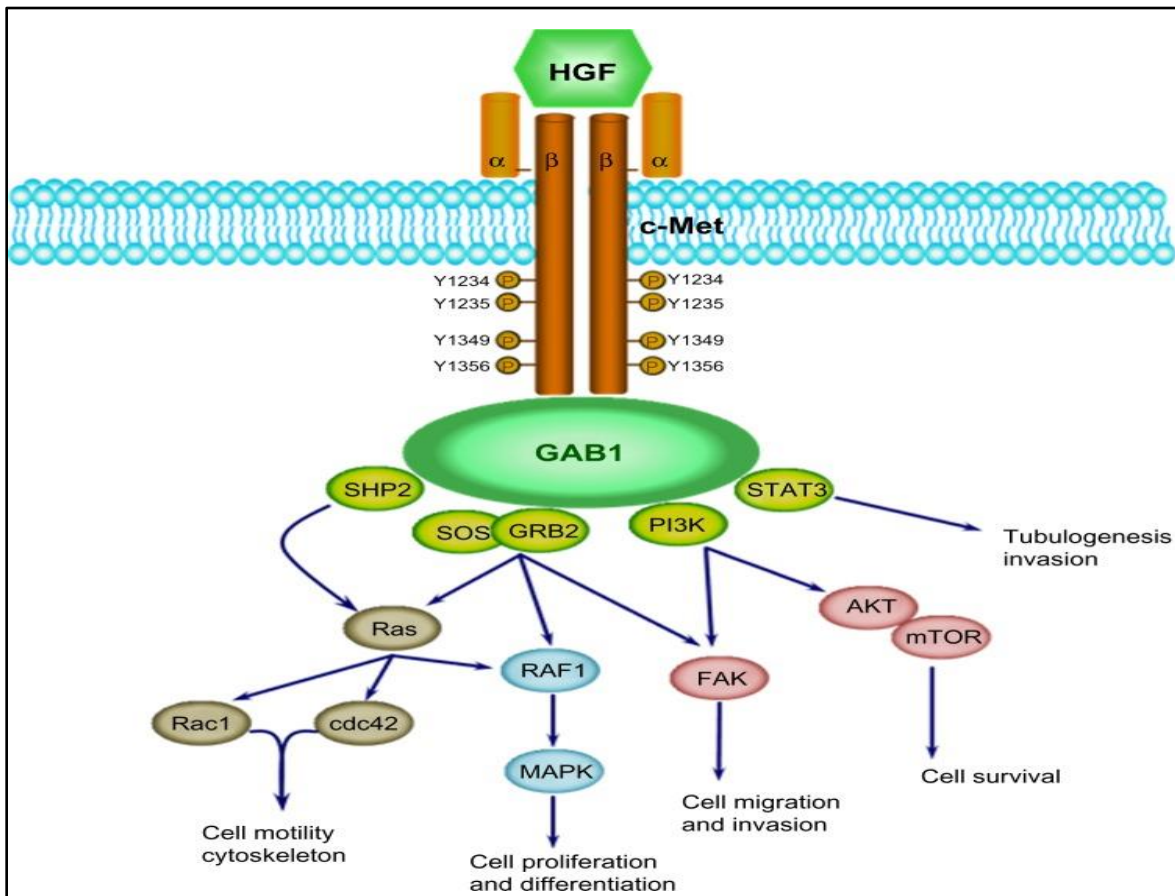


Figure 1.3 MET signaling pathways. Activated MET signals through multiple signaling cascades including the MAPK pathway (RAS/RAF/MEK/ERK) and the PI3K pathway (PI3K/AKT/MTOR) which in turn regulates multiple cellular processes highlighted in the figure (29, 30).

*Reprinted with permission of Immunotargets and Therapy by Dove Medical Press Ltd. This work is published by Dove Medical Press Limited, and licensed under Creative Commons Attribution: Non-Commercial (unported, v3.0) License (30).

Specifically, two studies have highlighted this correlation between MET amplification and poor survival outcomes in gastric cancer. The first study analyzed tissue from 472 gastric cancer patients who had undergone curative surgery and had DNA samples available for qPCR analysis (28). They found that 21.2% of the samples had amplified MET (>4.0 copies), and these patients experienced poorer overall survival as compared to the patients without MET amplification(28) (Figure 1.4 top panel) (28). The second study used silver in-situ hybridization (SISH) to identify MET gene amplification in tissue collected from a panel of 381 gastric cancer patients (25). They found that 3.4% of the tumors analyzed had MET gene amplification, and overall survival and disease-free survival decreased with increasing MET copy number (25) (Figure 1.4 bottom panel). Additionally they correlated overall survival according to the level of MET protein expression measured by IHC and found that 2.1% of the tumors had high levels (+3) of IHC staining and these patients had shorter survival time compared to the other groups (0, +1, +2).

This correlation between MET gene amplification and high grade MET protein expression link to poor outcome, coupled with the fact that MET has been credentialed as a viable RTK target made MET inhibitors attractive as tools for therapeutic intervention. Multiple preclinical studies indicate that MET amplification creates MET dependency in gastric cancer cells [27, 28] and recent clinical trials demonstrated that MET inhibitors had significant clinical activity (25, 26); particularly in patients whose tumors contained MET amplification (31-33).

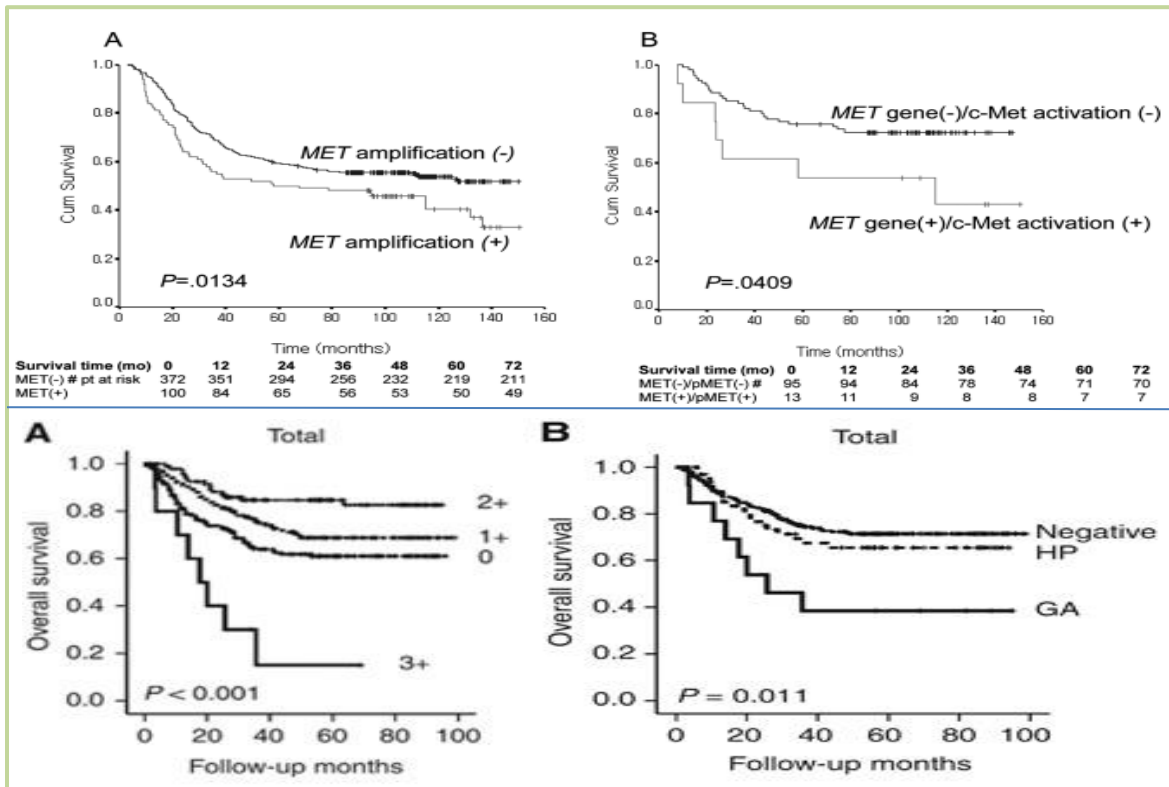


Figure 1.4 Overall survival based on MET amplification status. Top panel: MET status (amplification or protein expression) was correlated with survival data in a panel of 452 patients. (A) MET amplification (+) vs. (-). (B) MET amplification with c-Met protein activation (+) vs (-) status. MET amplification was determined using qPCR analysis and MET protein expression was determined using IHC staining against MET (total) and phospho-Met (pY1349) (28). Bottom panel: Overall survival (Kaplan–Meier curves) based on MET gene copy number and IHC MET activation for a panel of 438 patients. (A) IHC MET activation grade 0,1,2, or 3. (B) Gene amplification (GA) vs. high polysomy (HP) vs. wild-type MET (Negative) (25).

*Top Panel: Reprinted with permission of Oncology Reports. Impact of MET amplification on gastric cancer: possible roles as a novel prognostic marker and a potential therapeutic target. Lee J1, et al. *Oncol Rep.* 2011 Jun;25(6):1517-24. doi: 10.3892/or.2011.1219. Epub 2011 Mar 18 (28).

*Bottom Panel: Reprinted from *British Journal of Cancer*, (107), H E Lee, M A Kim, H S Lee, E- J Jung, H-K Yang et al., MET in gastric carcinomas: comparison between protein expression and gene copy number and impact on clinical outcome, 325–333, Copyright (2012), with permission from Nature Publishing Group.(25)

1.4 MET-targeted therapy in gastric cancer

Currently there are numerous therapeutic strategies aimed at targeting MET including 1) ATP-competitive MET and TKI inhibitors: foretinib (GSK1363089), crizotinib (PF-2341066), cabozantinib (XL184), S49076, MK-2461 and AMG 337; 2) allosteric tyrosine-kinase inhibitors (TKIs): tivantinib (ARQ197); and 3) anti-MET and anti-HGF monoclonal antibodies (mAbs): onartuzumab (MetMAb™), rilotumumab (AMG-102), ficlatuzumab (AV-299), TAK-701, emibetuzumab (LY-2875358), ARGX-111 and EM1-mAb (30, 34-37) [Figure 1.5 and Table 1.2](34, 38). These therapeutic strategies have an advantage over traditional chemotherapy and radiation as they have targeted mechanisms to induce cell death in tumor cells specifically and do not kill cells indiscriminately as is the case with traditional methods(39). ATP-competitive small molecule tyrosine inhibitors compete with the ATP binding site of the catalytic domain of tyrosine kinases and induce a cytotoxic response by inhibiting the sustained oncogenic signaling driven by the aberrant activation of the RTK (40). Monoclonal antibodies induce a cytotoxic response resulting in apoptosis by various antibody-directed mechanisms including the blockade of ligand-receptor growth or survival pathways, antigen crosslinking and activation of death receptors (41). The mechanism of action of each of these various classes of therapeutics ultimately leads to the induction of growth arrest and programmed cell death, apoptosis (39-41).

	DRUG	MOLECULAR TARGETS
HGF activation inhibitors	HGFAs (activators)	Pro-HGF
	HaIs (inhibitors)	Pro-HGF
HGF inhibitors	Rilotumumab (AMG102)	HGF
	Ficlatuzumab (AV-299)	HGF
	TAK701	HGF
MET antagonists	Onartuzumab	MET
	CE-355621	MET
	DN-30	MET
	LA480	MET
MET kinase inhibitors		
Selective	Tivantinib	MET
	Savolitinib	MET
	AMG 337	MET
	INC 280	MET
Nonselective	Crizotinib	MET, ALK, ROS, RON
	Cabozantinib	MET, VEGFR2, KIT, RET, AXL, FLT3

Table 1.2 Therapeutic strategies aimed at targeting MET.

* Reprinted with permission Creative Commons CC-BY-NC 3.0 license(38).

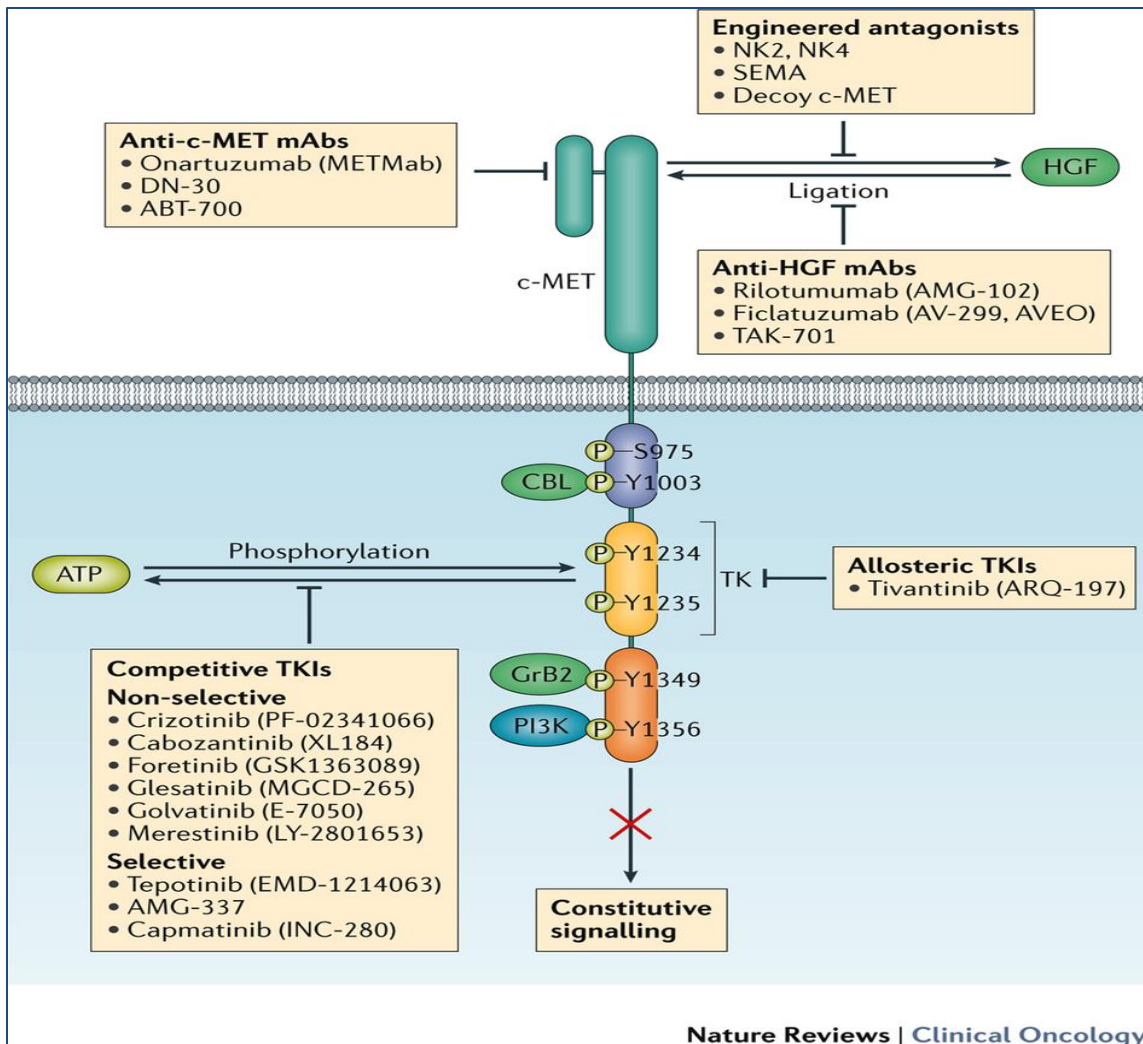


Figure 1.5 Therapeutic inhibitors targeting MET. Novel therapeutic strategies to target MET included: ATP-competitive inhibitors, tyrosine kinase inhibitors (TKIs), and anti-MET and anti-HGF monoclonal antibodies (mAbs) (34).

*Reprinted with permission of Nature Publishing Group. Conor A. Bradley, Manuel Salto-Tellez, Pierre Laurent-Puig, Alberto Bardelli, Christian Rolfo, Josep Tabernero Targeting c-MET in gastrointestinal tumours: rationale, opportunities and challenges. Nature Reviews Clinical Oncology 4.4.2017 (34).

1.5 Apoptosis

Although MET-targeted RTK inhibitors have clinical activity, not all MET-amplified tumors respond, and a deeper understanding of the molecular determinants of response and resistance is therefore crucial. MET inhibitors have both cytotoxic and cytostatic effects in MET-amplified cells, and two studies have highlighted the preclinical correlation between MET amplification and extreme sensitivity to MET inhibition in gastric cancer cells (42, 43). While profiling multiple cancer types for sensitive to two TKIs: PHA-665752 (MET tyrosine kinase inhibitor) and gefitinib (EGFR tyrosine kinase inhibitor), the Haber Lab identified a correlation between MET amplification and extreme sensitivity, via decreased cell proliferation and growth rates, to the MET inhibitor crizotinib (42). Okamoto and associates further investigated this finding by looking deeper into the anti-tumor mechanisms associated with MET inhibition in MET-amplified gastric cancers (43). They found that MET-amplified gastric cancer cells undergo growth arrest and apoptosis when MET is inhibited via chemical (crizotinib) and genetic (RNA interference) depletion methods. Also, MET depletion caused significant decreases in MET downstream signaling resulting in decreased AKT and ERK phosphorylation (43). Additionally, mechanistic studies implicated upregulation of the pro-apoptotic BCL2 family protein BIM and downregulation of several pro-survival genes, including the IAP family members c-IAP1, XIAP, and survivin, in crizotinib induced cell death (43). This suggests that BIM upregulation may contribute to the pro-apoptotic effects of crizotinib in MET-amplified gastric cancer cells, but further investigation is needed to identify the relative contributions of apoptosis and growth arrest in regards to the anti-tumor effects of MET inhibition.

Apoptosis is the process of programmed cell death commonly characterized by cell shrinkage, membrane blebbing, nuclear condensation, and DNA fragmentation [Figure 1.6] (44, 45). This process occurs via initiation through two distinct energy-dependent mechanisms, the intrinsic and extrinsic apoptotic pathways (44). Extrinsic apoptosis is death-receptor initiated, and intrinsic apoptosis is controlled by the mitochondria, but both pathways converge on the same execution pathway which is initiated by caspase 3 cleavage (44). Caspases are a family of proteolytic enzymes that help carry out the apoptotic cascade and are characterized into three main subcategories: initiator caspases (caspase 2, caspase 8, caspase 9, caspase 10), executioner caspases (caspase 3, caspase 6, and caspase 7), and inflammatory caspases (caspase 1, caspase 4 and caspase 5) (46). During times of cellular stress, the intrinsic pathway is activated by release of cytochrome c from the mitochondria into the cytosol resulting in the formation of the apoptosome from the activation and binding of cytochrome c, APAF-1 and caspase 9 (47). Apoptosome formation allows for the activation of executioner caspases and the degradation of cellular components that are subsequently phagocytosed by macrophages or adjacent normal cells and produce the hallmark characteristics associated with apoptosis, previously mentioned. Various anti-apoptotic proteins negatively control the two apoptosis pathways. Specifically for the extrinsic pathway activation of caspase 8 and caspase 3 are inhibited by c-FLIP and XIAP and regulation of the intrinsic pathway is controlled by the balance of proapoptotic (*i.e.* Bax, Bak, and Bid) and anti-apoptotic (*i.e.* Bcl-2, Bcl-xL, Mcl-1, and XIAP) proteins (48). Apoptosis is distinct from other forms of cell death such as necrosis [39]. Necrosis is primarily triggered by external factors such as infection or trauma and does not require energy and

elicits an immune response from the release of its cellular components to neighboring cells through the loss of membrane integrity [35]. The understanding these distinct processes is important for characterization of molecular response to cancer therapeutics.

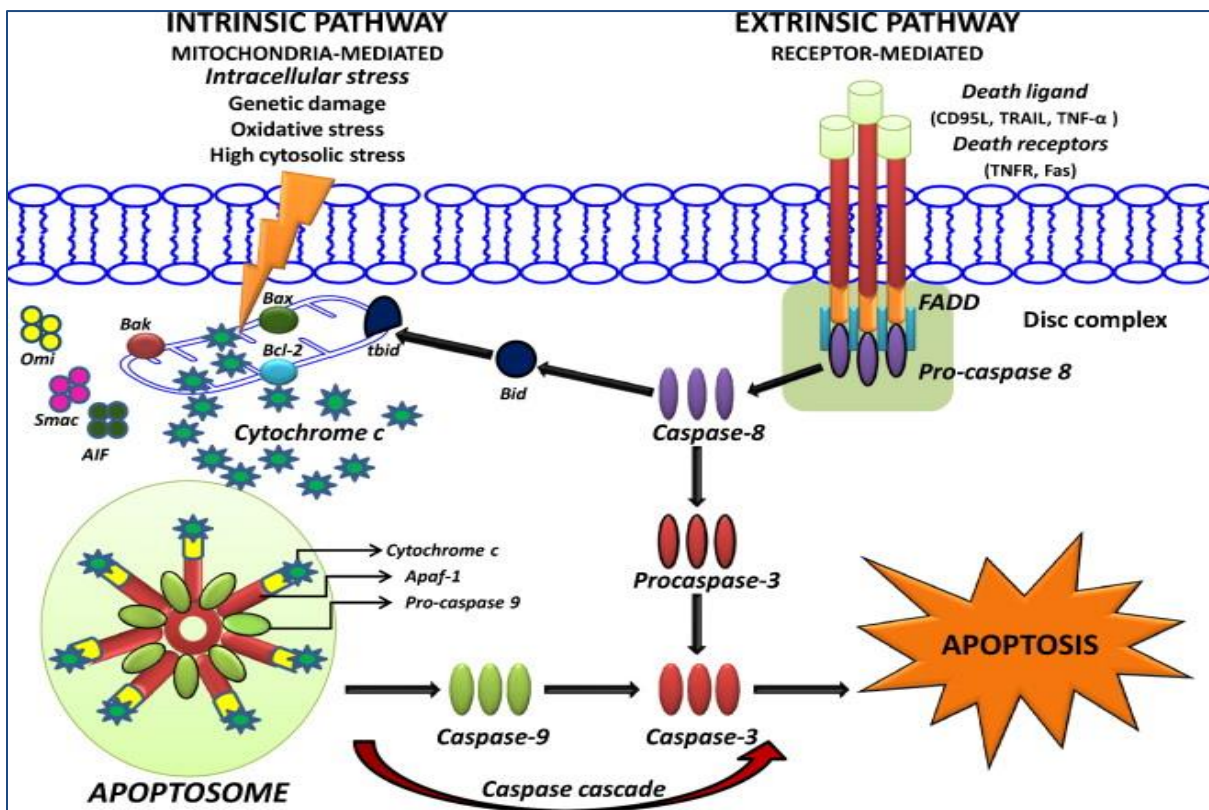


Figure 1.6 Extrinsic and intrinsic apoptotic pathways. Apoptosis is initiated through two distinct mechanisms. 1). Receptor-mediated induction, extrinsic signaling pathway, involves ligand-dependent activation of death receptors (Fas, TNF α R, DR3, DR4, and DR5) followed by activation of caspase 8 and caspase 3 resulting in apoptosis. 2) Mitochondria-mediated induction, intrinsic signaling pathway, is triggered by cellular stress (i.e. DNA damage, ER/metabolic stress, and hypoxia) and requires activation of BAX/BAK to initiate mitochondrial outer membrane permeabilization and cytochrome c release. The apoptosome is then formed, composed of caspase 9 and caspase 3, resulting in apoptosis.

*Reprinted from *Mutation Research/Fundamental and Molecular Mechanisms of Mutagenesis*, (768), Rima Beesoo, Vidushi Neergheen-Bhujun, Ranjeet Bhagooli, Theeshan Bahorun, Apoptosis inducing lead compounds isolated from marine organisms of potential relevance in cancer treatment, 84-97, Copyright (2014), with permission from Elsevier.(48)

1.6 Autophagy

In addition to apoptosis, macroautophagy (autophagy) is a well characterized process that has been implicated in the response as well as resistance to MET targeted therapies (49). Autophagy is an intracellular process that is involved in the degradation and recycling of damaged and dysfunctional cellular components via a lysosomal degradation pathway (50). The process of autophagy is important for the maintenance of overall cellular health by inhibiting the buildup of toxic cellular waste over time through the clearance of damaged proteins and organelles (51). The clearance and recycling of damaged cellular components allows for the preservation of cell viability during times of cellular stress that would otherwise lead to the activation of the apoptotic cascade (52). Autophagy is activated by cellular stress created through oxidative stress, protein aggregation and nutrient deprivation and is commonly associated with processes including differentiation, infection, and cancer (53).

The primary molecular signaling pathway associated with autophagy is the phosphoinositide 3-kinase (PI3K) pathway (53) [Figure 1.7]. This pathway is involved in regulating a multitude of cellular functions including metabolism, growth, proliferation, survival, transcription and protein synthesis. The PI3K pathway signals through protein kinase B (AKT) and the kinase mammalian target of rapamycin (mTOR), which is the primary regulator of autophagy within the cell (54). mTOR is comprised of two complexes, MTORC1 and MTORC2, that both play independent roles in the regulation of autophagy (55). As a result of this dynamic regulation, autophagy is controlled through the modulation of mTOR

to the extent of that when mTOR is activated through the AKT signaling autophagy is suppressed and when mTOR is inhibited through AMP-activated protein kinase (AMPK) activation autophagy is induced (53, 56, 57). Nutrient deprivation or cellular stress initiates a downstream cascade through multiple molecules, including MTOR inhibition, that ultimately leads to autophagosome formation. The autophagosome is a double-membrane vesicle that forms in a multi-step process and allows the process of autophagy (sequestration, transport to lysosomes, degradation, and utilization of degradation products) to occur [Figure 1.7] (58). The molecules involved in autophagosome formation are several kinases (serine/threonine) ULK1, ULK2, and UKL3 (UNC-51-like kinase -1, -2, and -3); the autophagy-related (Atg) genes ATG5, ATG7, ATG12, ATG10, and ATG16; and the microtubule-associated protein 1A/1B-light chain 3 (LC3) (59). Autophagy is often referred to as the double-edged sword of cancer modulation because it can act both as a tumor suppression mechanism and tumor cell survival mechanism (60). Autophagy is found to be both up-regulated and down-regulated in cancer and is highly dependent on cellular context as to which state is present within any given cell (61). Interestingly, there is evidence that indicates that there is significant overlap (crosstalk) between autophagy and apoptosis and that the two biologic processes are connected in both positive and negative manners (62). This dynamic relationship between autophagy and apoptosis functions in many capacities and is primarily determined by the state of the cell. Autophagy generally blocks apoptosis induction during times of cellular stress (acting as a survival mechanism) and apoptosis-initiated caspases block autophagy induction when the cells has reached a level of damage that is irreversible (acting as a cell death mechanism) (62). Also, in extreme

cases, autophagy can even act as an alternative cell death mechanism (63). Because of the diversity of activation mechanisms and biologic roles that autophagy plays within cells it has the distinct ability to both promote and inhibit tumorigenesis (50). This makes autophagy an attractive target for molecular therapies and further investigation into its role within specific subsets of cancer cells is a top priority for researchers.

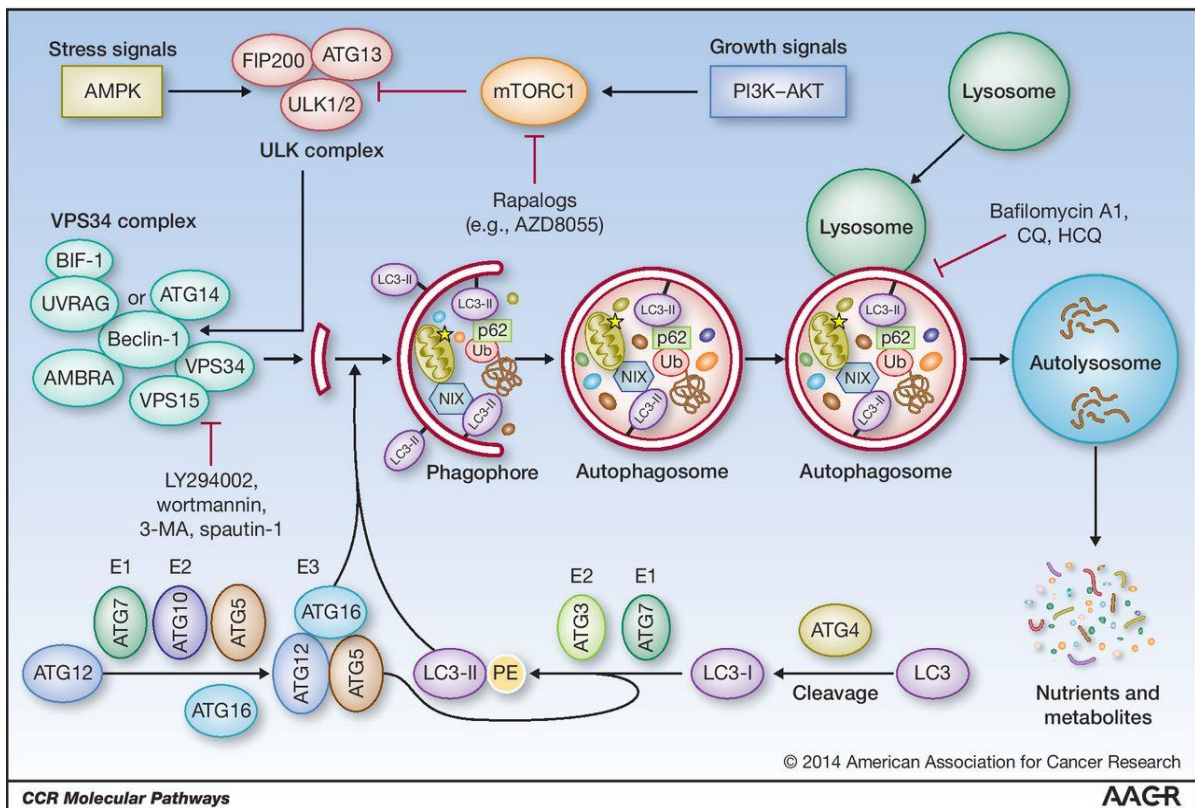


Figure 1.7 Autophagy. The molecular determinates of autophagy that control the highly conserved multi-step “self-digestive” process. These steps include vesicle nucleation, vesicle elongation, autophagosome fusion with the lysosome, and proteolytic degradation of engulfed molecules (61, 64).

*Reproduced with permission of Clinical Cancer Research by American Association for Cancer Research and HighWire Pres. Molecular Pathways: Autophagy in Cancer—A Matter of Timing and Context. Michelle Cicchini, Vassiliki Karantza and Bing Xia. Clin Cancer Res February 1 2015 (21) (3) 498-504.(61)

1.7 Summary and scope of dissertation

In this dissertation, I sought to better understand the molecular determinants of sensitivity and resistance to MET inhibition in human gastric cancer. Here I present the findings of one comprehensive study that is divided into two main parts pertaining to MET inhibitor sensitivity and subsequently the role of autophagy induction in response to MET inhibition in MET-amplified gastric cancer. First, in Chapters 3 and 4, I examined the effects of MET inhibition on gastric cancer cells as it pertains to cell death, growth arrest and global gene expression modulation. Using the data obtained from these experiments I identified two gastric cancer cell lines with extreme sensitivity to MET inhibition via incubation with a tyrosine kinase inhibitor, crizotinib. Both of the sensitive gastric cancer cell lines have amplified MET. Once I examined and identified the molecular determinants of sensitivity to MET inhibition, I sought to identify additional synergistic targets and potential resistance mechanisms. In Chapter 5, I evaluated the effects of crizotinib on gastric cancer cells with MET amplification and identified autophagy as a top biologic process modulated by MET inhibition. Then I sought to delve deeper into the understating of how autophagy modulation is interacting with MET inhibition in gastric cancer cells. Because autophagy has been shown to be both tumor suppressive and tumor promoting depending on cellular context, there is a need for a better understanding of how autophagy modulation influences response to MET inhibition and this dissertation seeks to contribute to this aim.

Chapter 2. MATERIALS AND METHODS

2.1 Materials and Methods for Chapter 3

2.1.1 Cell lines and culture: MKN45, MKN74, NUGC-3, NUGC-4, and IM95 gastric cancer cells were a gift from Julie G. Izzo, M.D., Department of Experimental Therapeutics, MD Anderson. KATOIII, NCI-N87, SNU-16, SNU-5, AGS, Hs746t, and SNU-1 gastric cancer cells were obtained from American Type Culture Collection (Manassas, VA). HGC-27 gastric cancer cells were obtained from Sigma-Aldrich (St. Louis, MO). All cells were validated by DNA fingerprinting using AmpFISTR® Identifiler® Amplification kit (Applied Biosystems, Foster City, CA), performed by the MD Anderson Characterized Cell Line Core. All gastric cancer cells (except for SNU-5) were maintained in RPMI-1640 medium supplemented with 10% FBS (HyClone/Thermo Scientific, Waltham, MA), minimum essential medium (MEM) vitamins, sodium pyruvate (Mediatech/Corning Cellgro, Manassas, VA), L-glutamine, non-essential amino acids, penicillin/streptomycin (Lonza, Switzerland), and HEPES buffer. SNU-5 cells were cultured in Iscove's modified Dulbecco's medium supplemented with 10% FBS, MEM vitamins, L-glutamine, sodium pyruvate, non-essential amino acids, penicillin/streptomycin, and HEPES. All cells were grown at 37° C in 5% CO₂.

2.1.2 Chemicals and antibodies: Crizotinib was purchased from Selleck Chemicals (Houston, TX). Bortezomib was purchased from ChemieTek (Indianapolis, IN). Propidium iodide was purchased from Sigma-Aldrich (St. Louis, MO). Antibodies were obtained from the following sources: MET, p-MET and cleaved PARP from Cell Signaling Technology (Beverly, MA); anti-mouse/ anti-rabbit HRP-labeled secondary antibodies from Promega (Madison, WI); and β -actin from Sigma-Aldrich (St. Louis, MO).

2.1.3. CCLE Methods: mRNA expression data was obtained using Affymetrix Human Genome U133 Plus 2.0 arrays according to the manufacturer's instructions. Copy number variation data was obtained using genome-wide human Affymetrix SNP Array 6.0. Pharmacological characterization was automated and performed with an ultra-high throughput screening using 72 to 84 hours Cell Titer Glo Assays (Promega) (65).

2.1.3 Cell proliferation assay: The panel of 13 gastric cancer cells was plated in quadruplet replicates in 96-well plates at a density of 5×10^3 cells per well. The cells were allowed to attach overnight before exposing them to the indicated concentrations of crizotinib (ranging from 0, .01-10uM) for 5 days. Conversion of MTT (3-(4,5-dimethylthiazol-2-yl)-2,5-diphenyltetrazolium bromide) to formazan salt was used to measure relative numbers of viable cells in each well (66). Following drug exposure, 50 μ L of MTT solution (50 μ g/ml in PBS) was added to each well and cells were incubated for 2 more hours. Next, the medium was aspirated and replaced with DMSO (100 μ L). A colorimetric assay using a standard micro-plate reader was used to determine the amount of MTT in each well via was quantified by measuring the optical densities (ODs). IC50 values were then correlated by using the raw absorbance values.

2.1.4 Copy number assay: DNA was isolated from gastric cell lines (MKN45, MKN74, NUGC-4, SNU-5 and Hs746t) using a genomic DNA extraction kit according to the manufacturer's protocol (Qiagen). *MET* gene copy number was determined using commercially available and pre-designed TaqMan Copy Number Assays (Applied Biosystems, Foster City, CA) as described previously (67). The primer used for the *MET* gene was Hs05005660_cn.

(Location: Chr.7:116778578 on GRCh38, Cytoband: 7q31.2). The *TERT* locus was used for the internal reference copy number. Real-time genomic PCR was performed in a total volume of 20 μ L in each well, which contained 10 μ L of TaqMan genotyping master mix and 20ng of genomic DNA and each primer. The PCR conditions were 95°C for 10 minutes, 40 cycles of 95°C for 15 seconds, and 60°C for 1 minute. Data were analyzed using SDS2.2 software and CopyCaller software (Applied Biosystems).

2.1.5 Cell death assay (apoptosis): Cells were plated in 6-well plates and were allowed to attach overnight. Cells were then exposed to crizotinib (0, .001 μ M, .01 μ M, .1 μ M, 1 μ M) for 48 hours and collected via trypsinization. Cell pellets were washed once in 2ml of cold PBS and resuspended in 0.5mL of PI-FACS buffer which contains: propidium iodide (PI) solution (100 μ g/mL), triton x-100, sodium citrate and PBS for 1-3 hours at 4° with limited exposure to light. Apoptosis was quantified by propidium iodide staining coupled with flow cytometry by FACS (fluorescence activated cell sorting) analysis on the FL3 channel of a Beckman Coulter FC500 flow cytometer (68). The method involves propidium iodide staining of permeabilized cells; apoptotic cells release the DNA fragments produced as a consequence of the endogenous endonuclease activation that is associated with apoptosis, and they appear as hypodiploid cells when they are measured by flow cytometry.

2.1.6 Immunoblotting: Phospho and total MET: cells were harvested by scrapping and lysed in buffer containing 50mM Tris-HCL, 150mM NaCl, 1mM EDTA, 1% Triton X-100, 1% sodium deoxycholate, 0.01% SDS, 2mM sodium orthovanadate (Na₃VO₄), 1mM NaF, 1mM glycerophosphate, 1mM PMSF and complete mini protease/ phosphatase inhibitor tablets

(Sigma-Aldrich). PARP: cells were harvested by scraping and lysed in buffer containing 0.5% (w/v) SDS and then the membrane was disrupted by sonication for 30 seconds before being stored on ice. Protein concentrations were measured using the BCA Protein Assay Kit (Thermo Scientific, Rockford, IL). Lysates were boiled in sample buffer (62.5 mmol/L Tris-HCl (pH 6.8), 10% (w/v) glycerol, 100 mmol/L DTT, 2.3% SDS, 0.002% bromophenol blue) for 5 minutes and cooled at room temperature for 10 minutes. Samples were then separated on 2-12% gradient SDS-PAGE gels at 100 V in electrophoresis buffer (25 mmol/L Tris-HCl (pH 8.3), 192 mmol/L glycine, 0.1% SDS) and then electrophoretically transferred onto nitrocellulose membranes in transfer buffer (25 mmol/L Tris-HCl, 192 mmol/L glycine, 20% methanol) overnight at 10 mV. The membranes were incubated in blocking buffer (5% nonfat milk in PBS) for 1 hour at room temperature while shaking. The membranes were then rinsed with PBS containing 0.1% Tween-20. The membranes were incubated with primary antibodies diluted 1:1000 in 1% milk overnight, washed, and then incubated with second antibodies (anti-mouse or anti-rabbit immunoglobulin) diluted 1:10,000 in 5% milk for 1 hour at room temperature while shaking. Immunoreactive proteins were detected using enhanced chemiluminescence (Amersham Biosciences, Piscataway, NJ) (66, 69).

2.2 Materials and Methods for Chapter 4

2.2.1 Cell lines and culture: All cell lines (MKN45 and SNU-5) were maintained as previously described in 2.1.1 methods and grown at 37° C in 5% CO₂.

2.2.2 Chemicals and antibodies: Crizotinib was purchased from Selleck Chemicals (Houston, TX). Antibodies were obtained from the following sources: MYC from Cell Signaling Technology (Beverly, MA); Bim from BD Pharmingen (Piscataway, NJ); anti-mouse/ anti-rabbit HRP-labeled secondary antibodies from Promega (Madison, WI); and β -actin from Sigma-Aldrich (St. Louis, MO).

2.2.3 Gene expression profiling: SNU-5 and MKN45 cells were plated in 10cm dishes and exposed to 100nM crizotinib for 24 hours. Triplicate experiments were performed for each cell line and treatment group. Cells were harvested by scraping on ice and washed twice with cold PBS. Total RNA from cell pellets was isolated using the mirVana miRNA isolation kit (Ambion, Inc) according to manufactures protocol. RNA purity and integrity were measured by a NanoDrop ND-1000 spectrophotometer and Agilent Bioanalyzer, respectively, and only high-quality RNA was used for the cRNA amplification. The MET-amplified gastric cancer cell lines were analyzed by direct hybridization on Illumina Human HT12v4 chips (Illumina, San Diego, CA). The chips were then scanned on the HiScan or iScan systems. Quantile normalization in the Linear Models for Microarray Data (limma) package in the R language environment was used to normalize the data. BRB Array Tools version 4.5.1 (National Cancer Institute) was used to analyze the data. The significantly differentially expressed genes ($P < 0.001$ with FDR < 0.05 , 2-fold cut-off) were then extracted using class comparison tools with random variance t-test to yield 1734 differentially expressed probes for SNU-5 representing 1405 genes and 1919 differentially expressed probes for MKN45 representing 1517. Gene expression profiling data was uploaded to Gene Expression Omnibus with accession number GSE77320.

2.2.4 Pathway Analysis: Functional and pathway analyses were performed using Ingenuity Pathway Analysis (IPA) software (Ingenuity® Systems, CA), which contains a database for identifying networks and pathways of interest in genomic data. Based on the IPA knowledge database, p values and Z-scores can be calculated based on how many targets of each transcriptional factor were overlapped (p values) and the extent of concordance of the known effects (activation or inhibition) of the targets in the gene lists (Z-score) (70).

2.2.5 mRNA extraction, reverse transcription and quantitative real-time PCR: RNA was isolated from cells according to the manufacturer's protocol using the mirVana™ miRNA isolation kit (Ambion/Life Technologies). RNA quantity and quality was then measured by a NanoDrop ND-1000 spectrophotometer and samples were diluted to 20ng of RNA. One-Step RT-PCR kit (Applied Biosystems/Life Technology) was used for real-time (TaqMan-based) reverse transcription PCR using 96- wells plates. TaqMan primers for PPIA (Hs04194521_s1), MYC (Hs00153408_m1), ETV5 (Hs00927557_m1), MXD4 (Hs01555090_m1) and PIK3IP1 (Hs00364627_m1) were purchased from Applied Biosystems. The comparative $\Delta\Delta C_t$ method was used to estimate gene expression and the data were plotted as relative quantity (CQ) \pm min and max as previously described (71).

2.2.6 Immunoblotting Analysis: Cells were plated and allowed to attach in 6-well plates overnight. The cells were then exposed to 100nM crizotinib and harvested by scraping on ice at 24 hours. The western blots were performed as previously described 2.1.6. The membranes were incubated with primary BIM and MYC antibodies diluted 1:1000 in 1% milk overnight, washed, and then incubated with second antibodies (anti-mouse or anti-

rabbit immunoglobulin) diluted 1:10,000 in 5% milk for 1 hour at room temperature while shaking. Immunoreactive proteins were detected using enhanced chemiluminescence (Amersham Biosciences, Piscataway, NJ) (69).

2.3 Materials and Methods for Chapter 5

2.3.1 Cell lines and culture: All cell lines (MKN45, SNU-5, NUGC-4 and MKN74) were maintained as previously described in 2.1.1 methods and grown at 37° C in 5% CO₂.

2.3.2 Chemicals and antibodies: Crizotinib was purchased from Selleck Chemicals (Houston, TX). Bortezomib was purchased from ChemieTek (Indianapolis, IN). Cisplatin was purchased from EMD Millipore Corp (Billerica, MA). Propidium iodide, oligomycin A, chloroquine and acridine orange were purchased from Sigma-Aldrich (St. Louis, MO). The following antibodies were purchased from the indicated sources: Cytochrome C (BD Pharmingen); and β -actin (Sigma-Aldrich).

2.3.3 Acridine orange autophagy detection: Cells were plated and allowed to attach overnight. At 30% confluence the cells were exposed to 0, .001, .01, .1 and 1 μ M crizotinib. After 72 hours the cells were washed with cold PBS and dissociated from the plate using Accumax to allow for the generation of a single cell suspension. Autophagy levels were measured using a lysotropic dye, acridine orange, which accumulates in acidic organelles in a pH-dependent manner, becomes protonated and trapped, and emits a bright red fluorescence. The red fluorescence was then detected by fluorescence-activated cell sorting (Coulter, FL2 channel). Bafilomycin A1 (Sigma Chemical Co.) was dissolved in DMSO and added to the cells 30 min before the addition of acridine orange as a positive control. A

negative control containing no AO dye was also generated to accurately gate the experiment.

2.3.4 Cyto-ID autophagy detection: The second method employed to measure autophagy within the cells was the use of the CYTO-ID® Autophagy detection kit (Enzo Life Sciences, Inc). The cells were plated in 96 well plates at 100µL cells/well (3.0×10^5 cells/ml), 24 hours before the experiment and then exposed to increasing concentrations of crizotinib for 48 hours. The cells were then washed once with 100 µL of 1X Assay Buffer and then the cells were incubated with 100µL of dual color detection solution at 37° for 30 minutes according to the manufacturer's protocol. After 30 minutes the cells were washed twice 1X Assay buffer and finally 100µL of 1X Assay Buffer was added to each well. The cells were then immediately analyzed by fluorescence microplate reader using the FITC filter (Excitation ~480 nm, Emission~530) to detect the CYTO-ID® Green detection reagent and the DAPI filter set (Excitation ~340, Emission ~480) to detect the nuclear stain (72).

2.3.5 Immunoblotting Analysis: Cells were plated and allowed to attach in 6-well plates overnight. The cells were then exposed to 100nM crizotinib, 50uM chloroquine or the combination of both and harvested at 24 hours. The western blots were performed as previously described 2.1.6. The membranes were incubated with primary LC3B antibodies diluted 1:1000 in 1% milk overnight, washed, and then incubated with second antibodies (anti-mouse or anti-rabbit immunoglobulin) diluted 1:10,000 in 5% milk for 1 hour at room temperature while shaking. Immunoreactive proteins were detected using enhanced chemiluminescence (Amersham Biosciences, Piscataway, NJ) (69).

2.3.6 Cell death assay (apoptosis): Cells were plated in 6-well plates and were allowed to attach overnight. Cells were then exposed to various concentrations of crizotinib, chloroquine, bortezomib or cisplatin for 48 hours and collected via trypsinization. Cell pellets were washed once in 2ml of cold PBS and resuspended in 0.5mL of PI-FACS buffer which contains: propidium iodide (PI) solution (100µg/mL), triton x-100, sodium citrate and PBS for 1-3 hours at 4° with limited exposure to light. Apoptosis was quantified by propidium iodide staining coupled with flow cytometry as previously described 2.1.5 (68).

2.3.7 Cell viability assay: Cell death was measured using the Vi-CELL XR Cell Viability Analyzer (Beckman Coulter) following incubation with the inhibitor for 48 hours. This analyzer processes and analyzes cells using the trypan blue dye exclusion method to determine the number of viable cells present in a cell suspension. Live cells have uncompromised cell membranes that exclude trypan blue dye whereas dead cells do not. Viable cells have a clear cytoplasm whereas nonviable cells have a blue cytoplasm. This automated process takes the average of 50 unique images to calculate cell viability as well as the cell count (73).

2.3.8 ATP quantification: Cellular ATP levels were measured via the CellTiter-Glo Luminescent Cell Viability Assay (Promega). Using the CellTiter-Glo assay, the cell provides the ATP needed for the conversion of luciferin so that the luminescence produced is directly proportional to the amount of ATP present. Cells were plated in 96 well black plates and exposed to increasing doses of crizotinib with or without chloroquine. At 24, 48 and 72 hours 100ul of CellTiter-Glo reagent was added to each well, and the plate was placed on a

shaker for 2 minutes to lyse the cells. The plate was incubated at room temperature for 10 minutes, and luminescence was then recorded (74).

2.3.9 Cytochrome c release: Release of cytochrome c from the mitochondria was measured by immunoblotting as previously described (75). Cells were incubated with or without 100nM crizotinib, 50uM chloroquine, or 100nM crizotinib + 50uM chloroquine for 6 hours. The cells were then obtained by scraping followed by gentle centrifugation at 1700rpm for 3 minutes. The pellets were then washed with cold PBS and re-spun for 3 minutes. Next the cells were lysed in an ice-cold buffer containing 250 mM Sucrose, 1 mM EDTA, 25 mM Tris, pH 6.8, 0.05% IGEPAL and a Complete Mini protease inhibitor tablet (Sigma-Aldrich) until the cells outer membrane was compromised as determined by the trypan blue exclusion assay. The cells were then centrifuged at 14,000 rpm for 5 min at 4 °C and the supernatant, containing the cytosolic fraction, was transferred to new tubes. The pellet containing the mitochondrial fraction was then suspended in lysis buffer, and cytochrome c was measured in each fraction by immunoblotting.

**Chapter 3. SENSITIVITY TO
CRIZOTINIB IN GASTRIC
CANCER CELLS IS ASSOCIATED
WITH MET AMPLIFICATION**

3.1 Introduction

As detailed in Chapter 1, genes related to receptor tyrosine kinase (RTK) signaling have been identified as therapeutically viable targets in gastric cancer (40). Specifically, MET has become a target of interest in gastric cancer cells following positive effects seen in preclinical studies by two different groups (Haber and Nakagawa) (42, 43). Both groups showed that MET amplification was associated with sensitivity to MET inhibition. Also, MET amplification has been associated with dramatic and prolonged response to MET inhibition in gastric cancer patients (76, 77). Although MET inhibitors have clinical activity, not all MET-amplified tumors respond, and a deeper understanding of the molecular determinants of response is therefore crucial. The results of previous efforts by other groups led to the hypothesis that gastric cancer cells with amplified MET are dependent on MET signaling for survival and therefore die in response to MET inhibition.

3.2 Results

3.2.1 Effects of crizotinib on cell proliferation

As a first step in defining the determinants of MET dependence, we examined pharmacologic profiling produced by the Broad Institute for the Cancer Cell Line Encyclopedia (CCLE) project. From the 504 cell lines profiled we extracted all gastric cancer cell lines and used this panel of 19 cell lines to examine the sensitivity to the two MET inhibitors, PF2341066 (crizotinib) and PHA-665752 [Figure 3.2.a and 3.2.b]. Of these 19 cell lines, the only cell line that was sensitive to both MET inhibitors at biologically significant

levels was MKN45. Crizotinib is a protein-kinase inhibitor that works by competitive binding within the ATP-binding pocket of target kinases [Figure 3.1] (78). Biologically significant levels of crizotinib were characterized as IC₅₀ levels less than the peak plasma concentration obtained in patients, 57nM (79). Crizotinib selectively targets MET and ALK at clinically relevant doses and has a low probability of pharmacologically relevant inhibition of other kinases at these doses [Table 3.1] (80).

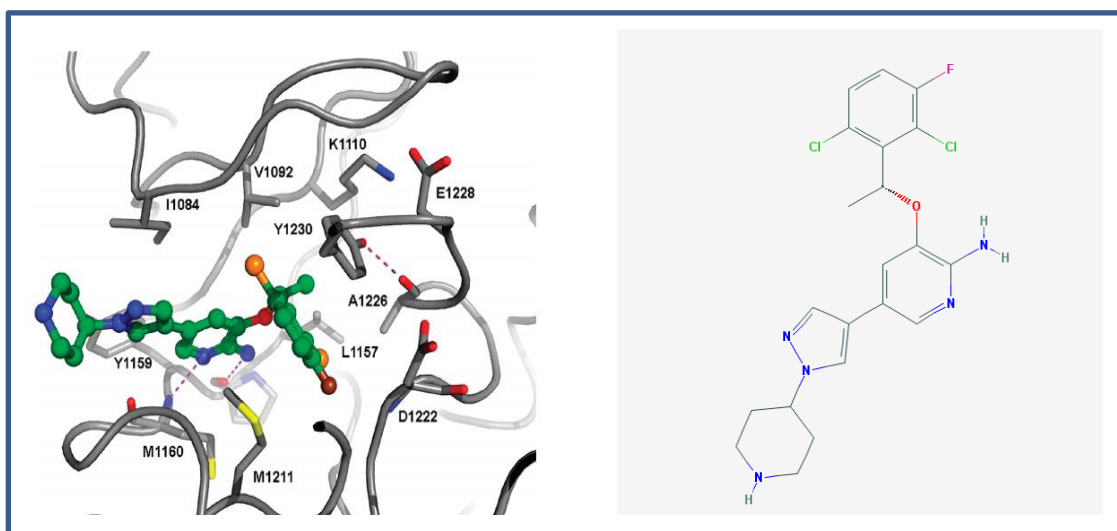


Figure 3.1 Crizotinib. (Left) Cocrystal structure of crizotinib bound to c-MET. Crizotinib binds in ATP-competitive manner with an auto-inhibitory kinase conformation of MET (80). (Right) 2D crizotinib structure (81).

*Reprinted with the permission of (80). Copyright 2011, American Chemical Society.

parameter	kinase									
	c-MET	ALK	RON	AXL	TIE2	TRKA	TRKB	ABL	IR	LCK
% inhib (1 μ M) ^a	97.0	99.0	97.0	93.0	97.0	99.3	99.7	91.5	67.7	96.5
enzyme IC ₅₀ (nM) ^a	<1.0	<1.0	NA	<1.0	5.0	<1.0	2.0	24	102	<1.0
cell IC ₅₀ (nM) ^b	8.0	20	80	294	448	580	399	1159	2887	2741

Table 3.1 Crizotinib kinase selectivity profile.

*Reprinted with the permission of (80). Copyright 2011, American Chemical Society.

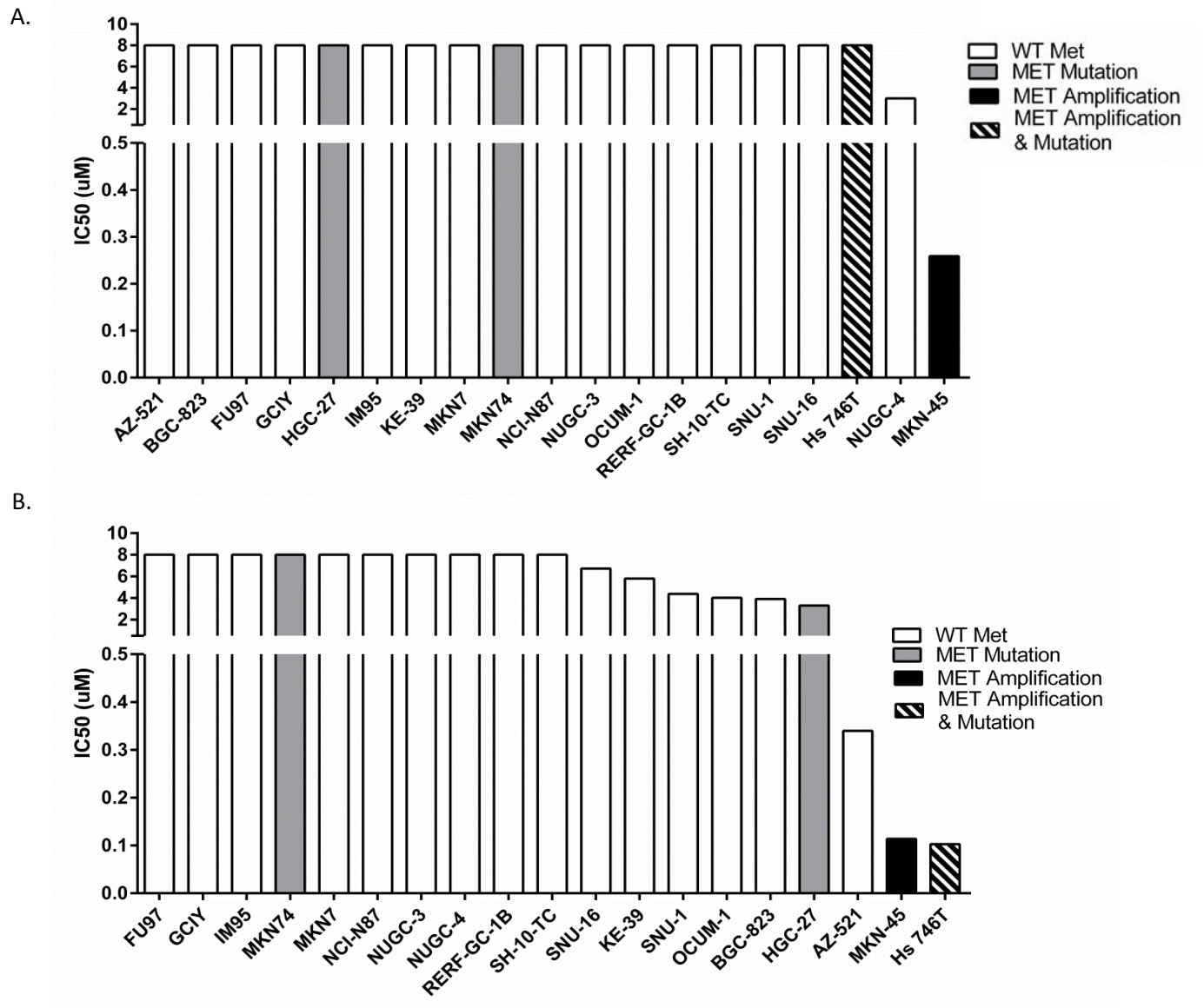


Figure 3.2 Drug sensitivity profiles of gastric human cancer cell lines treated with Crizotinib or PHA-665752. (A) Inhibitory concentration 50% (IC50) values of PHA-665752 in a panel of nineteen gastric cancer cell lines are compared using data generated by the CCLE. (B) Inhibitory concentration 50% (IC50) values of crizotinib in a panel of nineteen gastric cancer cell lines are compared using data generated by the CCLE.

Additionally, we extracted the crizotinib pharmacologic profiling data for all gastric cancer cell lines obtained from the Genomics of Drug Sensitivity in Cancer Project (GDSC) to be as comprehensive as possible with our interrogation of publically available pharmacologic profiling (82). The GDSC is collaboration between the Cancer Genome Project at the Wellcome Trust Sanger Institute (UK) and the Center for Molecular Therapeutics, Massachusetts General Hospital Cancer Center (USA). Using these data, of the five cell lines available (HSC-39, GCIY, SNU-16, SNU-1 and SNU-5) only one (SNU-5) had amplified MET and it was also the only cell line that was sensitive to crizotinib [Figure 3.3].

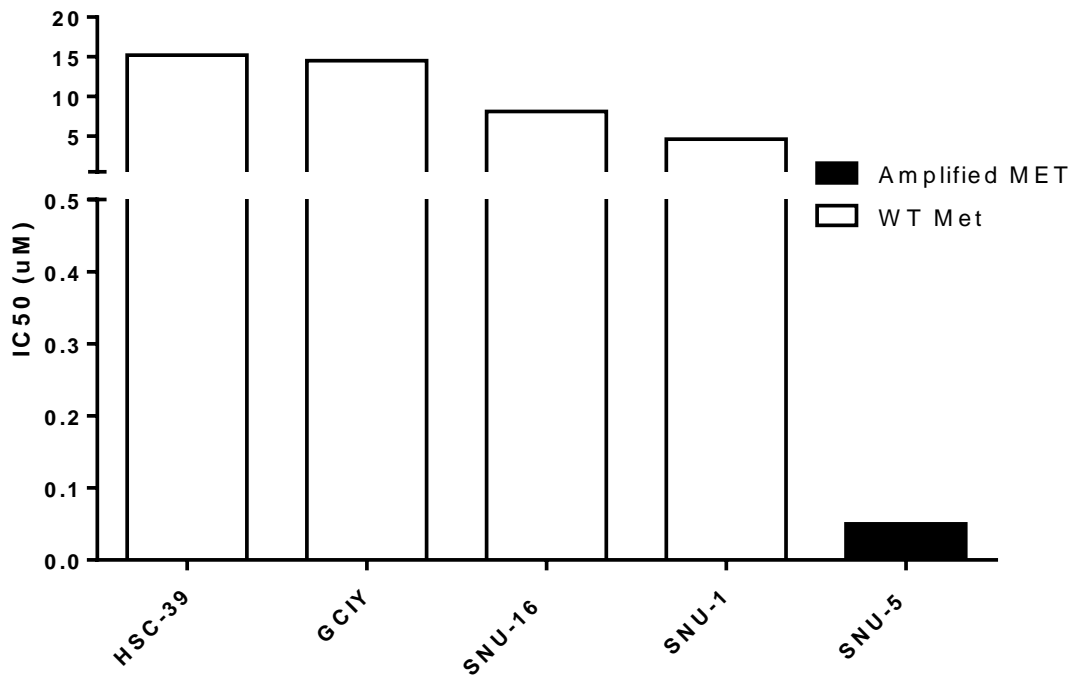


Figure 3.3 Drug sensitivity profiles of gastric human cancer cell lines treated with Crizotinib. Inhibitory concentration 50% (IC50) values of crizotinib in a panel of five gastric cancer cell lines are compared using data generated by the GDSC.

3.2.2 MET gene expression and copy number variation in panel of gastric cancer cell lines

We then correlated the IC50 values for the MET inhibitor crizotinib with MET gene expression and MET copy number variation using publicly available data from the Cancer Cell Line Encyclopedia (CCLE) project [Figure 3.4.a]. The results revealed that both of the cell lines identified as sensitive by the pharmacologic profiling experiments (SNU-5 and MKN45) had amplified MET with greater than 10 copies each. The other cell line, Hs746t, which had MET amplification and also harbored a MET mutation, was sensitive to only one of the two MET inhibitors used by the CCLE (83). The MET mutation identified in the Hs746t cell line and its potential consequences will be elaborated on further in the discussion.

We validated the MET copy number data produced by the CCLE in a panel of 5 cell lines, two with MET amplification only (SNU-5 and MKN45), one with wild-type MET (NUGC-4), one with a MET mutation only (MKN74) and one with MET amplification and a MET mutation (Hs746t) using the TaqMan Copy Number Assay [Figure 3.4.b].

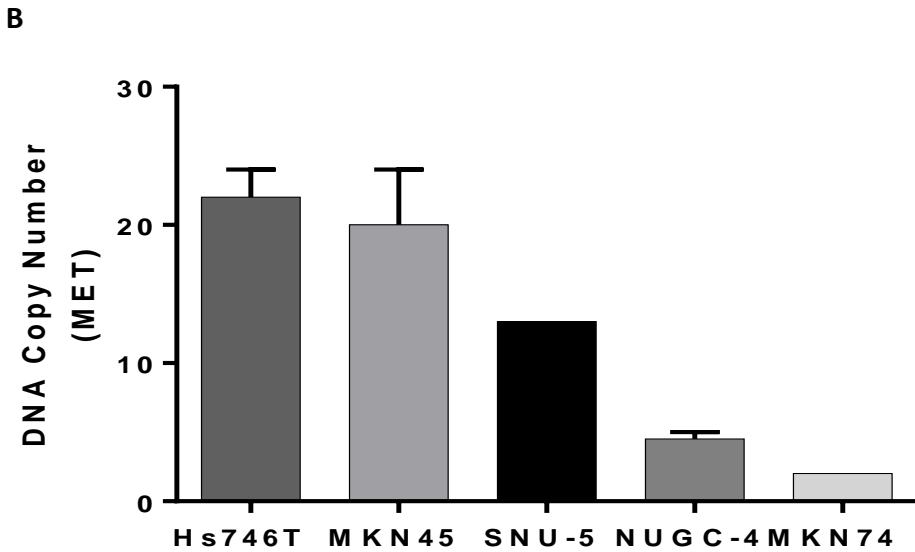
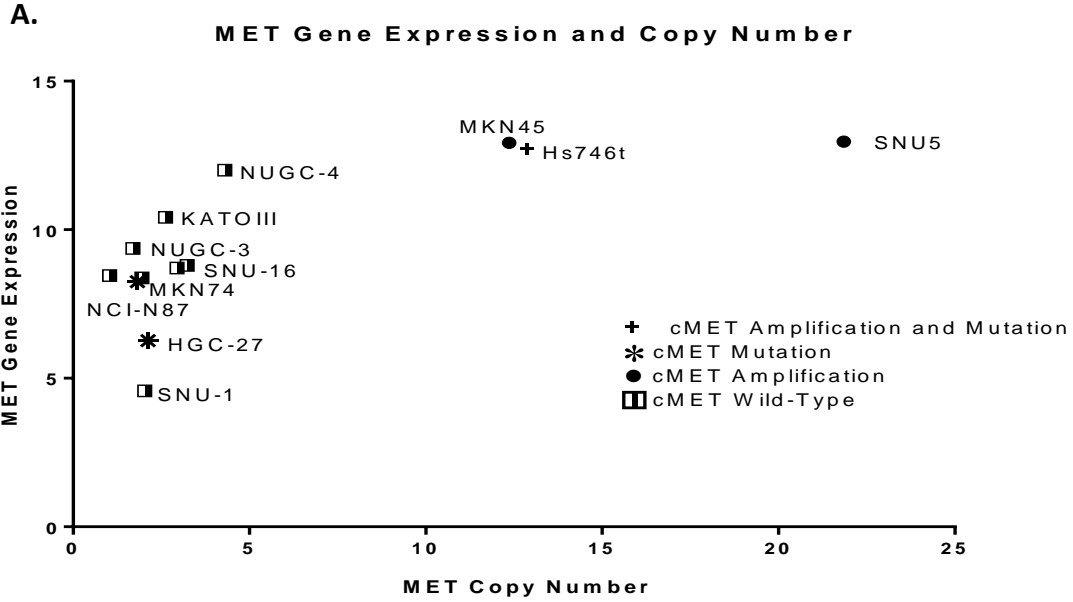


Figure 3.4 MET gene expression and copy number profile of gastric human cancer cell lines. (A) MET RNA expression levels were compared to MET copy numbers for a panel of thirteen gastric cancer cell lines using data generated by the CCLE (B) MET DNA copy numbers were analyzed using TaqMan copy number assays. Three cell lines Hs746t, SNU-5, and MKN45 had high level MET amplification with average copy numbers of 22, 13 and 20, respectively. Data are means \pm SEM from two biological replicates.

One interesting observation that warranted further investigation is that although the NUGC-4 cell line had relatively high levels of MET gene expression, no growth arrest was exhibited following MET inhibition. To further interrogate this finding, we used immunoblotting to look at the total and phospho-MET levels in the panel of 5 cell lines [Figure 3.5]. The results demonstrated that the amplified cell lines (SNU-5, MKN45, and Hs746t) had higher levels of both total and phospho-MET as compared to the MKN74 cells that contained mutated MET or the NUGC-4 cells that contained wild-type MET.

While measuring mRNA is a valid gauge of gene regulation, it cannot be assumed that there is a direct correlation between the amount of mRNA and protein expression since post-transcriptional processes are key to the final synthesis of the protein (84). Therefore, even though the NUGC-4 cells had relatively high mRNA expression they had significantly lower levels of total MET and phospho-MET, which appeared to be the primary predictor of response to crizotinib, as compared to the amplified cell lines (SNU-5 and MKN45) [Figure 3.5]. This is reinforced by reports showing a link between phospho-MET levels and sensitivity to the MET Inhibitor PHA665752 in lung cancer cells (85). This supports the idea that high levels of phospho-MET may be required for drug sensitivity, an idea which merited further inquiry.

3.2.3 Validation of effects of crizotinib on cell proliferation

Next, we attempted to confirm the results produced by the CCLE and GDSC in an independent (but overlapping) panel of 13 gastric cancer cell lines (MKN45, SNU-5, MKN74, NUGC-3, NUGC-4, IM95, KATOIII, NCI-N87, SNU-16, HGC-27, AGS, Hs746t, and SNU-1).

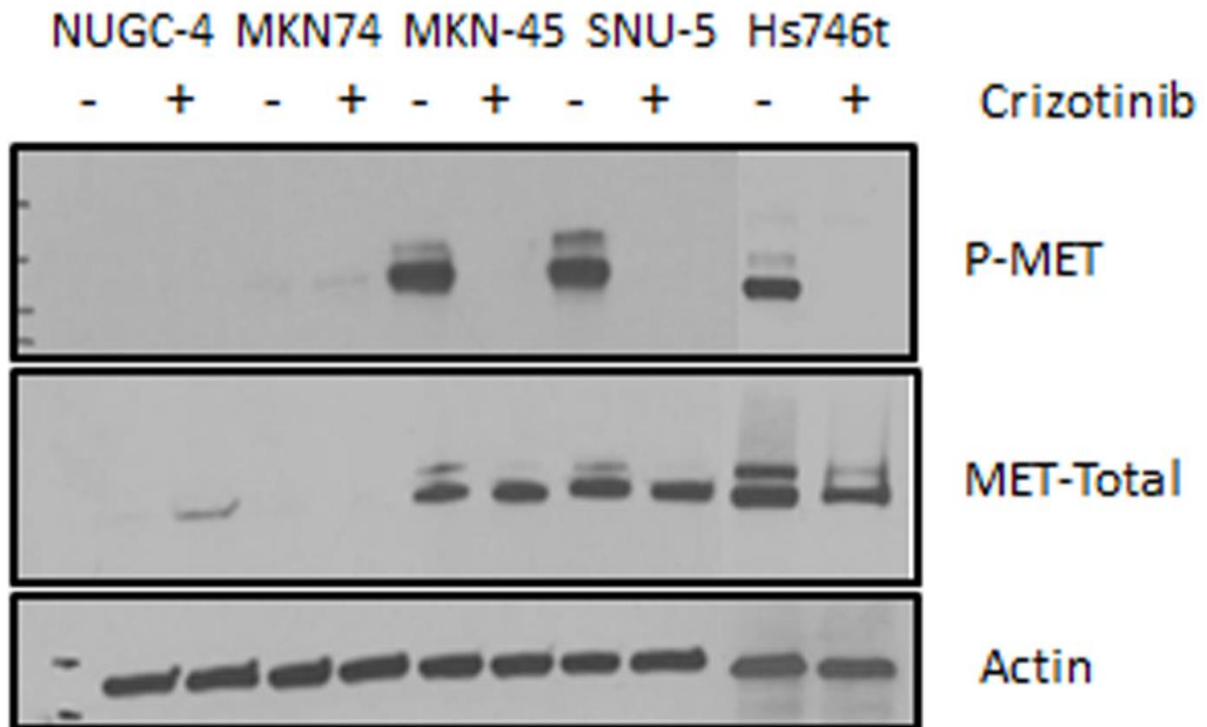


Figure 3.5 Crizotinib sensitivity correlates with MET phosphorylation in human gastric cancer cells. Three MET amplified (Hs746t, SNU-5, and MKN45) and two non-amplified cell lines (MKN74 and NUGC-4) were incubated with or without 100nM crizotinib 24 hours, and total protein was extracted using RIPA lysis buffer. Total lysates were then analyzed by immunoblotting using anti-phospho-MET, anti-total-MET, and β -actin antibodies.

For the results produced by the CCLE, the cells were incubated for 72 to 84 hours followed by ATP measurement by luminescence using the Cell Titer Glo assay (Promega) to correlate ATP levels to cell survival. For our analysis, we performed 5-day MTT (3-(4,5-dimethylthiazol-2-yl)-2,5-diphenyltetrazolium bromide) assays using increasing concentrations of crizotinib (ranging from 0, .01-10uM) to measure proliferation inhibition and determine IC50 values. At the conclusion of the 5-days conversion of MTT to formazan salt was used to measure relative numbers of viable cells in each well. These data were then analyzed and transformed to generate a crizotinib IC50 for each of the cell lines. Then we classified the cell lines as either sensitive (<57nM) or resistant (>57nM), based on the clinically achievable plasma level of crizotinib in patients. In our panel, the only cell lines that were sensitive to clinically achievable concentrations of crizotinib were two of the three that contained amplified MET (SNU-5 and MKN45), whereas in our hands the Hs746t cells were resistant [Figure 3.6]. Hs764t cells were also resistant to one of the MET inhibitors, PHA-665752, tested in the pharmacologic profiling experiments done by the CCLE [Figure 3.2.b]. Published data on this cell line presents conflicting results of the total and phospho-MET levels as well as sensitivity to MET inhibition which will be elaborated on further in the discussion (42, 83). This expands on the idea that although high levels of phospho-MET may be required for drug sensitivity, they may not be sufficient for drug sensitivity alone.

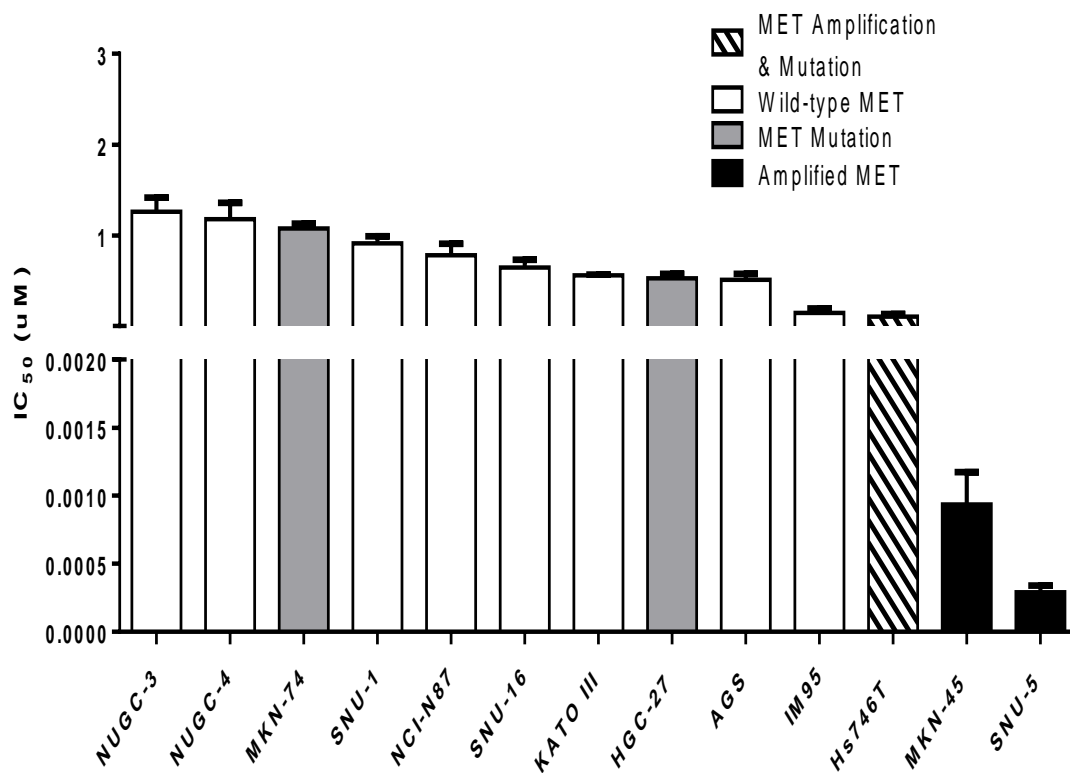


Figure 3.6 Drug sensitivity profile of gastric human cancer cell lines treated with Crizotinib. Thirteen human gastric cancer lines were used to independently determine IC₅₀ values of crizotinib in a panel of cancer cell lines. Cells were exposed to increasing concentrations of crizotinib for 5 days, and viable cells were assessed using the MTT colorimetric assay. Data are means \pm SEM from two biological replicates.

3.2.4 Effects of crizotinib on cell death in gastric cancer cells

Based on the previous observation that treatment with crizotinib has cytostatic effects on gastric cancer cells containing amplified MET, we speculated that these same cells would die via apoptosis following exposure to crizotinib. We then performed a time course and dose response in response to crizotinib treatment in a subset of gastric cancer cell lines and measured apoptosis by propidium iodide staining coupled with FACS analysis. PI/FACS analysis is used to identify cells with hypodiploid DNA content (68). In this assay cells are permeabilized during the PI staining, which results in loss of DNA fragments, produced by apoptosis-associated endogenous endonuclease activation, from the cells. From this preliminary analysis we decide to move forward with profiling the entire thirteen cells lines at the 48 hour time point using the two lowest available concentrations of crizotinib that produced significant levels of apoptosis (10nM and 100nM crizotinib) in the two MET amplified cell lines. When the entire panel of cell lines was profiled, only the SNU-5 and MKN45 cell lines displayed significant increases in crizotinib-induced apoptosis at 10nM and 100nM crizotinib [Figure 3.7]. This finding that only the MET amplified cell lines responded to MET inhibition is consistent with the results of the MTT assays previously reported.

Although the PI-FACS technique has been validated and widely used for the analysis of apoptosis since its original publication (68) we sought to confirm these effects using an independent assay. For this, we selected immunoblotting for cleaved poly-(ADP-ribose) polymerase (PARP). PARP (116kDA) is involved in DNA damage repair by modifying nuclear

proteins and binding DNA breaks. PARP is cleaved by caspase-3 into an 89kDa fragment during apoptosis thus preventing its repair functionality allowing for the progression of apoptosis and the resulting hallmark DNA laddering [Figure 3.8.a]. Using the PARP cleavage assay, we confirmed that only the cell line with amplified MET (MKN45) responded to crizotinib by undergoing apoptosis. To investigate further the effects of crizotinib on two MET amplified cell lines (SNU-5 and MKN45) we examined the modulation of two well-characterized proteins involved in apoptosis, BIM and XIAP. As mentioned in the introduction, BIM upregulation may contribute to the pro-apoptotic effects of crizotinib in MET-amplified gastric cancer cells (43). The BH3-only protein BIM is a Bcl-2 family member that is essential for the initiation of apoptosis following growth-factor withdrawal (86, 87). X-linked Inhibitor of apoptosis (XIAP) is a member of the family of proteins that antagonizes apoptosis through binding to inhibits caspase 3, 7 and 9 and deregulation of XIAP has been associated with cancer development (88). Based on the PI-FACS and PARP cleavage results [Figure 3.7 and 3.8.a] we would anticipate that level of anti-apoptotic protein XIAP (89) would decrease, and the level of pro-apoptotic protein BIM (90) would increase following exposure to crizotinib in the two MET amplified cell lines. Consistent with our expectations, we observed statistically significant changes in protein expression levels between the control and crizotinib-treated samples for XIAP and BIM in each cell line (SNU-5 and MKN45) [Figure 3.8.b]. Overall, the results demonstrate that MET amplification promotes crizotinib induced apoptosis.

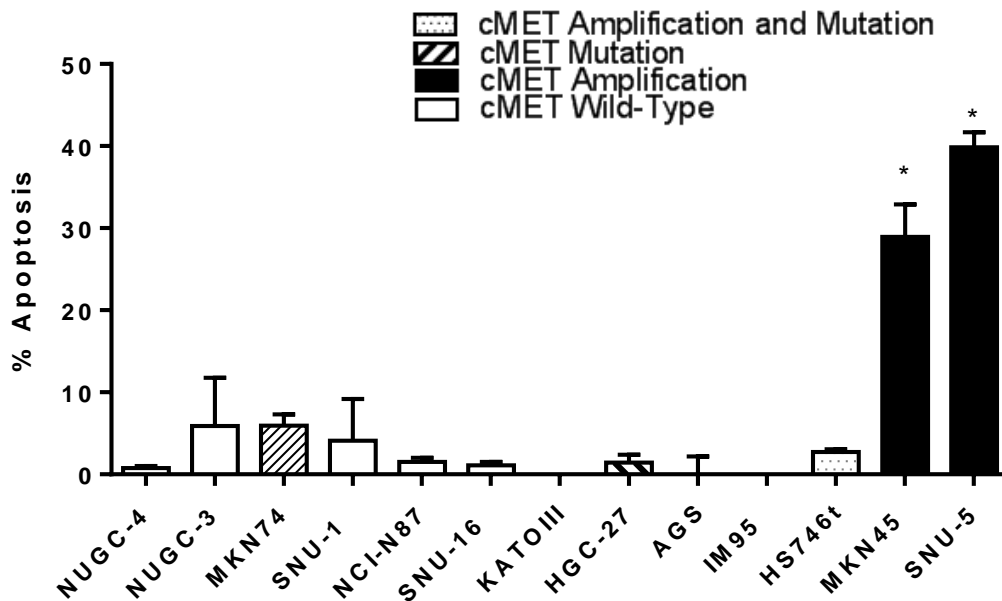
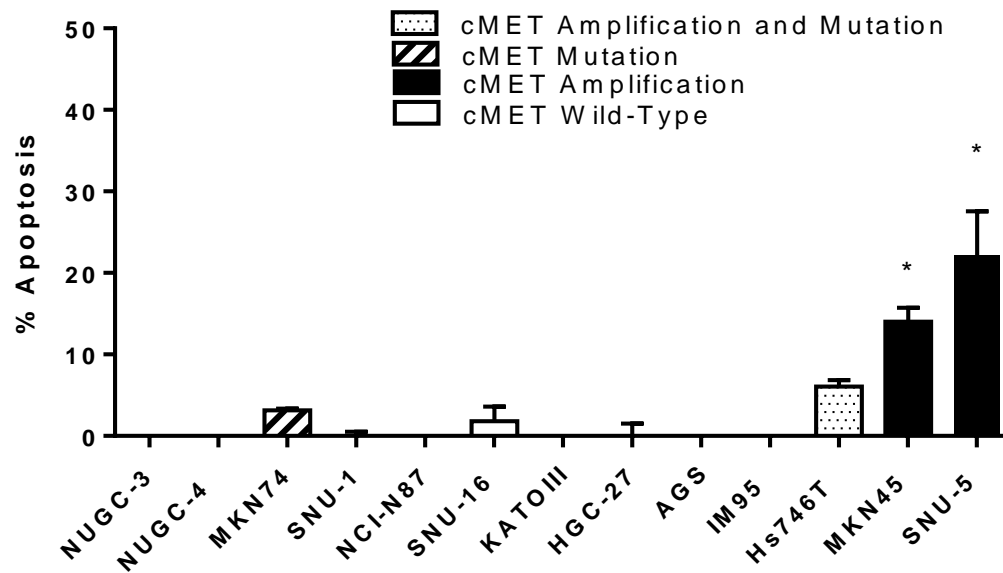


Figure 3.7 Effects on apoptosis of the MET inhibitor crizotinib on human gastric cancer cells. Thirteen human gastric cancer lines were incubated with or without (A) 10nM crizotinib or (B) 100nM crizotinib for 48 hours, and DNA fragmentation characteristic of apoptosis was measured by propidium iodide (PI) staining and FACS analyses. Values represent normalized results subtracting untreated controls, which were all less than 15%. Student t-test, * $p \leq 0.005$ crizotinib versus untreated control.

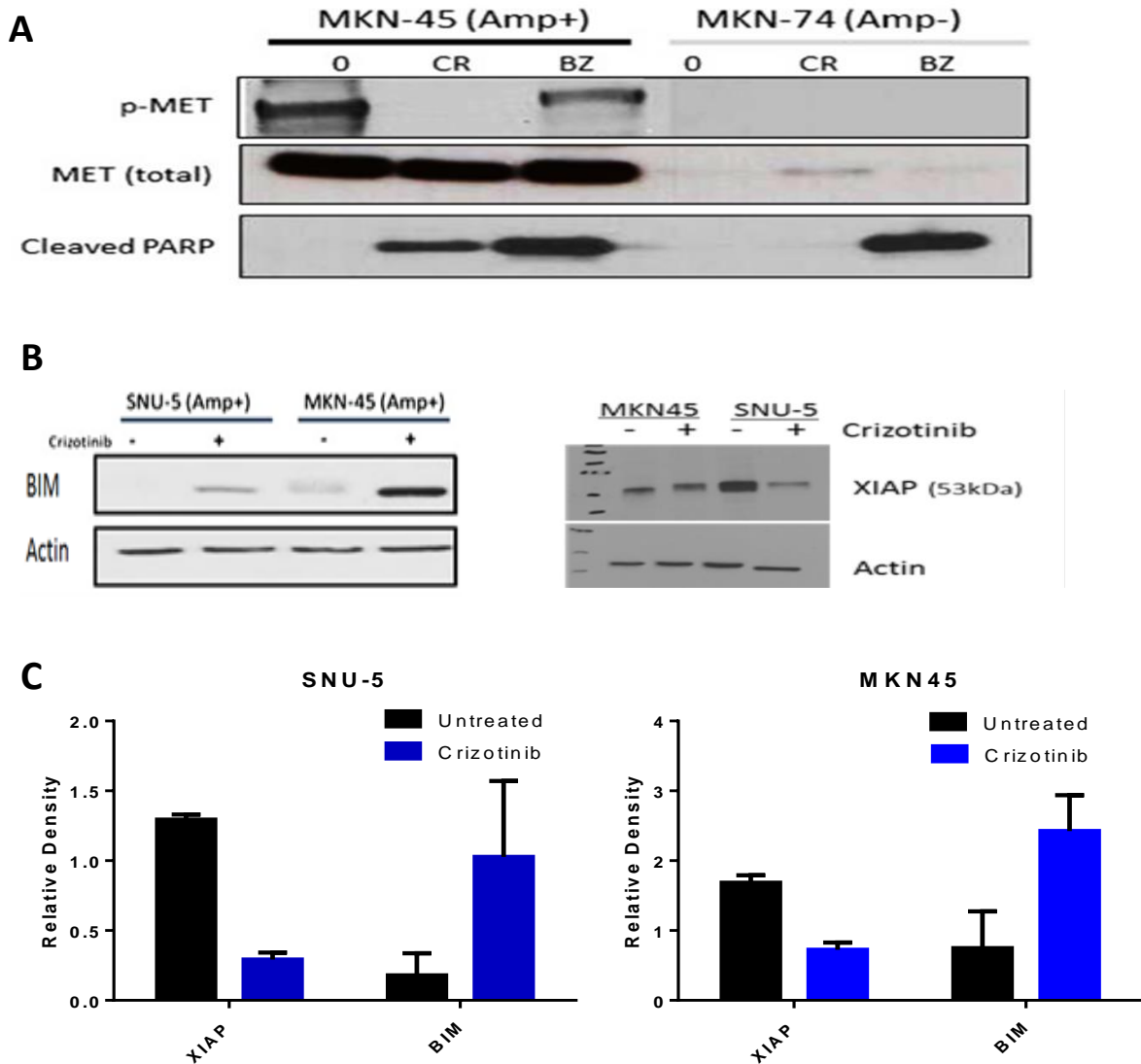


Figure 3.8 Effects on apoptosis related proteins of the MET inhibitor crizotinib on human gastric cancer cells. (A) One MET amplified and one non-amplified cell line were incubated with or without 100nM crizotinib or 1uM bortezomib for 48 hours. The cells were then lysed, and total protein was extracted using RIPA lysis buffer. Total lysates were then subjected to immunoblotting analysis using anti-phospho-MET, anti-total-MET, and anti-cleaved-PARP antibodies. (B) Two MET amplified cell lines (SNU-5 and MKN45) were incubated with 100nM crizotinib for 24hrs and the effects on the anti-apoptotic protein XIAP and the pro-apoptotic protein BIM were measured via western blotting. (C) Bar graphs represent quantitative densitometry of the XIAP and BIM protein expression. Data are means \pm SEM from two independent biological replicates. Student t-test, all groups had statistically significant changes in expression between the treated and untreated groups. * $p \leq 0.05$

3.3 Discussion

MET amplification is present in 9-30% (24-26) of gastric cancers and is associated with the proximal non-diffuse subtype and generally confers poor patient outcomes (10, 25, 28). MET has been clinically validated as a therapeutic target in gastric cancer based on recent clinical experience (31, 77, 91-93). We demonstrate that MET-amplified gastric cancer cells exhibit growth arrest and cell death in response to incubation with the MET inhibitor crizotinib whereas MET inhibition had no significant effects in cells without MET amplification, irrespective of whether they had high MET expression or contained MET mutations. We show a clear correlation between crizotinib sensitivity and MET amplification and identified apoptosis as the mechanism by which the cells are responding to MET inhibition. Our results are consistent with previous preclinical observations (42, 43) and expand upon these findings by delving deeper into the molecular determinates of response to MET inhibition in MET-amplified gastric cancer cells. We confirmed that in the MET-amplified cells, expression of BIM (a pro-apoptotic member of the Bcl-2 family) increased and X-linked inhibitor of apoptosis protein (XIAP) (anti-apoptotic member survivin) decreases following exposure to crizotinib.

Nevertheless, it was surprising to us that MET inhibitors had no measurable effects in the gastric cancer cell lines that contained activating MET mutations, Hs746t and MKN74. In particular, one cell line contained a MET mutation in combination with MET amplification and was resistant to crizotinib (Hs746t). One plausible explanation for this observation is that Hs746t has a very slow growth rate with a long doubling rate which could account for

the lack of apoptosis and growth arrest observed because it would take much longer for these processes to occur. The Hs746t cell line is a mix of epithelial cells and fibroblasts that exhibits gross alteration in size, shape, and staining of cells with curious nuclear and nucleolar shapes (94). The published literature about this cell line contains conflicting results as to its sensitivity to MET inhibitors as well as its level of MET protein expression (42, 76, 83, 95).

Hs746t harbors a splice site mutation (Deletion: L982_D1028del) of MET leading to juxtamembrane domain deletion (83). RTKs contain several receptor domains including: 1) extracellular domain (EC), 2) single transmembrane domain (TM) and 3) Intracellular domain (ICD) (96, 97) [Figure 3.9]. Each domain plays an important role for RTKs. Specifically the EC domain contains the ligand binding site and the TM domain allows for and maintains receptor dimerization which is the mechanism by which RTK signal transduction is accomplished (97). The intracellular domain consists of three regions the juxtamembrane domain (JM), kinase domain, and carboxy-terminal region (96). The kinase domain is the site of the ATP-binding pocket which is where crizotinib and other small-molecule inhibitors bind to prevent RTK activation. Because Hs746t harbors a JM mutation this site is not affected and inhibitor binding is not inhibited (98). The juxtamembrane domain works synergistically with the TM and amino acids on the JM serve as binding and phosphorylation site for various signaling molecules (99). JM regulate kinase activity by serving as an auto-inhibitory segment, and as a result mutations, deletions and insertions in the JM lead to cancer development (100). Specifically, JM mutations found on MET have been implicated in inhibiting MET receptor degradation (83, 97). Although, these mutations

have been validated as constitutive activators of MET in other cancer types the exact effects of these mutations have yet to be elucidated in gastric cancer (101). Perhaps MET JM mutations control some aspect of cancer biology that was not measured in the preclinical studies that have been performed to date. Alternatively, it is possible that activating MET mutations act at an early stage in tumor progression and/or become less important in established human gastric cancer cell lines. A deeper understanding of these mutations is important for the selection of patients for targeted therapeutics and further research into this is warranted, albeit outside of the scope of this project. A top priority for ongoing investigation for our study focused on identifying strategies that increase MET inhibitor sensitivity and overcome the development of the acquired resistance that is likely to emerge following prolonged MET inhibition.

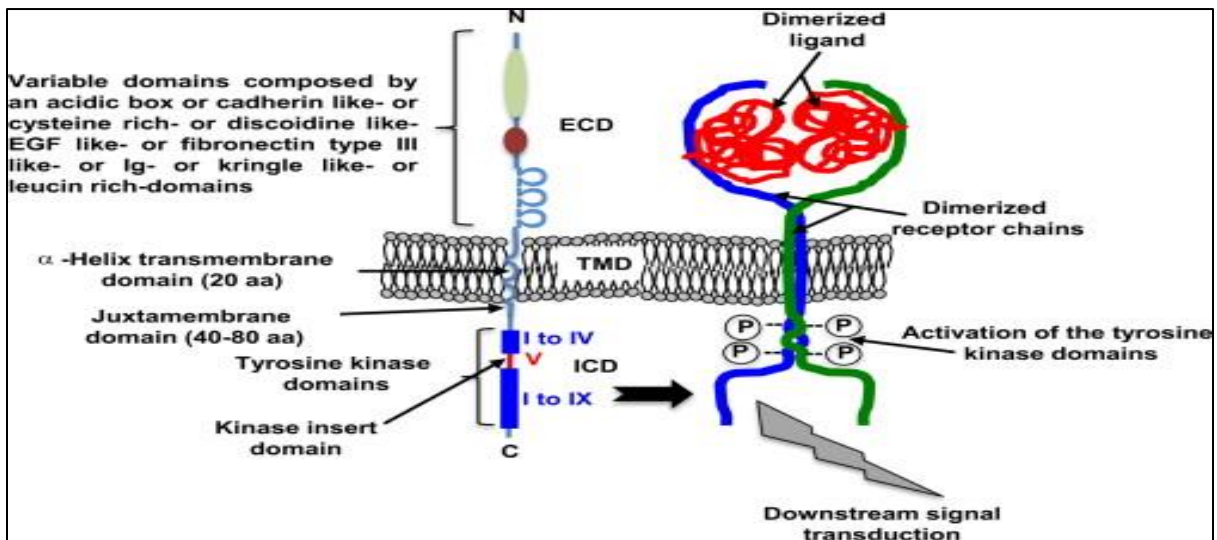


Figure 3.9 Receptor tyrosine kinase molecular domains. Schematic of the various domains that comprise RTKs: 1) extracellular domain (EC), 2) single transmembrane domain (TM) and 3) Intracellular domain (ICD) (96, 97).

*Reprinted with the permission of the Journal of Bone Oncology. Segaliny, A. I., Tellez-Gabriel, M., Heymann, M. F., Heymann, D. Receptor tyrosine kinases: Characterization, mechanism of action and therapeutic interests for bone cancers. Bone Oncology (2015) (96)

Chapter 4.EFFECTS OF CRIZOTINIB ON GLOBAL GENE EXPRESSION IN GASTRIC CANCER CELLS

4.1 Introduction

Aberrant tyrosine kinase (TK) signaling is involved in the oncogenic transformation of malignant cells, thereby promoting tumor development and progression (102). This abnormal signaling results in “oncogenic addiction” within the cells resulting in the ability to impair cell growth and survival by the inactivation of a single oncogene (103). As a result of this “oncogenic addiction,” therapeutics targeting tyrosine kinases and their related molecular partners have been developed and extensively tested both pre-clinically and clinically (16). Numerous TK inhibitors have had great clinical success initially, but overall TK inhibitors have proven to have limited long-term clinical efficacy due to the emergence of adaptive resistance mechanisms (102). These resistance mechanisms are primarily achieved through the emergence of additional mutations, modifications to gene copy number and protein expression, and rewiring of the molecular pathway [Figure 4.1] (104, 105). One famous example of this phenomenon of oncogenic addiction coupled with *de novo* resistance is the use of trastuzumab in the treatment of HER2 positive breast cancer (106). Upon its release Trastuzumab was hailed as the “magic bullet” of cancer therapeutics and is a very effective anti-cancer agent. Unfortunately, trastuzumab also proves to be a cautionary tale as many patients ultimately go on to have progressive disease following their initial response due to the development of acquired resistance (106).

Therefore gaining a deeper understanding of the molecular determinants of response by delving deeper into the gene expression changes is critical to being able to predict synergistic and resistance mechanisms. Here we compared the effects of MET

inhibition on gene expression in MET two amplified gastric cancer cell lines. We hypothesized that overlapping changes in gene expression between the two distinct cell lines would identify candidate molecular pathways and biologic mechanisms associated with resistance to small-molecule MET inhibitors.

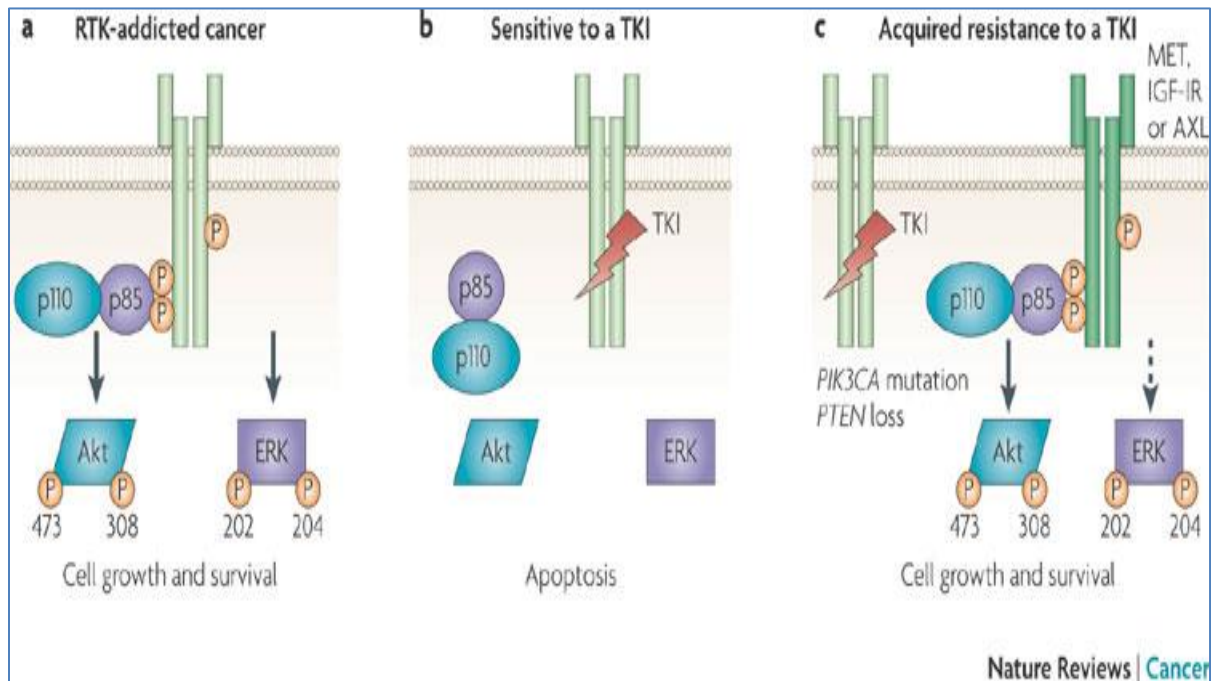


Figure 4.1 Acquired resistance mechanisms to TK inhibitors. Multiple mechanisms of acquired resistance can occur in response to exposure of TK inhibitors within cancer cells. This figure highlights the progression of acquired resistance in the PI3K signaling pathway, but the mechanism applies to other growth-factor receptors. (A) Oncogenic addiction to RTK signaling in cancer cells. (B) TK inhibition induces apoptosis in TK addicted cells. (C) Acquired resistance mechanisms to TK inhibitors.

*Reprinted with the permission of Nature Publishing Group. Targeting PI3K signalling in cancer: opportunities, challenges and limitations. Jeffrey A. Engelman, Nature Reviews Cancer 9, 550-562 (August 2009) (107).

4.2 Results

4.2.1 Effects on gene expression of the MET inhibitor crizotinib on MET amplified human gastric cancer cells.

We sought to define better MET-dependent signaling and mechanisms mediating resistance to MET inhibitors in gastric cancers with amplified MET. To accomplish this, we examined changes in gene expression by performing whole-genome mRNA expression profiling. We incubated the inhibitor-sensitive cell lines (MKN45 and SNU-5) with or without crizotinib for 24 hours and harvested cell pellets and extracted high-quality RNA to use for microarray analysis. We were then able to look modulation of 47,000 probes using the HumanHT-12 v4 Expression BeadChip [Figure 4.2 and 4.3]. In both cell lines, >1400 genes were differentially expressed under the two conditions [Figure 4.2]. We observed substantial overlap between the two cell lines with regard to the genes that were differentially expressed following incubation with crizotinib – 406 downregulated and 246 upregulated genes were shared [Figure 4.2]. We extracted the top 25 upregulated and downregulated transcripts in each cell line and observed that this subset was enriched for numerous genes related to cell death and cell growth/proliferation [Figure 4.3]. Further analyses resulted in the identification of eleven overlapping genes between the two cell lines in this subset. Of these, ten genes have been implicated as being directly linked to cell death and cell growth/proliferation. Specifically, we observed downregulation of MYC, ETV5, TRIP13, DUSP6, CDC45L, and CALB2 and upregulation of PI3KIP1, SEPP1, ABCA1, and HIST1H2AC. The involvement in tumorigenesis and the modulation of cellular mechanisms

pertaining to apoptosis and cell growth proliferation for all of the ten overlapping transcripts will be further elaborated on in the discussion section.

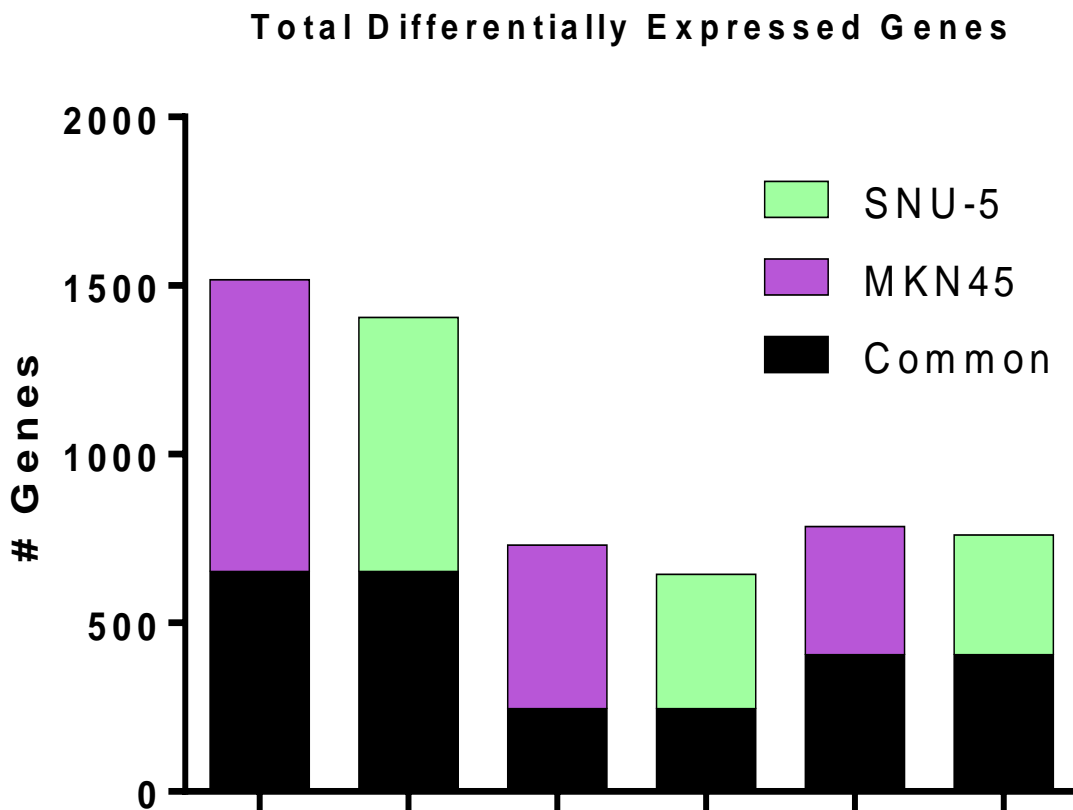


Figure 4.2 MET inhibition results in significant changes in gene expression in MET-amplified gastric cancer cell lines. Graph representing the total number of genes that had a $P < 0.001$ with $FDR < 0.05$ and 2-fold cut-off in the two MET amplified cell lines following incubation with crizotinib for 24 hours (left). The total number of genes up-regulated (middle) and down-regulated (right) following incubation with crizotinib for 24 hours, with the number of common genes between the two cell lines shaded in black.

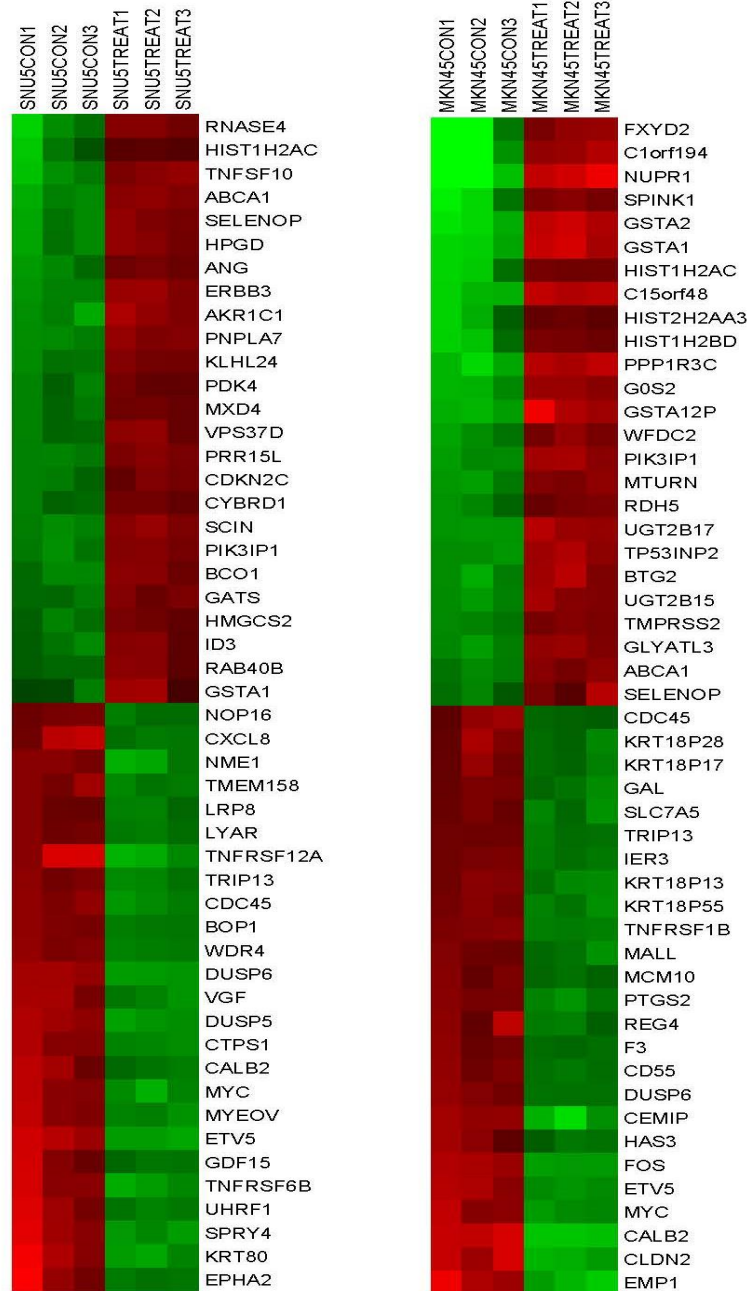


Figure 4.3 Effects on gene expression of the MET inhibitor crizotinib on MET amplified human gastric cancer cells. Heat map of the top 50 differentially expressed genes for each cell line following incubation with crizotinib for 24 hours. Red, higher relative expression; green, lower relative expression.

We then performed numerous control experiments to verify the biologic relevance of the gene expression profiling experiments. Using these experiments we wanted to confirm that top differentially expressed genes related to cell death and cell growth/proliferation identified by gene expression profiling were also differentially expressed when they were measured by RT-PCR or immunoblotting in the same cell lines [Figure 4.4]. We generated RNA from SNU-5 and MKN45 cells exposed to crizotinib for 24 hours and measured the relative expression of MYC, ETV5, MXD4, and PIK3IP1 by quantitative one-step RT-PCR [Figure 4.4.a and 4.4.b]. Next, we generated protein from SNU-5 and MKN45 cells exposed to crizotinib for 24 hours and measured the protein levels of MYC by western blotting [Figure 4.4.c]. From these additional analyses, we were able to validate that the modulation of the genes and protein measured were consistent with the gene expression profiling results.

4.2.2 Ingenuity Pathway Analysis.

To more clearly define the molecular pathways and biologic functions that were altered by drug exposure, we used Ingenuity Pathway Analysis (IPA, Ingenuity Systems; <http://www.ingenuity.com>) to analyze the gene expression profiling data (108). IPA uses a global perspective to interpret the context of biological processes, pathways, and networks. This is an ideal method since genes cooperate via an intricate network of interactions and do not work alone. Using the IPA analysis, we were able to gain a global insight into the changes occurring through use of the core analysis feature which generates outputs for

canonical pathways, upstream regulators, networks, diseases and biologic functions, toxicity functions, and analysis-ready molecules [Figure 4.5].

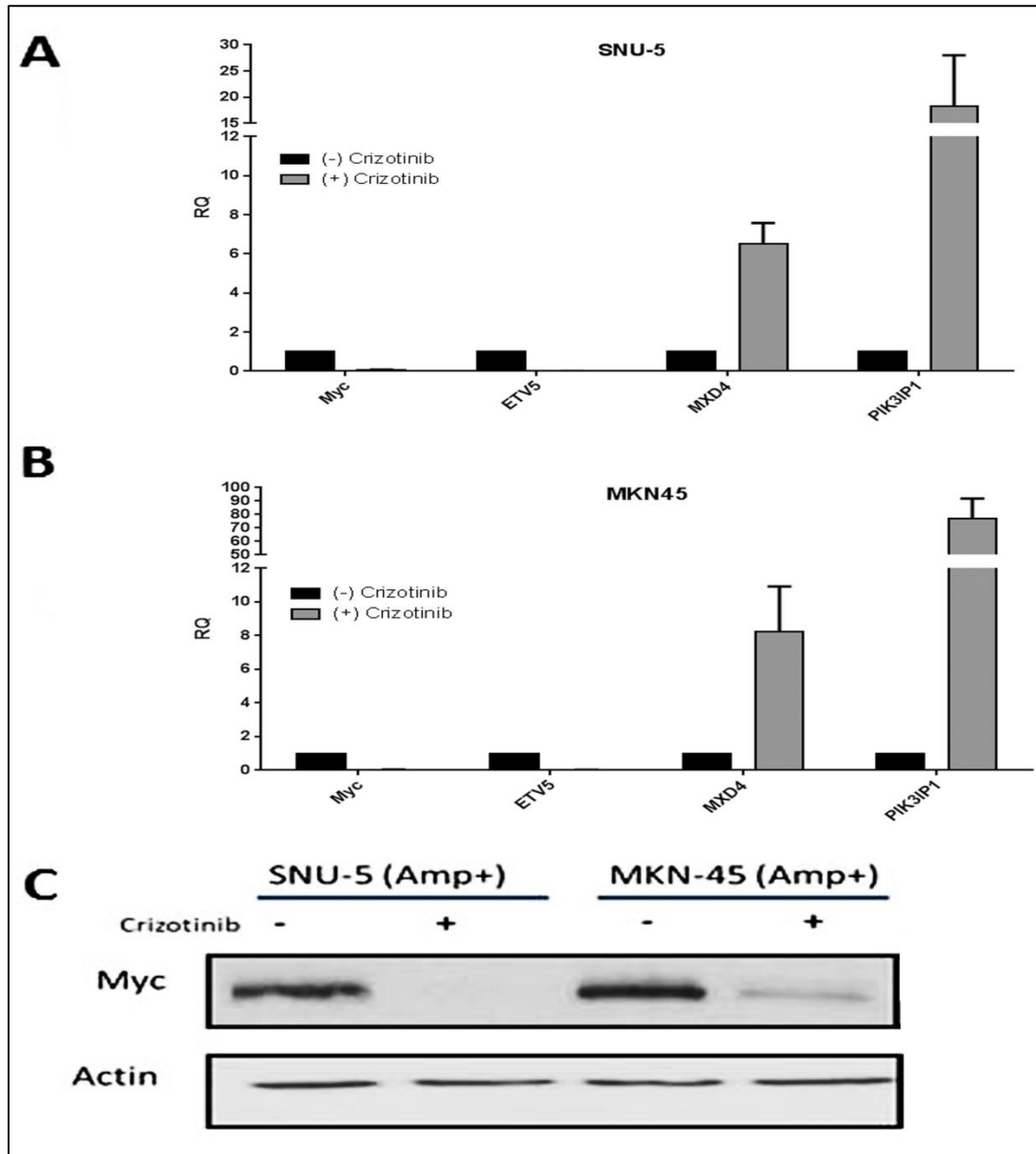


Figure 4.4 Quantitative RT-PCR was used to evaluate the accuracy of the gene expression profiling results. (A) Selection of the top down-regulated and up-regulated genes following treatment with crizotinib in the SNU-5 MET amplified cell line. (B) Selection of the top down-regulated and up-regulated genes following treatment with crizotinib in the MKN45 MET amplified cell line. (C) Immunoblotting analysis was used to confirm significant changes in selected up-regulated and down-regulated genes at the protein level.

SNU-5 IPA Summary of Analysis

Top Canonical Pathways

Name	p-value	Overlap
Estrogen-mediated S-phase Entry	6.38E-10	54.2 % 13/24
Aryl Hydrocarbon Receptor Signaling	9.96E-10	23.0 % 31/135
Cell Cycle Control of Chromosomal Replication	7.15E-08	36.8 % 14/38
GADD45 Signaling	9.26E-08	52.6 % 10/19
Cell Cycle: G1/S Checkpoint Regulation	5.23E-07	27.0 % 17/63

Top Upstream Regulators

Upstream Regulator	p-value of overlap	Predicted Activation
beta-estradiol	3.29E-33	Inhibited
ERBB2	5.17E-31	Inhibited
TP53	1.21E-30	Activated
FOXO3	3.79E-30	Activated
MYC	1.34E-28	Inhibited

MKN45 IPA Summary of Analysis

Top Canonical Pathways

Name	p-value	Overlap
Cell Cycle Control of Chromosomal Replication	2.79E-11	47.4 % 18/38
Estrogen-mediated S-phase Entry	1.97E-09	54.2 % 13/24
GADD45 Signaling	1.40E-08	57.9 % 11/19
Aryl Hydrocarbon Receptor Signaling	1.25E-07	21.5 % 29/135
Cell Cycle: G1/S Checkpoint Regulation	3.67E-07	28.6 % 18/63

Top Upstream Regulators

Upstream Regulator	p-value of overlap	Predicted Activation
ERBB2	5.55E-44	Inhibited
TP53	2.76E-43	Activated
beta-estradiol	5.41E-40	Inhibited
E2F4	9.89E-40	
MYC	2.93E-39	Inhibited

Figure 4.5 IPA core analysis results. Core analysis results for the top canonical pathways and upstream regulators for both SNU-5 and MKN45.

We then queried “molecular and cellular functions” in IPA to get a sense of the core pathway modulation occurring in response to crizotinib exposure in both MET amplified cell lines [Table 4.1]. Molecular and cellular function changes related to cell death, cell cycle, cell growth, and proliferation were among the top alterations observed in both MET-amplified cell lines (SNU-5 and MKN45).

SNU-5		
Molecular and Cellular Functions	P-Value	# Molecules
Cellular Growth and Proliferation	4.48E-06 - 9.67E-23	516
Cell Cycle	9.39E-06 - 2.15E-16	263
Cellular Development	2.41E-07 - 1.16E-14	281
Cell Death and Survival	8.96E-06 - 1.02E-12	470
DNA Replication, Recombination and Repair	4.55E-06 - 1.84E-10	151
MKN45		
Molecular and Cellular Functions	P-Value	# Molecules
Cell Cycle	1.77E-06 - 1.34E-24	320
Cellular Growth and Proliferation	1.24E-06 - 8.08E-22	550
Cellular Development	1.24E-06 - 9.69E-19	341
Cell Death and Survival	1.72E-06 - 1.65E-18	524
Cellular Assembly and Organization	1.31E-06 - 4.94E-16	85

Table 4.1 Overall IPA analysis results. Results of IPA analyses of the top molecular and cellular functions for MKN45 and SNU-5.

A deeper investigation of the “Diseases or Functions Annotation” within the cell cycle and cell death categories uncovered extensive overlap between the two cell lines in regards to the distinct mechanisms that make up the comprehensive categories [Figure 4.6]. Within the cell cycle category, the two cell lines shared significant modulation of seven distinct functions including interphase, S phase, M phase, cell cycle progression of tumor cell lines, entry into interphase, entry into S phase, and interphase of fibroblast cell lines. Within the cell death category, the two cell lines shared significant modulation of seven distinct functions including cell death of tumor cell lines, necrosis, cell death, apoptosis of tumor cell lines, cell survival, cell viability of tumor cell lines, and cell viability. This overlap also extended to the cell growth and proliferation category with the overlap of five distinct functions including cell proliferation of breast cancer cell lines, cell proliferation of tumor cell lines, proliferation of cells, proliferation of connective tissue cells, and proliferation of fibroblast cell lines [Figure 4.7].

IPA also predicts which transcriptional regulators are involved in the upstream cascade that can explain the observed gene expression changes. IPA can then visualize this network of regulators and targets to explain how the regulators interact with one another and their targets to provide a testable hypothesis for gene regulatory networks. We extracted the top inhibited and activated transcriptional regulators for each cell line and observed extensive overlap between the two cell lines [Figure 4.8 and 4.9]. The activated population was highly enriched with transcription factors involved in cell cycle/proliferation arrest and apoptosis activation, whereas the inhibited population was enriched for transcription factors involved in cell cycle progression and cellular proliferation.

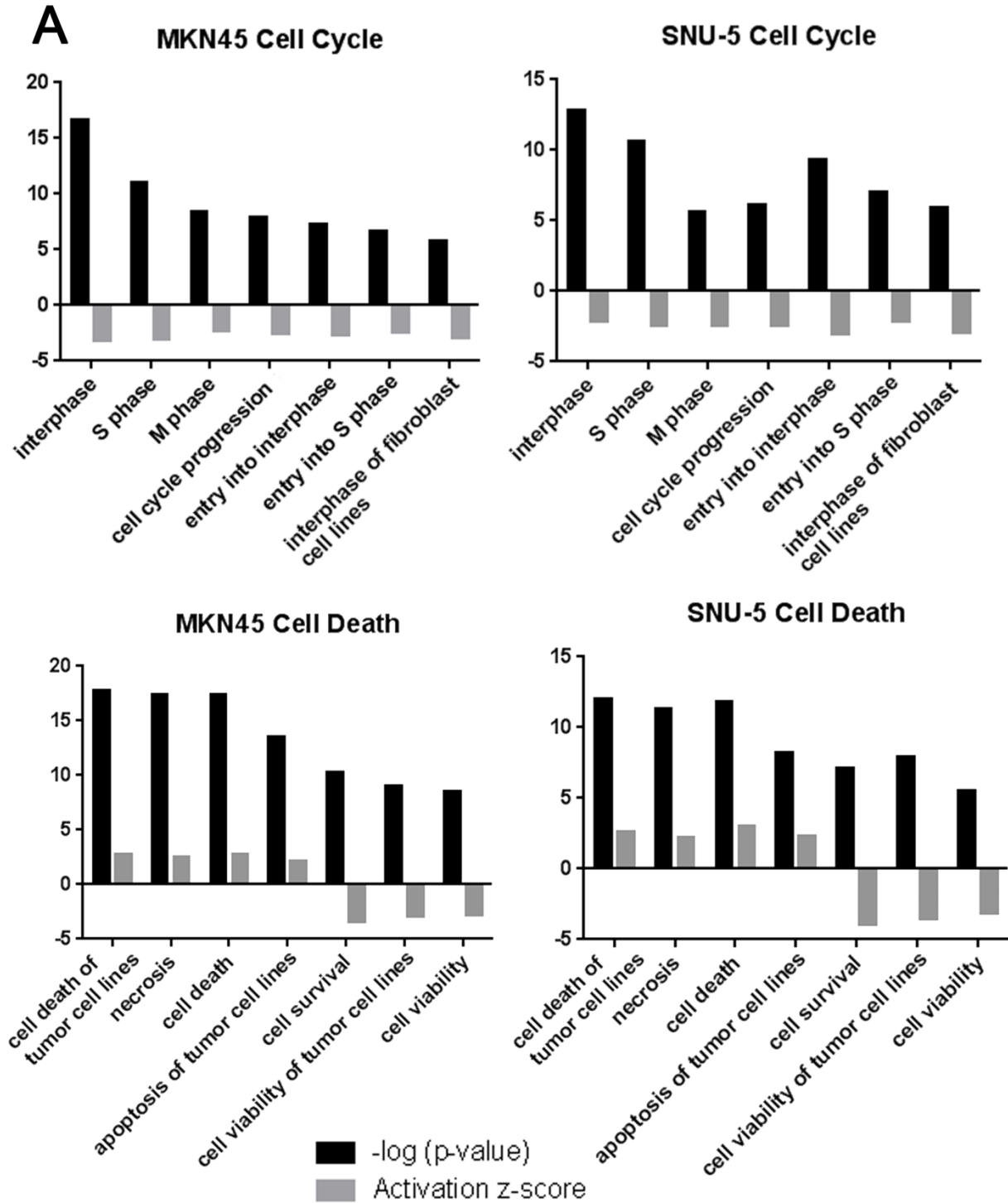


Figure 4.6 Pathway analyses of crizotinib-induced changes in gene expression. Significant changes in gene expression were analyzed using Ingenuity Pathway Analysis (IPA) using the molecular and cellular functions of the platform. And the cell lines showed significant overlap in the identified functions for cell death and cell cycle.

Cell Growth and Proliferation

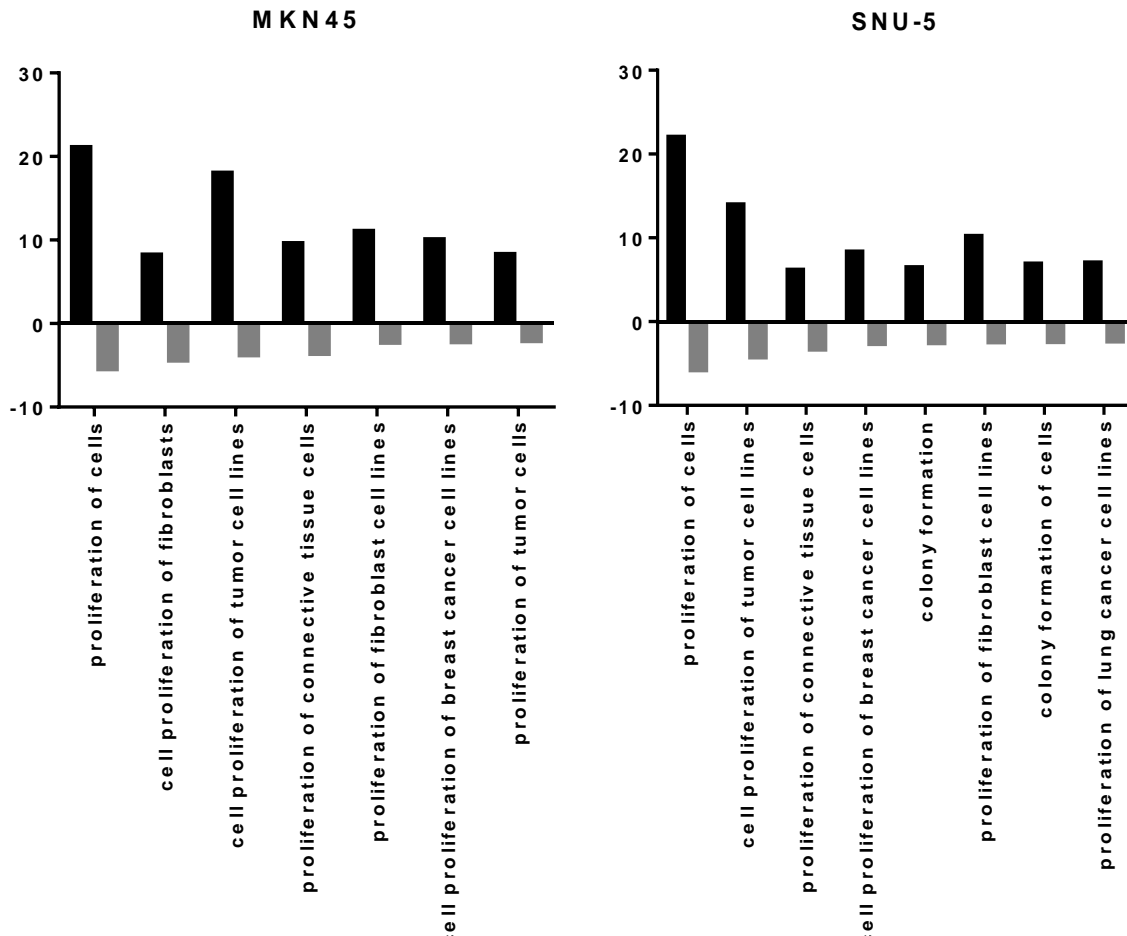


Figure 4.7 Additional IPA analysis results. Effects of crizotinib on the IPA “cell growth and proliferation” canonical pathway.

Transcription Regulators [Activated]

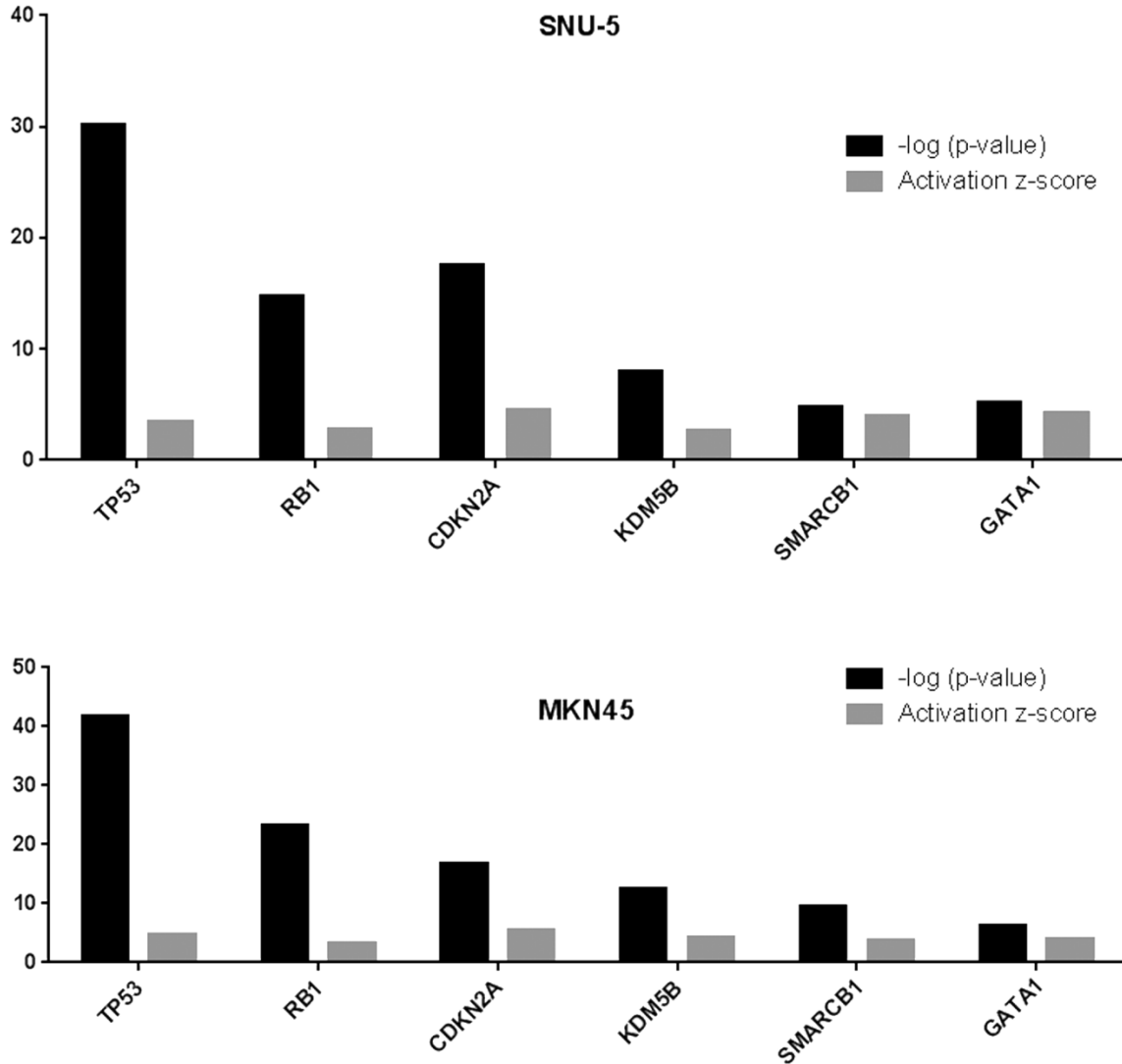


Figure 4.8 Transcriptional analyses of crizotinib-induced changes in gene expression. Activation z-score and p-value (-log transformed) for significantly activated transcriptional regulators from whole genome mRNA expression profiling using IPA.

Transcription Regulators [Inhibited]

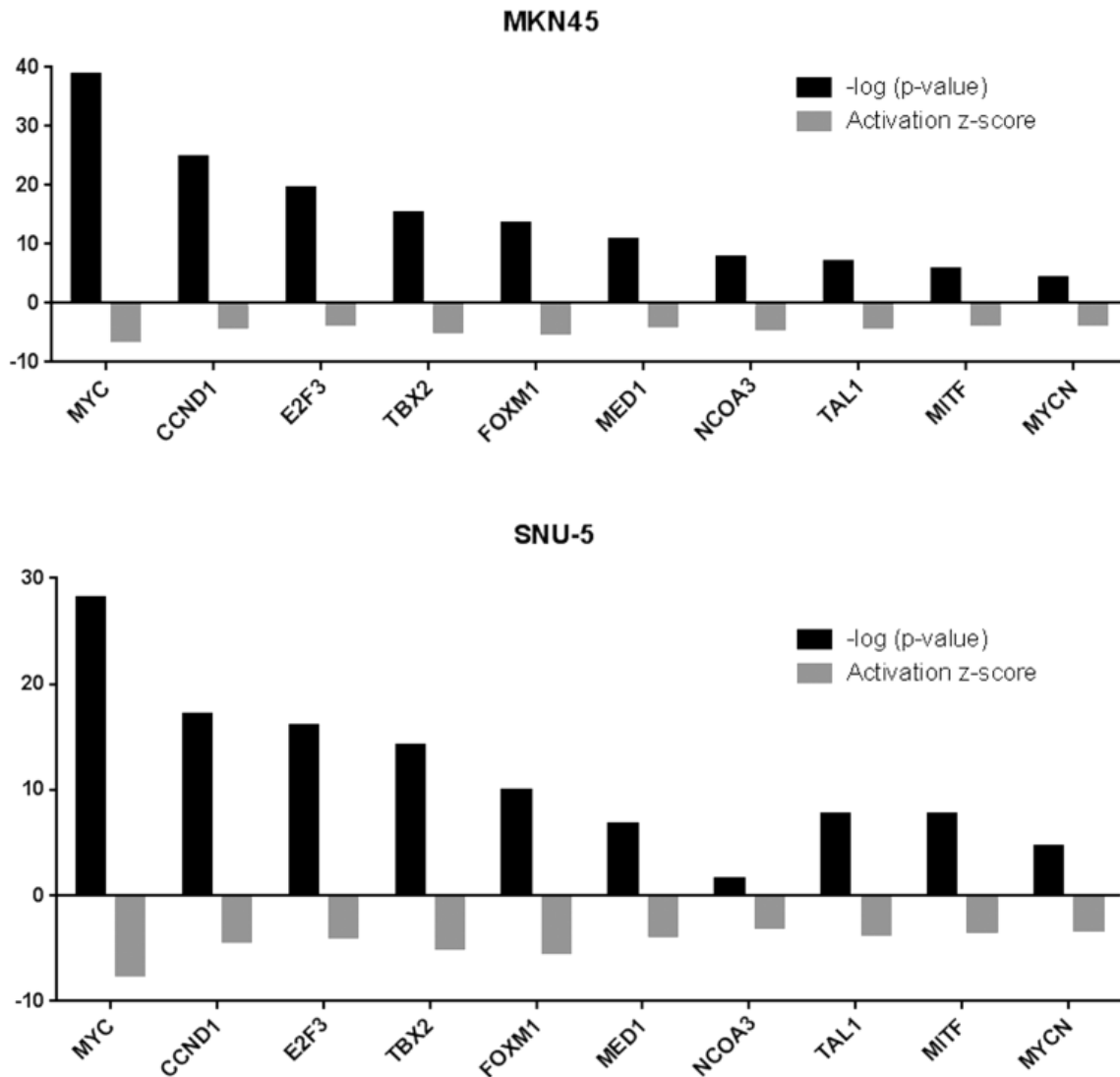


Figure 4.9 Transcriptional analyses of crizotinib-induced changes in gene expression. Activation z-score and p-value ($-\log$ transformed) for significantly inhibited transcriptional regulators from whole genome mRNA expression profiling using IPA.

4.2.3 Gene set enrichment analyses.

We further expanded on our analysis of the gene expression profiling experiments by performing gene set enrichment analysis (GSEA) which is a complementary analysis to the previous pathway analyses performed using IPA. We began the gene set enrichment analysis by using previously identified gene sets available from the molecular signature database within GSEA (MSigDB; www.broadinstitute.org/gsea/) (109). Initially, we queried our data using the H: hallmark resource which contains 50 gene sets and is designed to be a starting point for exploration within the molecular signature database. The gene sets within this collection condense and characterize specific biological processes including P53 pathway, MYC targets and KRAS signaling just to name a few. We observed that in the SNU-5 and MKN45 cells 36 and 30 gene sets were significantly enriched, respectively [Table 4.2 and 4.3]. Of these significantly enriched gene sets, 22 were shared between the two cell lines. P53 signaling was positively enriched, and MYC signaling was negatively enriched in the treated group following crizotinib exposure [Figure 4.10], which is consistent with the IPA results and with the idea that MET inhibition causes decreased cell proliferation/growth and apoptosis induction. We also discovered that in addition to the previously mentioned processes, MTORC1 signaling was downregulated by crizotinib in both cell lines [Figure 4.11]. MTORC1's ability to suppress autophagy is well established, and inhibition of MTORC1 induces autophagy (110, 111). This was of great interest because autophagy is well documented as having both tumor suppressive and promoting properties, making it an ideal target for our study looking at both synergistic and resistance mechanisms to MET inhibition in gastric cancer(50).

	GENE SET NAME	# GENES	NES	NOM p-val	FDR q-val
SNU-5	HALLMARK_BILE_ACID_METABOLISM	112	1.986628	0	0
	HALLMARK_PROTEIN_SECRETION	96	1.856694	0	3.14E-04
	HALLMARK_HEME_METABOLISM	195	1.759858	0	0.001867
	HALLMARK_FATTY_ACID_METABOLISM	156	1.778577	0	0.002002
	HALLMARK_ADIPOGENESIS	197	1.725787	0	0.002696
	HALLMARK_XENOBIOTIC_METABOLISM	199	1.684998	0	0.003608
	HALLMARK_INTERFERON_ALPHA_RESPONSE	96	1.660124	0	0.003756
	HALLMARK_KRAS_SIGNALING_DN	198	1.5909	0	0.007554
	HALLMARK_P53_PATHWAY	196	1.566838	0	0.008672
	HALLMARK_MYOGENESIS	199	1.551734	0	0.009115
	HALLMARK_COAGULATION	138	1.52902	0.00339	0.010355
	HALLMARK_INTERFERON_GAMMA_RESPONSE	198	1.446082	0.005068	0.02209
	HALLMARK_PEROXISOME	102	1.470179	0.01005	0.018397
	HALLMARK_ESTROGEN_RESPONSE_LATE	200	1.272327	0.0384	0.099368
HALLMARK_APOPTOSIS	161	1.230343	0.049474	0.132614	
MKN45	GENE SET NAME	# GENES	NES	NOM p-val	FDR q-val
	HALLMARK_BILE_ACID_METABOLISM	112	1.627883	0.001439	0.02106
	HALLMARK_P53_PATHWAY	196	1.653042	0	0.031423
	HALLMARK_PANCREAS_BETA_CELLS	40	1.536858	0.023438	0.036237
	HALLMARK_KRAS_SIGNALING_DN	198	1.487999	0	0.048577
	HALLMARK_APICAL_JUNCTION	199	1.450285	0.002732	0.060757
	HALLMARK_MYOGENESIS	199	1.431041	0.003979	0.06274
	HALLMARK_HEME_METABOLISM	195	1.38405	0.009383	0.088198
HALLMARK_INTERFERON_ALPHA_RESPONSE	96	1.348254	0.047267	0.108533	

Table 4.2 GSEA molecular signature database hallmarks gene sets. Gene sets upregulated in the crizotinib treatment phenotype with p-values <.05 and NES of <.25 as per the suggested cut-offs from GSEA. The gene sets in blue are shared between the two cell lines.

	GENE SET NAME	SIZE	NES	NOM p-val	FDR q-val
SNU-5	HALLMARK_E2F_TARGETS	189	-3.03282	0	0
	HALLMARK_MYC_TARGETS_V1	193	-2.93968	0	0
	HALLMARK_G2M_CHECKPOINT	190	-2.8404	0	0
	HALLMARK_MYC_TARGETS_V2	57	-2.76023	0	0
	HALLMARK_UNFOLDED_PROTEIN_RESPONSE	113	-2.23322	0	0
	HALLMARK_MTORC1_SIGNALING	196	-2.09654	0	0
	HALLMARK_MITOTIC_SPINDLE	196	-1.89872	0	0
	HALLMARK_TNFA_SIGNALING_VIA_NFKB	199	-1.83644	0	0
	HALLMARK_UV_RESPONSE_UP	158	-1.56692	0	0.012095
	HALLMARK_DNA_REPAIR	148	-1.47698	0	0.02139
	HALLMARK_IL6_JAK_STAT3_SIGNALING	87	-1.5602	0.00232558	0.011774
	HALLMARK_GLYCOLYSIS	198	-1.45701	0.00472813	0.023496
	HALLMARK_INFLAMMATORY_RESPONSE	200	-1.4008	0.00491401	0.03165
	HALLMARK_EPITHELIAL_MESENCHYMAL_TRANSITION	200	-1.41353	0.00497512	0.030683
	HALLMARK_SPERMATOGENESIS	130	-1.41771	0.01173709	0.03122
	HALLMARK_ALLOGRAFT_REJECTION	200	-1.33962	0.01173709	0.054259
	HALLMARK_KRAS_SIGNALING_UP	200	-1.31931	0.02020202	0.061895
	HALLMARK_WNT_BETA_CATENIN_SIGNALING	42	-1.55194	0.02340426	0.01143
	HALLMARK_HEDGEHOG_SIGNALING	36	-1.48897	0.03393665	0.020886
	HALLMARK_IL2_STATS5_SIGNALING	193	-1.29652	0.03496504	0.071825
HALLMARK_HYPOXIA	197	-1.2337	0.04580153	0.114126	
	GENE SET NAME	SIZE	NES	NOM p-val	FDR q-val
MKN45	HALLMARK_E2F_TARGETS	189	-3.03686	0	0
	HALLMARK_MYC_TARGETS_V1	193	-2.91449	0	0
	HALLMARK_G2M_CHECKPOINT	190	-2.8715	0	0
	HALLMARK_MYC_TARGETS_V2	57	-2.64413	0	0
	HALLMARK_MTORC1_SIGNALING	196	-2.34046	0	0
	HALLMARK_UNFOLDED_PROTEIN_RESPONSE	113	-2.22047	0	0
	HALLMARK_OXIDATIVE_PHOSPHORYLATION	196	-1.94574	0	2.14E-04
	HALLMARK_MITOTIC_SPINDLE	196	-1.82597	0	0.001186
	HALLMARK_GLYCOLYSIS	198	-1.81079	0	0.001054
	HALLMARK_UV_RESPONSE_UP	158	-1.69578	0	0.002224
	HALLMARK_INFLAMMATORY_RESPONSE	200	-1.69074	0	0.00233
	HALLMARK_ESTROGEN_RESPONSE_LATE	200	-1.68031	0	0.002715
	HALLMARK_IL2_STATS5_SIGNALING	193	-1.53183	0	0.013003
	HALLMARK_SPERMATOGENESIS	130	-1.52127	0.00346021	0.013476
	HALLMARK_EPITHELIAL_MESENCHYMAL_TRANSITION	200	-1.42877	0.00362319	0.026598
	HALLMARK_ESTROGEN_RESPONSE_EARLY	194	-1.35522	0.00364964	0.043127
	HALLMARK_DNA_REPAIR	148	-1.38107	0.00716846	0.039951
	HALLMARK_TNFA_SIGNALING_VIA_NFKB	199	-1.37308	0.01260504	0.041666
	HALLMARK_COMPLEMENT	199	-1.26369	0.01960784	0.079206
	HALLMARK_ANDROGEN_RESPONSE	101	-1.36401	0.02380952	0.043446
HALLMARK_KRAS_SIGNALING_UP	200	-1.31319	0.0239726	0.056981	
HALLMARK_CHOLESTEROL_HOMEOSTASIS	74	-1.43686	0.02760736	0.027138	

Table 4.3 GSEA molecular signature database hallmarks gene sets. Gene sets negatively enriched in the crizotinib treatment phenotype with p-values <.05 and NES of <.25 as per the suggested cut-offs from GSEA. The gene sets in blue are shared between the two cell lines.

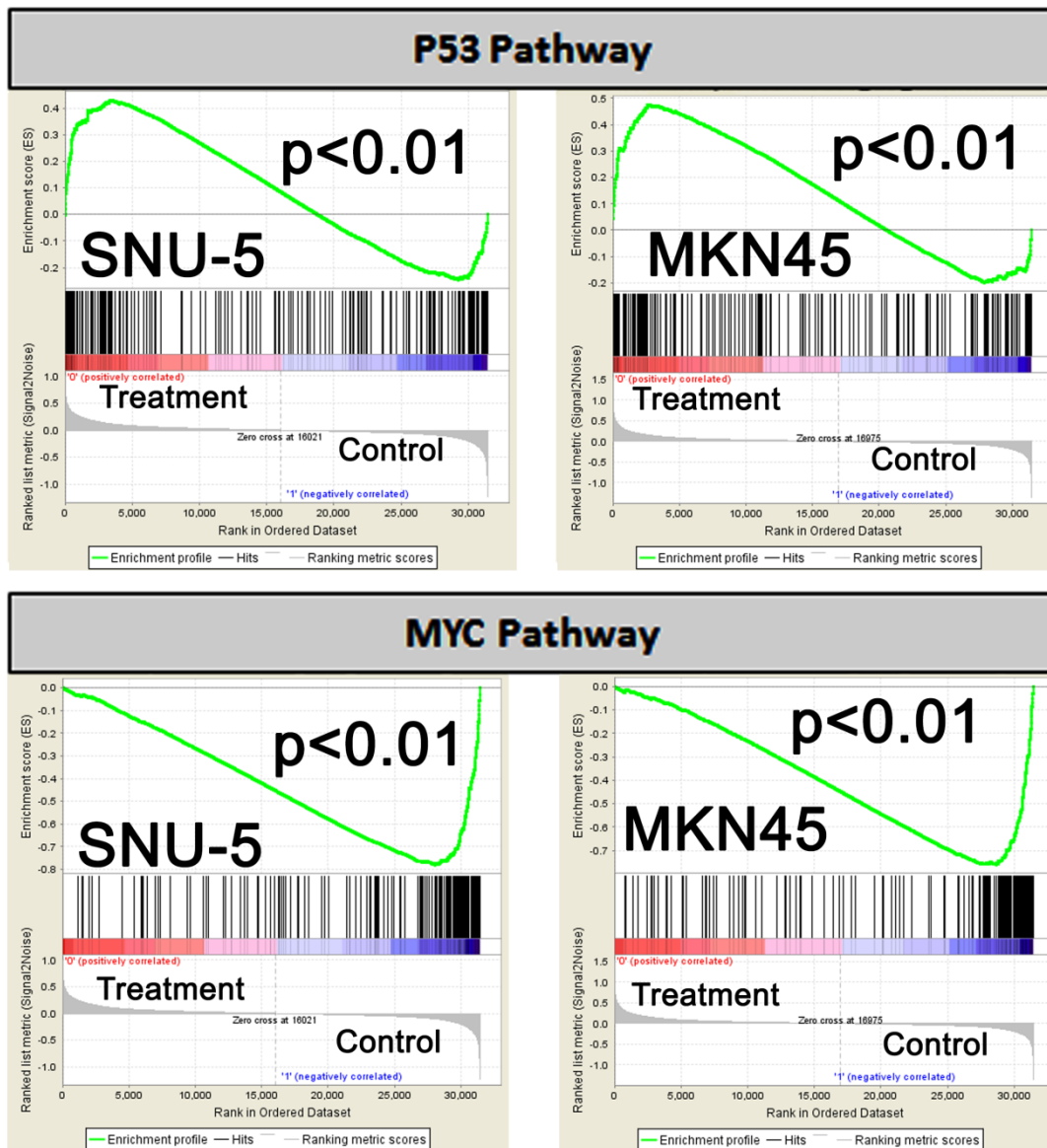


Figure 4.10. GSEA analyses of crizotinib-induced changes in gene expression. Selection of the top common results within GSEA H: hallmark gene sets from the molecular gene sets database are displayed for each of the cell lines. All results have a $P < .01$ and $FDR < .05$.

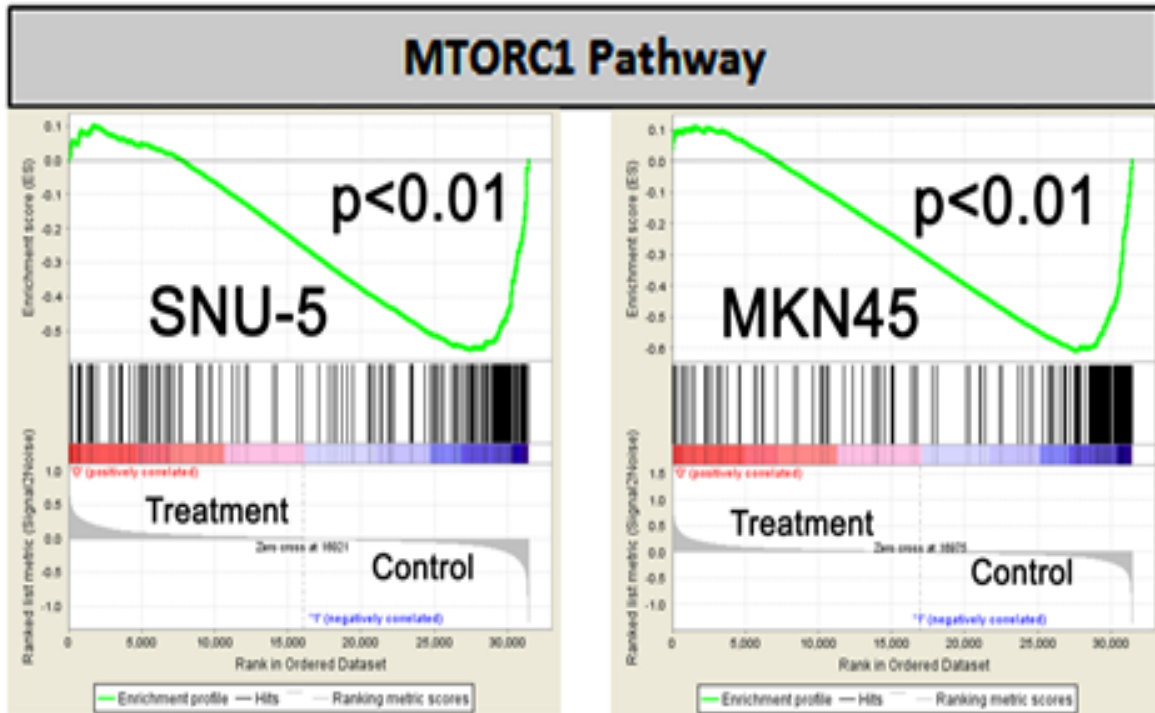


Figure 4.11. GSEA analyses of crizotinib-induced changes in gene expression. MTORC1 is among the top results for both cell lines when using the GSEA curated H: hallmark gene sets from the molecular gene sets database with $P < .01$ and $FDR < .05$.

4.2.4 MET inhibition stimulates an autophagy gene expression signature.

The discovery that MTORC1 was among the top negatively enriched hallmarks gene sets in both cell lines prompted us to query the Gene Ontology Consortium (GO): Biologic Processes (BP) resource. The GO: BP resource contains 4653 gene sets identified by the Gene Ontology Consortium (GO) as enriched in various biologic processes. GO uses ontologies to support biologically meaningful annotation of genes and their products as determined by the association between specific references, GO terms, and gene products (<http://geneontology.org/page/guide-go-evidence-codes>) (112, 113).

These analysis identified autophagy as among the top thirty biologic processes enriched in both of the two MET-amplified cell lines [Table 4.4]. We looked at all of the upregulated gene sets included in the GO: BP resource and identified that of the eight autophagy-related gene sets MKN45 and SNU-5 each had at least four that were enriched with a p-value <.05 [Table 4.5]. Further investigation of the enrichment plots for the top overlapping autophagy gene set between the two cell lines showed great similarities [Figure4.12] and, we observed concordance in the modulation of the top autophagy-related gene set in both cell lines [Figure 4.13]. This data adds to the GSEA Hallmarks results implicating autophagy as a top biologic mechanism that is modulated by MET inhibition in MET-amplified gastric cancers and served as a benchmark for the next phase of this project.

	NAME	SIZE	NES	NOM p-val	FDR q-val
SNU-5	GO_LIPID_CATABOLIC_PROCESS	239	2.152469	0	0
	GO_Glutathione_derivative_metabolic_process	22	2.064683	0	4.92E-04
	GO_FATTY_ACID_METABOLIC_PROCESS	286	2.07081	0	6.56E-04
	GO_Glutathione_derivative_biosynthetic_process	22	2.081848	0	9.84E-04
	GO_CELLULAR_LIPID_CATABOLIC_PROCESS	147	2.028686	0	0.001779
	GO_ETHANOLAMINE_CONTAINING_COMPOUND_METABOLIC_PROCESS	84	2.034813	0	0.001943
	GO_PRIMARY_ALCOHOL_METABOLIC_PROCESS	47	2.009606	0	0.002068
	GO_ENDOSOME_TO_LYSOSOME_TRANSPORT	40	1.989965	0	0.00325
	GO_RETINOL_METABOLIC_PROCESS	29	1.977568	0.0018018	0.003849
	GO_UNSATURATED_FATTY_ACID_METABOLIC_PROCESS	105	1.979623	0	0.003851
	GO_MONOCARBOXYLIC_ACID_CATABOLIC_PROCESS	92	1.967976	0	0.004441
	GO_CARBOXYLIC_ACID_CATABOLIC_PROCESS	199	1.96395	0	0.004742
	GO_POST_GOLGI_VESICLE_MEDIATED_TRANSPORT	82	1.969099	0	0.004809
	GO_ICOSANOID_METABOLIC_PROCESS	93	1.968001	0	0.004811
	GO_RESPONSE_TO_XENOBIOTIC_STIMULUS	105	1.958727	0	0.004813
	GO_FATTY_ACID_DERIVATIVE_METABOLIC_PROCESS	93	1.943206	0	0.005458
	GO_ORGANIC_ACID_CATABOLIC_PROCESS	199	1.946657	0	0.005657
	GO_LONG_CHAIN_FATTY_ACID_METABOLIC_PROCESS	87	1.943881	0	0.005665
	GO_ARACHIDONIC_ACID_METABOLIC_PROCESS	49	1.926438	0	0.007601
	GO_VACUOLE_ORGANIZATION	158	1.922182	0	0.008038
	GO_PHOSPHATIDYLCHOLINE_METABOLIC_PROCESS	63	1.917608	0	0.008205
	GO_CHOLESTEROL_EFFLUX	26	1.90631	0	0.010277
	GO_ALDITOL_PHOSPHATE_METABOLIC_PROCESS	35	1.902618	0	0.010669
	GO_PHOSPHATIDYLETHANOLAMINE_ACYL_CHAIN_REMODELING	22	1.896524	0	0.011586
	GO_PHOTORECEPTOR_CELL_MAINTENANCE	33	1.886789	0.0018282	0.013055
GO_POSITIVE_REGULATION_OF_AUTOPHAGY	74	1.88253	0	0.013233	
GO_GOLGI_TO_PLASMA_MEMBRANE_TRANSPORT	41	1.87981	0.0018349	0.013344	
GO_MEMBRANE_INVAGINATION	28	1.882854	0	0.013594	
GO_CILIIUM_MORPHOGENESIS	188	1.875818	0	0.013979	
MKN45	NAME	SIZE	NES	NOM p-val	FDR q-val
	GO_INNATE_IMMUNE_RESPONSE_IN_MUCOSA	21	2.064134	0	0.002695
	GO_Glutathione_derivative_biosynthetic_process	22	1.952886	0	0.020348
	GO_Glutathione_derivative_metabolic_process	22	1.956883	0	0.026568
	GO_PHOTORECEPTOR_CELL_MAINTENANCE	33	1.923241	0	0.030552
	GO_Glutathione_metabolic_process	59	1.905583	0	0.036876
	GO_ANTIMICROBIAL_HUMORAL_RESPONSE	45	1.856053	0.0016026	0.05441
	GO_RESPONSE_TO_XENOBIOTIC_STIMULUS	105	1.859418	0	0.057542
	GO_CILIIUM_MOVEMENT	33	1.866313	0	0.05789
	GO_CHROMATIN_SILENCING	92	1.845917	0	0.058887
	GO_CELLULAR_RESPONSE_TO_ZINC_ION	16	1.87169	0.0034722	0.062079
	GO_AXONEME_ASSEMBLY	40	1.837052	0	0.064109
	GO_EPOXYGENASE_P450_PATHWAY	18	1.815891	0.0017452	0.065947
	GO_EPITHELIAL_CILIIUM_MOVEMENT	16	1.818705	0	0.067234
	GO_DEFENSE_RESPONSE_TO_GRAM_POSITIVE_BACTERIUM	68	1.820362	0	0.0709
	GO_AUTOPHAGOSOME_ORGANIZATION	39	1.796441	0.0048	0.071785
	GO_REGULATION_OF_ACROSOME_REACTION	15	1.797629	0	0.074436
	GO_VACUOLE_ORGANIZATION	158	1.821857	0	0.074893
	GO_VACUOLE_FUSION	22	1.797934	0.0034014	0.078451
	GO_CILIIUM_MORPHOGENESIS	188	1.79916	0	0.081689
	GO_FLAVONOID_METABOLIC_PROCESS	28	1.779221	0.0017036	0.085202
	GO_POSITIVE_REGULATION_OF_TRANSCRIPTION_FROM_RNA_POLYMERASE	27	1.77964	0	0.088974
	GO_ORGAN_OR_TISSUE_SPECIFIC_IMMUNE_RESPONSE	31	1.773162	0	0.089679
	GO_PROTEIN_LOCALIZATION_TO_CILIIUM	25	1.751528	0.0035524	0.104682
	GO_CELLULAR_GLUCURONIDATION	22	1.75883	0	0.105871
GO_GLUCURONATE_METABOLIC_PROCESS	27	1.755923	0	0.105969	
GO_CELLULAR_RESPONSE_TO_CADMIUM_ION	15	1.751699	0.0034722	0.108408	
GO_DORSAL_VENTRAL_NEURAL_TUBE_PATTERNING	17	1.7451	0	0.110837	
GO_POSITIVE_REGULATION_OF_ADHERENS_JUNCTION_ORGANIZATION	21	1.738033	0.0017007	0.113464	
GO_URONIC_ACID_METABOLIC_PROCESS	27	1.73937	0.0050251	0.115453	

Table 4.4 GSEA molecular signature database GO:BP gene sets. Gene sets upregulated in the crizotinib treatment phenotype with p-values <.05 and NES of <.25 as per the suggested cut-offs from GSEA. The gene sets in blue are shared between the two cell lines.

	NAME	SIZE	NES	NOM p-val
SNU-5	GO_POSITIVE_REGULATION_OF_AUTOPHAGY	74	1.88253	0
	GO_AUTOPHAGOSOME_ORGANIZATION	39	1.75685	0.001760563
	GO_REGULATION_OF_AUTOPHAGY	240	1.619914	0
	GO_AUTOPHAGY	375	1.495902	0
	GO_MACROAUTOPHAGY	264	1.432912	0
	NAME	SIZE	NES	NOM p-val
MKN45	GO_AUTOPHAGOSOME_ORGANIZATION	39	1.796441	0.0048
	GO_REGULATION_OF_AUTOPHAGY	240	1.576546	0
	GO_MACROAUTOPHAGY	264	1.498016	0.002564103
	GO_REGULATION_OF_AUTOPHAGOSOME_ASSEMBLY	34	1.496375	0.03322785

Table 4.5 Autophagy gene sets enriched in the GO:BP gene sets. Autophagy gene sets upregulated in the crizotinib treatment phenotype with p-values <.05. The gene sets in blue are shared between the two cell lines.

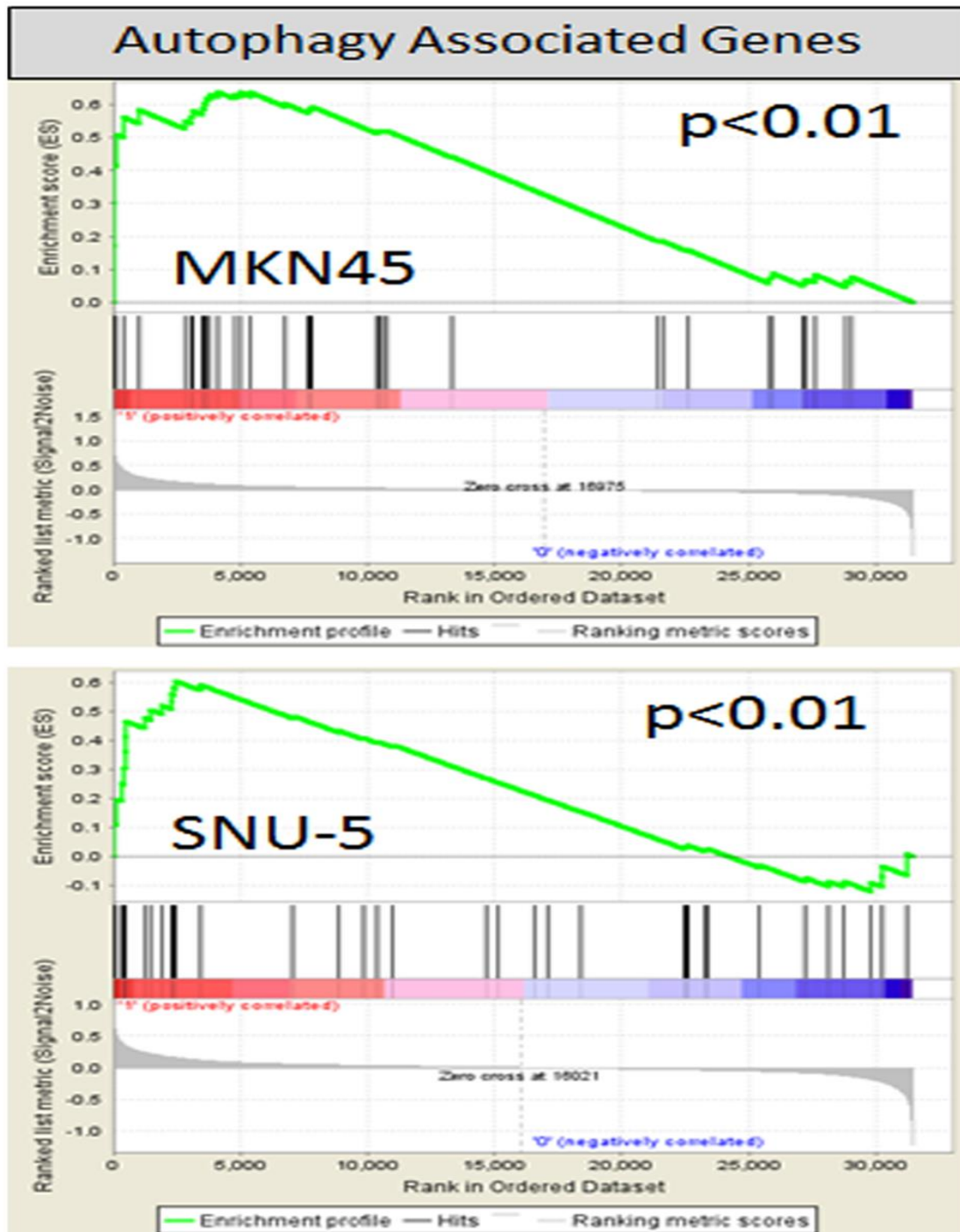


Figure 4.12. MET inhibition stimulates an autophagy gene expression signature. Gene set enrichment analysis (GSEA) was used to determine whether a gene expression signature associated with autophagy (BP: GO biological process gene set) was stimulated by crizotinib in the SNU-5 ($P < .01$, FDR = .04) and MKN45 ($P < .01$, FDR = .07) cells.

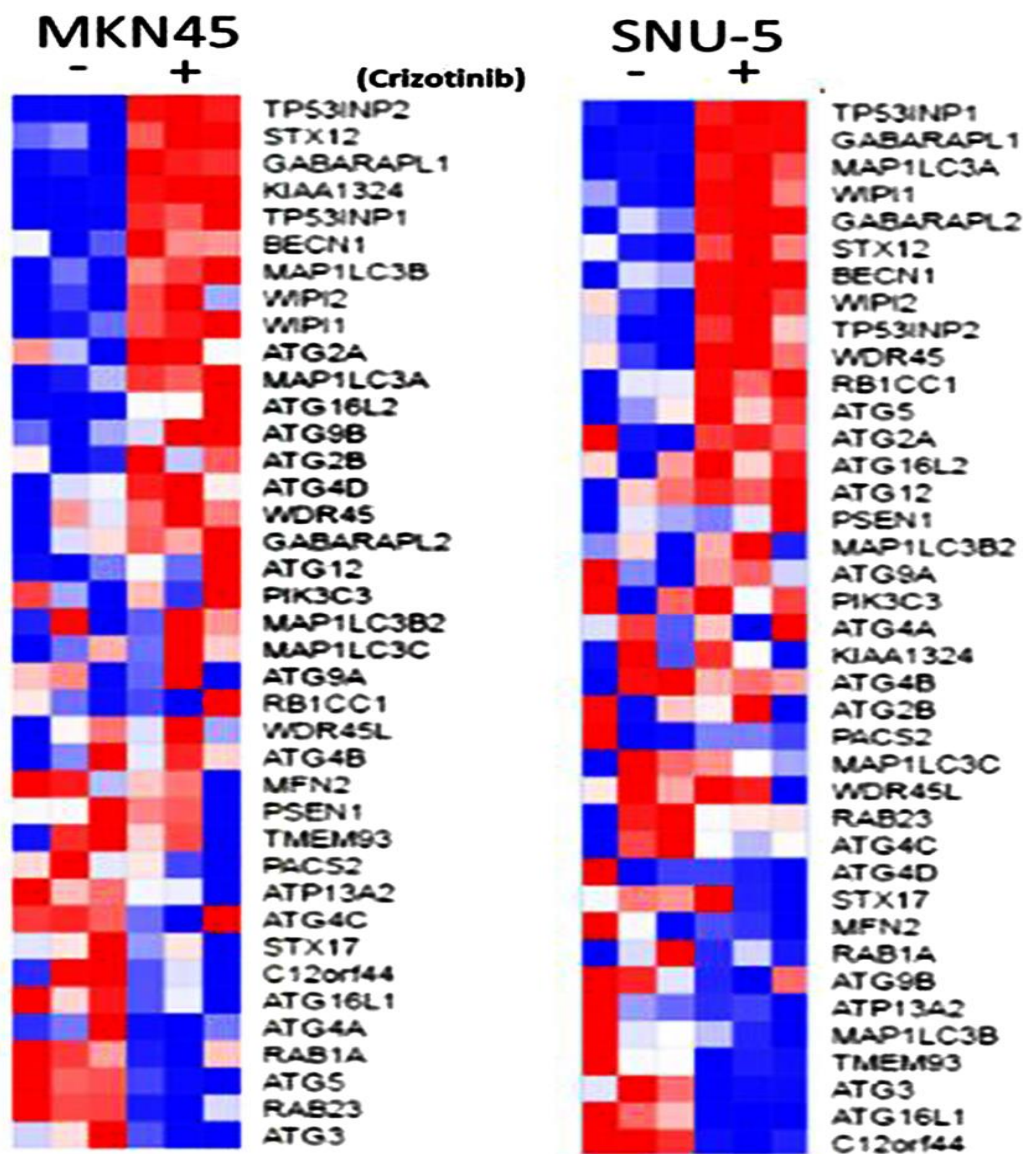


Figure 4.13. MET inhibition stimulates an autophagy gene expression signature. Expression of the top differentially expressed autophagy-associated genes included in the GSEA data set (GO autophagosome organization) used in Figure 4.11. The heat maps depict relative expression of autophagy markers in two MET amplified cell lines following incubation with crizotinib for 24 hours. Red, higher relative expression; blue, lower relative expression.

4.3 Discussion

We observed that several of the 50 modulated genes shared between the two cell lines were related to cellular proliferation, growth, and apoptosis. Of the eleven genes shared between the two cell lines, ten have been directly implicated as involved in the previously mentioned cellular processes and their deregulation is associated with tumorigenesis. These included downregulation of MYC, ETV5, TRIP13, DUSP6, CDC45L, and CALB2 and upregulation of PI3KIP1, SEPP1, ABCA1, HIST1H2AC following exposure to crizotinib. For the most part, this is consistent with the direction of modulation we would expect if crizotinib is indeed shutting down proliferation and inducing apoptosis in these cells, with the exception being DUSP6 modulation. Dual specificity phosphatase 6 (DUSP6) is a member of the family of MAPK phosphatases and modulates BCL-2 family members (Bcl-2, Bcl-xL, and Bad) expression levels to regulate p53-induced apoptosis (103). DUSP6 also inhibits MAPK signal transduction, and previous studies have shown that DUSP6 siRNA knockdown results in increased ERK signaling and cellular proliferation (114, 115). Since DUSP6 has multiple tumor suppressive mechanisms it was surprising that DUSP6 expression decreased following exposure to crizotinib. By delving deeper into this phenomenon, we found that other groups have shown that there is significant interaction between crizotinib, DUSP6, and ERK which may account for this unexpected finding (116).

The remaining genes exhibit the expected direction of modulation, and we have briefly highlighted the molecular mechanisms involved in cell growth/proliferation and apoptosis for each. The transcription factor ETV5 (Ets-transcript variant 5) is involved in

multiple tumorigenic mechanisms in the cell including promoting invasion through increased epithelial to mesenchymal transition (EMT) and matrix metalloproteinase 2 (MMP-2) expression, as well as promoting proliferation through increased downstream signaling of the RAS/MAPK pathway (117, 118). MYC is a well-characterized signal transducer that promotes cellular growth and proliferation, and MYC deregulation has been linked to the tumorigenesis (119, 120). Thyroid hormone receptor interactor 13 (TRIP13) is an ATPase associated with spindle assembly checkpoint inactivation leading to aberrant cell transformation due to chromosomal abnormalities (121). Inhibition of TRIP13 is associated with decreased cell proliferation, migration, and invasion (122). Cell division cycle protein 45 (CDC45L) is replication factor that is required for the initiation of DNA replication (123-125). CDC45L is found at much higher levels in cancer cells compared to normal human cells and overexpression has a positive correlation to proliferation (124). CALB2 (Calretinin) is a calcium binding protein that is involved in cell cycle progression (126). Cells with depleted CALB2 have decreased proliferation due to G1 cell cycle arrest (127). PI3KIP1 (phosphoinositide-3-kinase interacting protein 1) is a well characterized negative regulator of PI3K's that are vital for cell survival and proliferation (128, 129). Upregulation of PI3KIP1 is associated with apoptosis and tumor suppression (128). Selenoprotein P (SEPP1) is a glycoprotein that transports 60% of selenium in the plasma as well as functioning as a potent antioxidant (130). Inhibition of SEPP1 is associated with tumor initiation through Wnt signaling and overexpression inhibits proliferation (131). ABCA1 (ATP-binding cassette transporter) is a membrane transporter that is upregulated at the mRNA and protein level by apoptosis and function to promote the clearance of apoptotic cells by phagocytosis (132,

133). Histone H2A type 1-C (HIST1H2AC) is a core histone that helps to make up the nucleosome, and its decreased expression is associated with increased proliferation and tumorigenicity (134). Overall, the diverse mechanisms that are modulated by just these ten defined genes shared between the two cell lines highlights the wide spectrum of molecular and biologic mechanisms that are modulated by MET antagonists in MET-amplified cells.

Because of the diverse mechanisms being modulated by MET inhibition a top priority for our ongoing investigation was to identify strategies that increase MET inhibitor sensitivity and overcome the development of the acquired resistance that is likely to emerge following prolonged MET inhibition. By using whole-genome mRNA expression profiling, we were able to identify that genes involved in the regulation of autophagy were modulated in both MET inhibitor-sensitive cell lines, and GSEA confirmed that genes associated with autophagy were highly enriched following MET inhibition. Furthermore, direct measurements of autophagy are needed to characterize the functional effect that exposure to crizotinib causes in both MET amplified gastric cancer cell lines (49, 135). Autophagy is a complex process that mediates a variety of different physiological functions, including degrading dysfunctional cellular components, protection of organelle function, promoting cell survival, decreasing metabolic stress, and executing apoptosis (50, 136). As we highlighted in the introduction with regard to cell death, the effects of autophagy are context-dependent, resulting in cytoprotective or cytotoxic effects depending on the specific physiological or pathological context (136-139). Because of the complexity of the role autophagy plays within the cell and the interest in targeting autophagy to improve the

effects of cancer therapies, it was important to understand the role of autophagy following MET inhibition in the MET-amplified gastric cancer cells (135, 138, 140).

Chapter 5.
CHARACTERIZATION OF
AUTOPHAGYS INVOLVEMENT
IN RESPONSE TO MET
ANTAGONIST

5.1 Introduction

Previous studies have demonstrated that MET inhibitors induce increases in autophagy and autophagy-associated gene expression, but the effect autophagy had on cell death, and cell survival in this context was not determined (49, 135). Autophagy has been shown to promote cell death, raising the possibility that blocking autophagy may prevent the pro-apoptotic effects of MET antagonist (141-143). Likewise, autophagy inhibitors have been known to promote cell death in cancer cells exposed to other pro-apoptotic agents (136, 137, 144), raising the possibility that autophagy inhibitors might promote the effects of MET antagonists in human gastric cancer cells. We, therefore, recognized the clinical importance of understanding autophagy's involvement as it relates to cell death and cell survival and therefore sought to evaluate the effects that blocking autophagy has on MET inhibitor-induced cell death.

5.2 Results

5.2.1 Induction of autophagy in response to MET inhibition in MET-amplified gastric cancer

We used functional assays in an attempt to confirm the gene expression profiling results implicating autophagy as among the top upregulated biologic processes in response to MET antagonist in MET-amplified gastric cancer cell lines SNU-5 and MKN45. We used two of the drug-resistant gastric cancer cell lines (NUGC-4, MKN74) as controls. We exposed the cells to increasing concentrations of crizotinib for 72 hours and then measured

autophagy by acridine orange staining coupled with FACS analysis (145-147). Crizotinib caused concentration-dependent increases in autophagy in both MET-amplified cell lines but not in the drug-resistant cells [Figure 5.1].

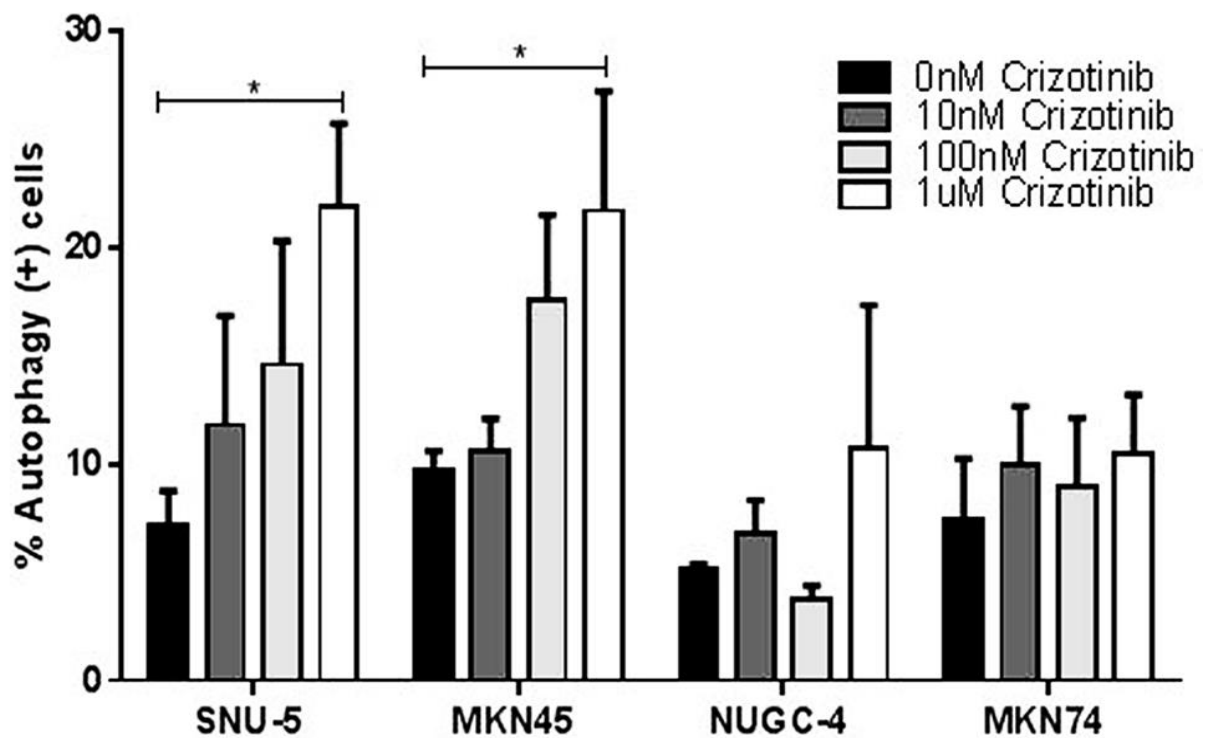


Figure 5.1 MET inhibition induces autophagy in the crizotinib-sensitive cells. (A) Crizotinib induces autophagy in a concentration-dependent fashion. The gastric cancer cell lines were incubated with increasing concentrations of crizotinib (0, 10, 100, 1000nM) for 72 hours and autophagy was accessed by acridine orange staining coupled with flow cytometry. The SNU-5 and MKN45 cells contain high level MET amplification, whereas the NUGC-4 and MKN74 cells do not.

Next, we confirmed the autophagy results using two supplementary independent assays. First, we measured autophagic flux using the CYTO-ID autophagy assay which utilizes a cationic amphiphilic tracer (CAT) dye that rapidly partitions into cells. This CAT dye works in a similar manner as drugs that induce phospholipidosis (from Enzo Life Sciences, Inc). Careful selection of titratable functional moieties on the dye prevents its accumulation within lysosomes, but enables labeling of vacuoles associated with the autophagy pathway. [Figure 5.2, top panel] (72). We observed significant increases in autophagy in both MET-amplified cell lines following exposure to crizotinib.

Next, we used immunoblotting to detect conversion of LC3B I to LC3II [Figure 5.2, bottom panel]. Microtubule-associated protein 1A/1B-light chain 3 (LC3) plays a role in autophagy whereas during autophagy the cytosolic form LC3-I is conjugated to phosphatidylethanolamine to form LC3-II which is recruited to the autophagosome (59). Degradation (lysosomal turnover) of LC3-II is directly proportional to autophagy activation within the cell and is routinely used to monitor autophagy through measurement via immunoblotting, immunoprecipitation, and immunofluorescence (59). Following exposure to crizotinib, we observed an increase in autophagy in both MET amplified cell lines, as determined by an increase in LC3-II conversion [Figure 5.2, bottom panel]. Overall, the results of these three assays were consistent with each other and expanded on the results of the gene expression profiling by confirming that autophagy is activated following MET-inhibition.

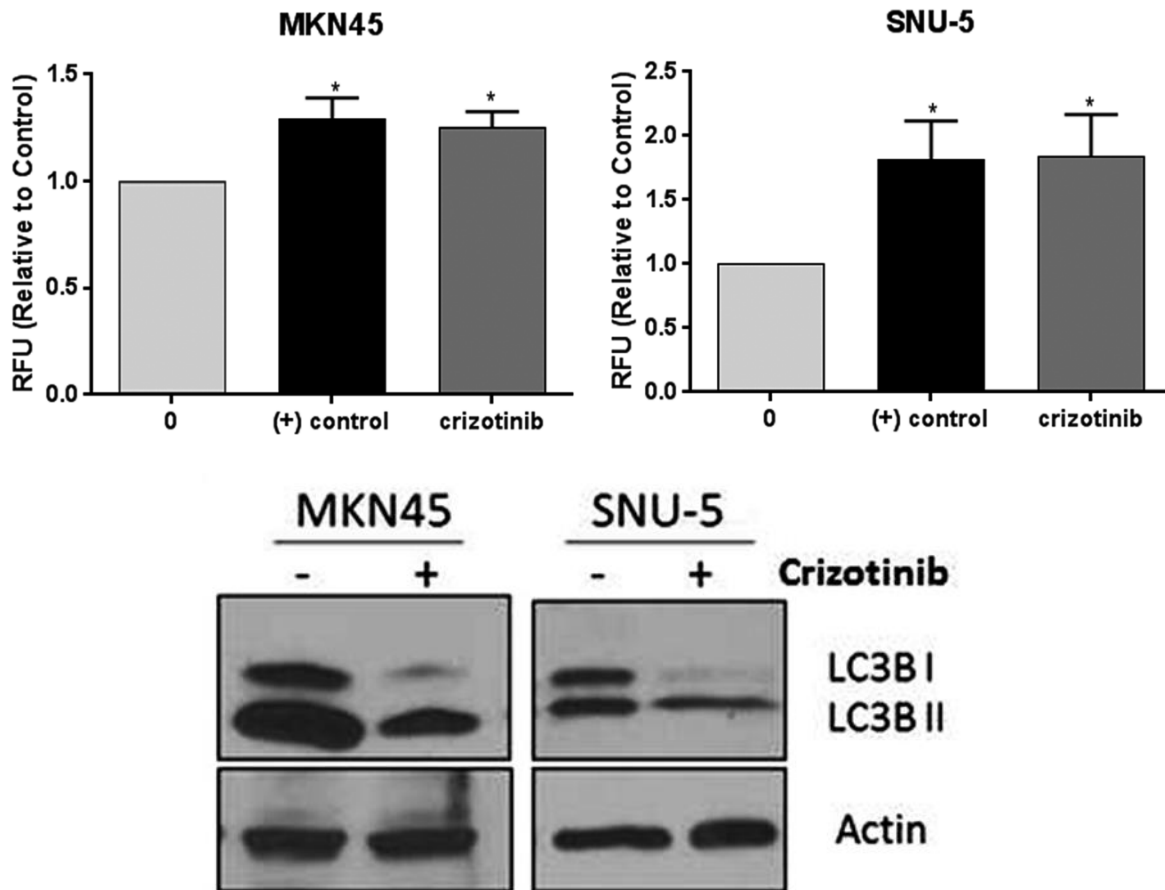


Figure 5.2 MET inhibition induces autophagy in the crizotinib-sensitive cells. Conformation of the acridine orange autophagy assay using two additional autophagy assays. (Top Panel) Crizotinib causes increased autophagic flux in the drug-sensitive cells. SNU-5 and MKN45 cells were incubated with 100nM crizotinib with for 24hrs and autophagy was accessed by fluorescence microplate reader with the application of Cyto-ID autophagy detection kit. Data are means \pm SEM from three independent experiments. Student *t*-test, * $p \leq 0.05$. (Bottom Panel) Crizotinib induces LC3-II processing. SNU-5 and MKN45 cells were incubated with 100nM crizotinib with for 24hrs, and LC3 expression was analyzed by Western blotting.

5.2.2 Effects of autophagy inhibition on apoptosis

As detailed in the introduction, depending on the particular biological context, autophagy can either promote or inhibit cancer cell death (136, 148). Therefore, we designed mechanistic experiments to define the role of autophagy in crizotinib-induced cell death. First, we examined the effects of blocking autophagy with chloroquine, a clinically approved anti-malarial drug that inhibits autophagy by raising lysosomal pH (149, 150). Chloroquine did not induce statistically significant increases in the levels of apoptosis in any of the cell lines on its own or in combination with crizotinib [Figure 5.3]. On the other hand, chloroquine caused a statistically significant decrease in crizotinib-induced apoptosis in the MET amplified cell lines (MKN45 and SNU-5) [Figure 5.3].

We then looked at the effects of chloroquine on other forms of cell death (i.e. necrosis) and proliferation. We observed that chloroquine alone induces significant increases in the numbers of trypan blue-positive (necrotic) cells in all of the cell lines except for the MET-amplified cell line MKN45 [Figure 5.4.A]. We also measured total cell numbers following exposure to chloroquine with or without crizotinib and did not observe statistically significant decreases in cell numbers, indicative of proliferation inhibition, in any of the cell lines [Figure 5.4.B]. We expanded on these results by using live cell imaging at 72 hours and measuring trypan-blue positivity at 96 hours and observed the same trends as the 48-hour data even at these extended time points [Figure 5.5]. Therefore, the decreased apoptosis in the chloroquine-exposed MKN45 and SNU-5 cells was not caused by a

reduction in total cell numbers due to anti-proliferative effects or alternative cell death mechanisms.

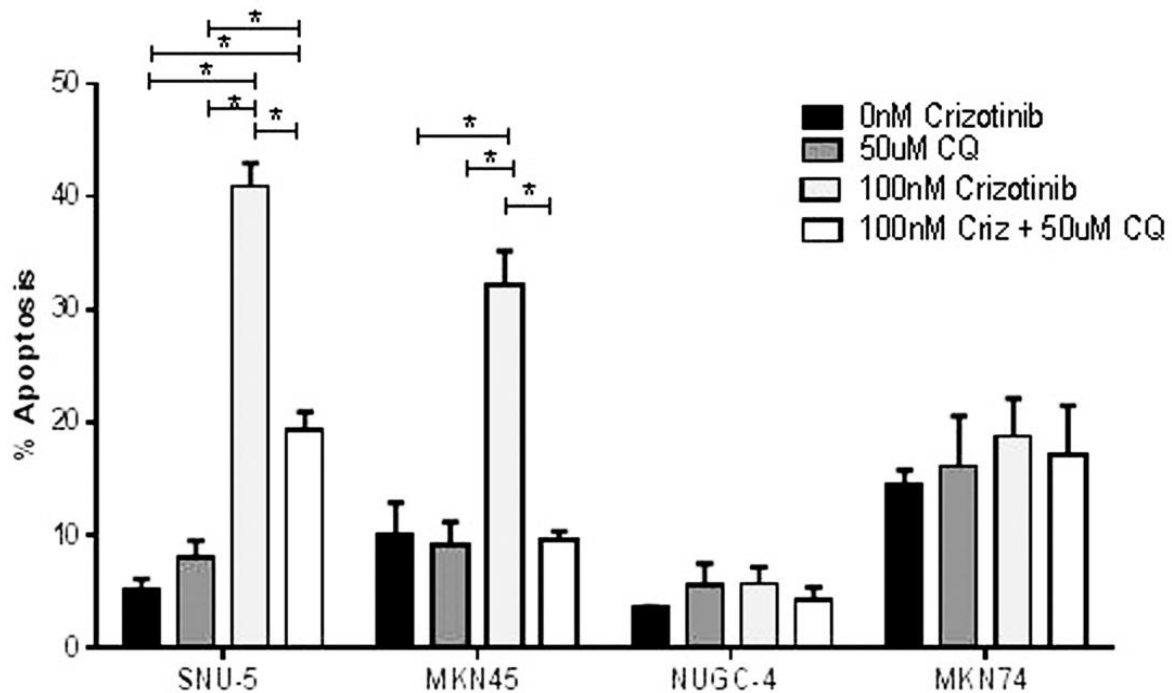


Figure 5.3 Autophagy is required for crizotinib-induced apoptosis. Gastric cancer cell lines (SNU-, MKN45, MKN74, and NUGC-4) were incubated with or without 100nM crizotinib, 50uM chloroquine (CQ) and 100nM crizotinib + 50uM chloroquine for 48 hours and PI-FACS was used to quantify cells with fragmented DNA due to apoptosis. Student t test, * $p \leq 0.0005$.

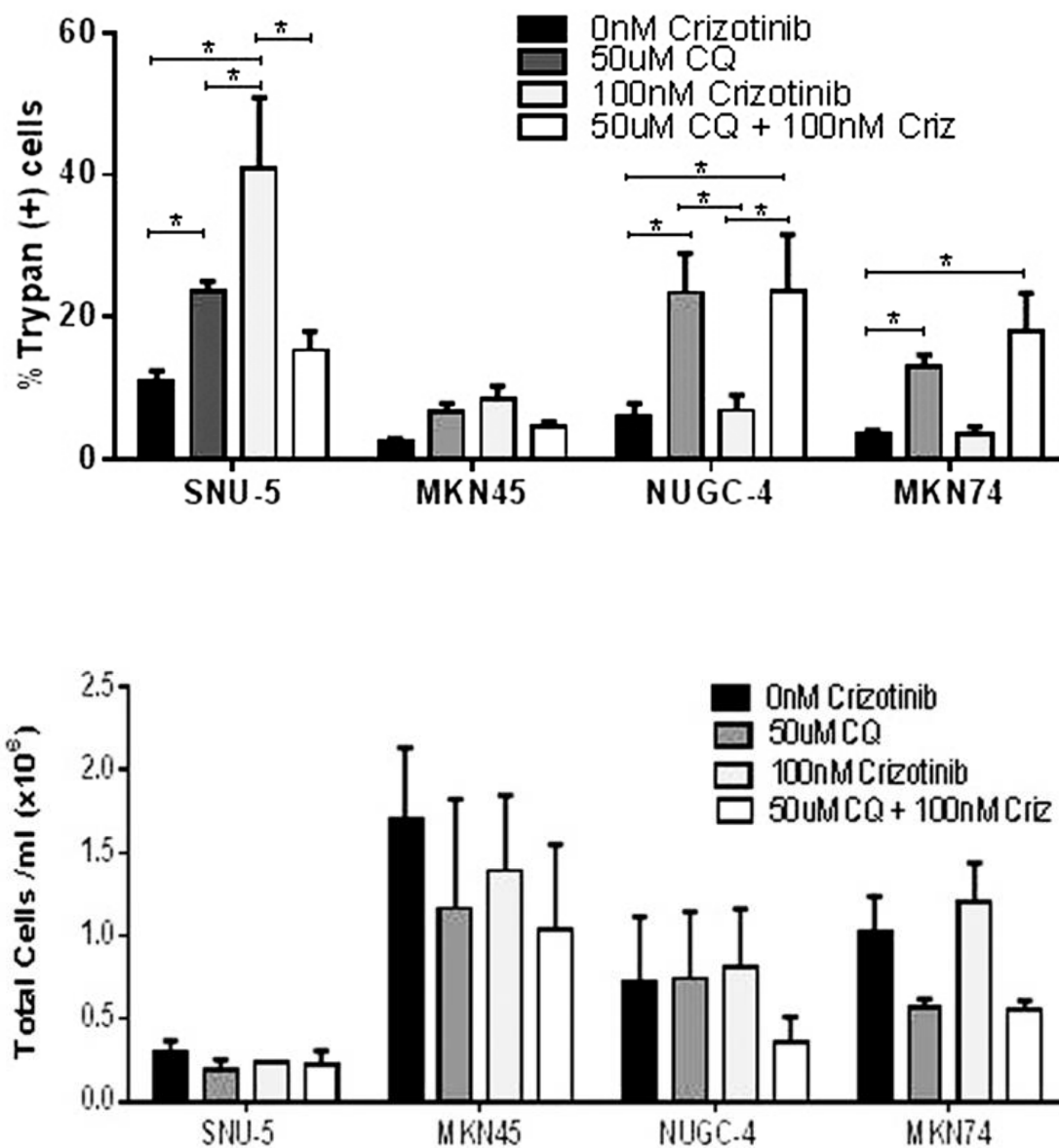


Figure 5.4 Autophagy inhibition effects on cell death and proliferation. Effects on total cell death. Gastric cancer cell lines (SNU-5, MKN45, MKN74, and NUGC-4) were incubated with or without 100nM crizotinib, 50uM chloroquine (CQ) or 100nM crizotinib + 50uM chloroquine for 48 hours and trypan blue exclusion/ ViCELL was used to quantify total cell death (top) and absolute cell numbers (bottom). Data are means \pm SEM from three independent experiments. Student t-test, *p<0.05.

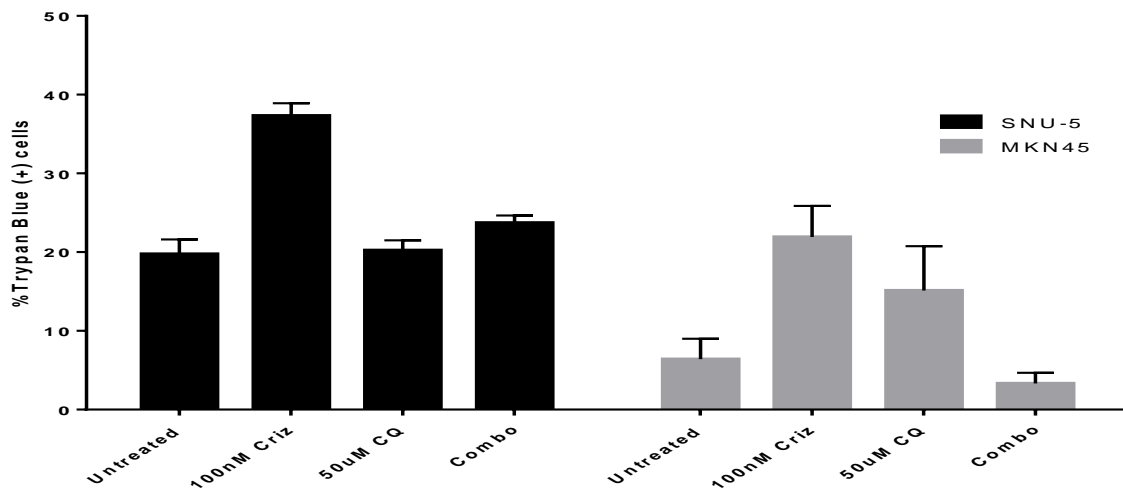
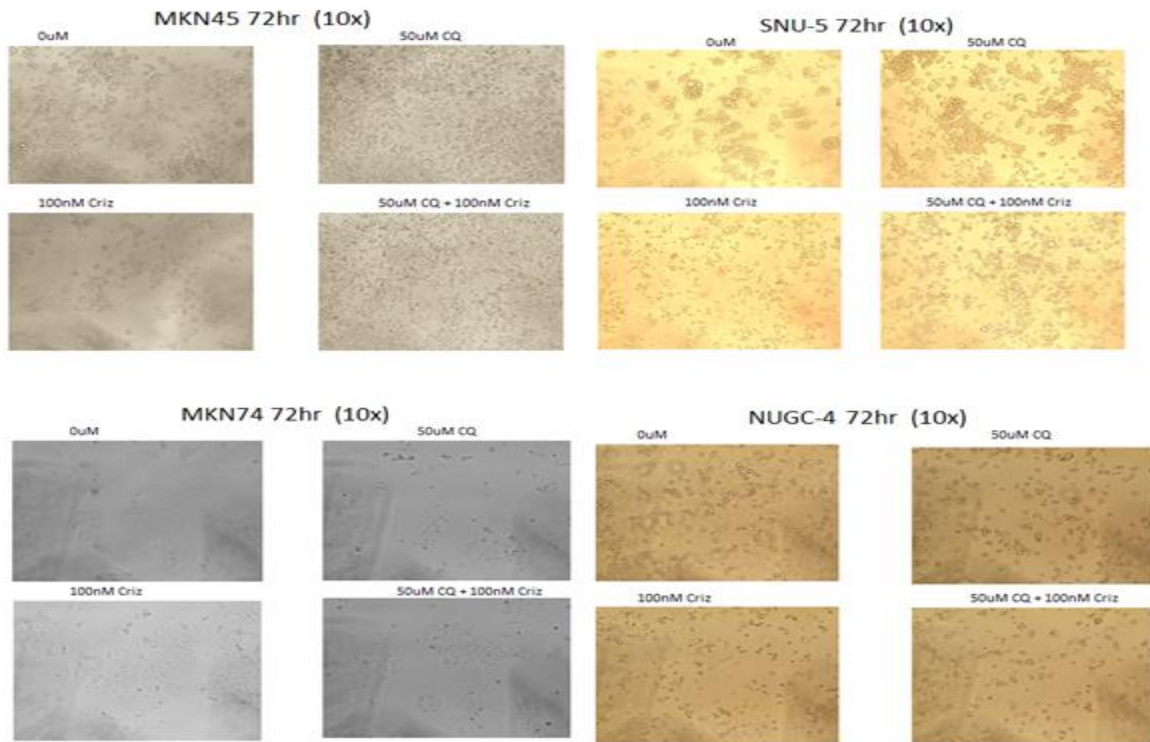


Figure 5.5 Effects of chloroquine at 72 and 96 hours. Effects on total cell death. Gastric cancer cell lines (SNU-5 and MKN45) were incubated with or without 100nM crizotinib, 50uM chloroquine (CQ) or 100nM crizotinib + 50uM chloroquine for 72 hours and live cell imaging was performed (top panel) and 96 hours trypan blue exclusion was used to quantify total cell death (bottom panel). Data are means \pm SEM from three independent experiments. Student t-test, * $p \leq 0.05$.

5.2.3 Anti-apoptotic effects of chloroquine are due autophagy inhibition

We sought to confirm that the anti-apoptotic effects of chloroquine were due to autophagy inhibition and not due off-target effects of the drug. We used RNA interference to knock down two obligate components of the autophagy pathway (ATG5 and ATG7) and measured the effects of molecular interruption of autophagy on apoptosis induced by MET knockdown. We confirmed the knockdown efficiencies of the siRNA silencing by RT-PCR [Figure 5.6]. Our results revealed that similar to what we observed in Figure 5.3 knockdown of ATG5/7 blocked MET knockdown-induced apoptosis in both of the crizotinib-sensitive cell lines but had no effect on the non-amplified cell lines where little apoptosis is observed [Figure 5.6]. Next, we measured LC3 conversion by immunoblotting and witnessed a buildup of the ratio of LC3-II and LC3-I as expected [Figure 5.7] (150). Chloroquine is a lysosomotropic agent that prevents endosomal acidification and leads to inhibition of lysosome-autophagosome fusion and lysosomal protein degradation (151). We also sought to confirm that the effects of chloroquine weren't due to differences in MET expression (i.e. an endosome-dependent protein turnover mechanism). To examine whether chloroquine affects steady-state MET levels and/or MET turnover, we examined MET stability in cells exposed to chloroquine with or without cycloheximide, an inhibitor of translation [Figure 5.7]. Although MET levels were indistinguishable in cells that were incubated with or without chloroquine alone, they were significantly lower in the cells exposed to chloroquine plus cycloheximide compared as compared with cycloheximide alone. Therefore, chloroquine does appear to increase MET turnover, although not enough to inhibit MET expression in the absence of cycloheximide. These effects do not account for the inhibitory

effects of chloroquine on crizotinib-induced apoptosis. From the correlation of previously described data, we can conclude that autophagy is directly responsible for the anti-apoptotic effects of chloroquine.

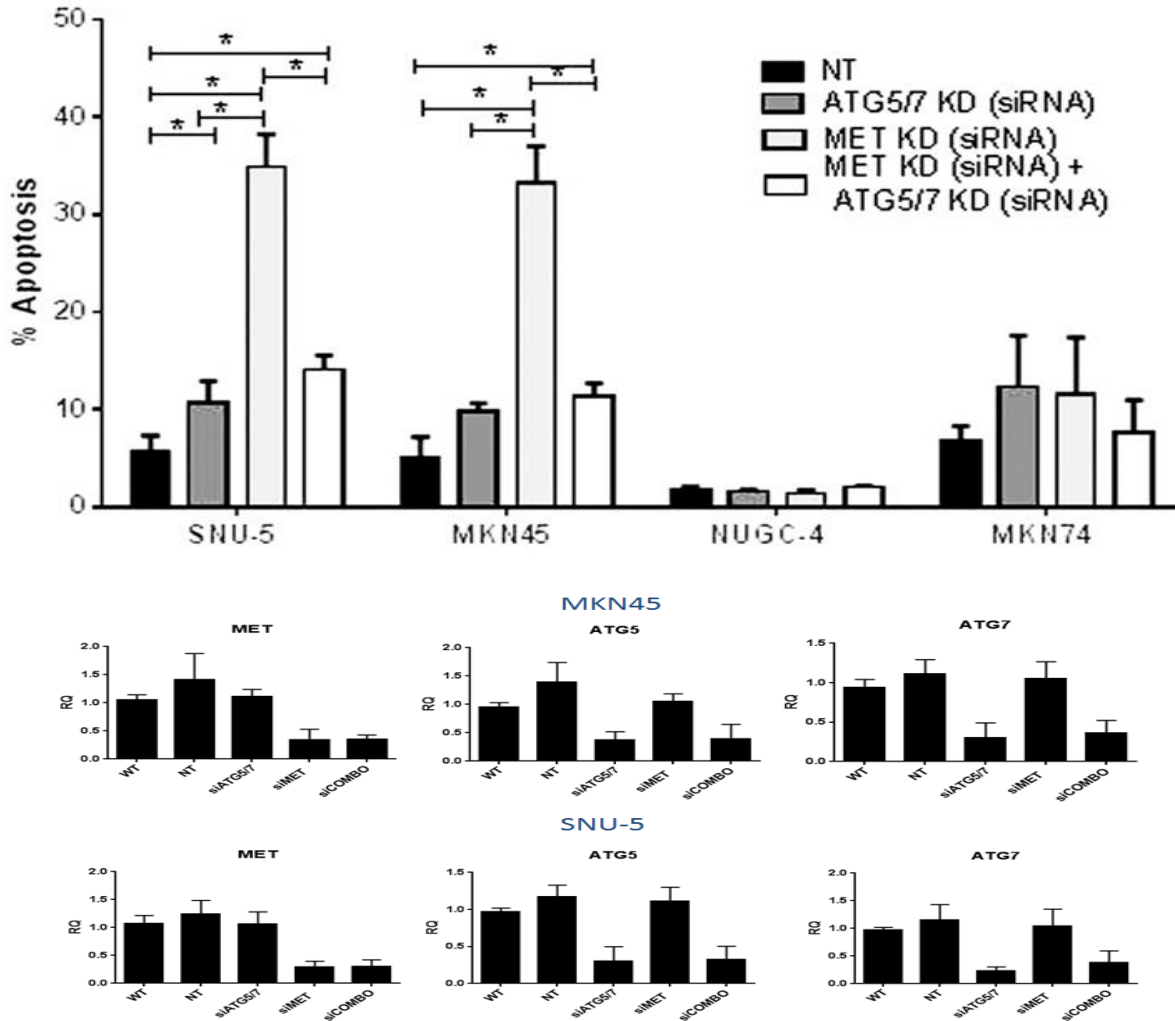


Figure 5.6 Autophagy is required for crizotinib-induced apoptosis. (A) Effects on apoptosis. Gastric cancer cell lines (SNU-5, MKN45, MKN74, and NUGC-4) were transfected with a non-targeting (NT) or MET siRNA, ATG5/7siRNA or MET siRNA + ATG5/7 siRNA for 48 hours and PI-FACS was used to quantify apoptotic cell death. (B) Knockdown efficiencies for MET, ATG5, and ATG7 siRNAs in MKN45 and SNU-5 cells transfected with siRNA for 48 hours. Expression levels were measured by one-step quantitative RT-PCR. Data are means \pm SEM from three independent experiments.

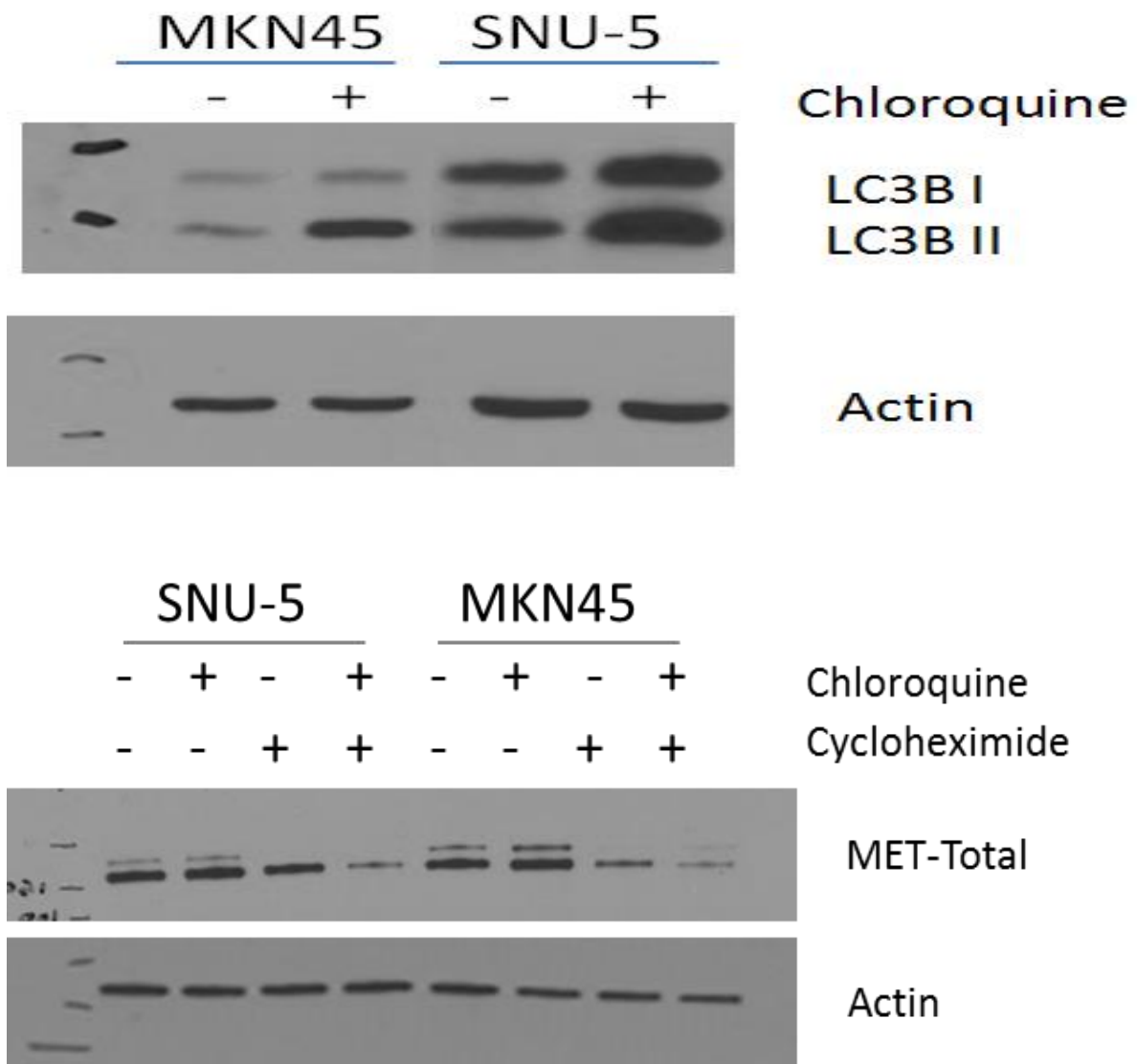


Figure 5.7 Chloroquine directly modulates autophagy. (Top) Gastric cancer cell lines (SNU-N and MKN45) were incubated with 50uM CQ, and LC3 conversion was used to quantify autophagy levels. (Bottom) Gastric cancer cell lines (SNU-N and MKN45) were incubated with 50uM CQ +/- cyclohexamide and total MET levels were measured via western blotting.

5.2.4 MET and Autophagy antagonists modulate metabolic pathways in MET-amplified gastric cancer cells.

The anti-apoptotic effects observed following exposure to chloroquine implicates autophagy as a key pro-apoptotic mechanism that warrants further investigation. Additional interrogation of the gene expression profiling data revealed that gene signatures associated with the two main metabolic pathways, oxidative phosphorylation and glycolysis, were negatively enriched following MET inhibition in both of the MET amplified cell lines [Figure 5.8]. Previous studies demonstrated that apoptosis is an ATP-dependent process, such that artificially lowering ATP levels can inhibit apoptotic cell death (152-154).

Because autophagy provides an energy source for cells undergoing growth factor withdrawal-induced stress (140, 155), we wondered whether decreased ATP levels might account for the effects of autophagy inhibition on apoptosis in the MKN45 and SNU-5 cells. To test this hypothesis, we measured ATP levels in cells at baseline and following exposure to chloroquine with or without crizotinib at 24, 48 and 72 hours using the CellTiter-Glo assay (156, 157). Consistent with the MTT results, crizotinib caused time- and concentration-dependent decreases in ATP levels in both drug-sensitive cell lines (SNU-5 and MKN45) but had much more modest effects in the two drug-resistant lines (NUGC-4 and MKN75) [Figure 5.9]. Chloroquine exposure caused major decreases in ATP levels in all of the cell lines, and crizotinib had minimal further effects, consistent with a role for autophagy in baseline energy homeostasis [Figure 5.10]. Importantly, the ATP levels reached following chloroquine exposure were very similar in all of the cell lines.



Figure 5.8 MET antagonist decrease metabolic pathways. Oxidative phosphorylation and glycolysis are among the top results negatively enriched for both cell lines when using the GSEA curated H: hallmark gene sets from the molecular gene sets database with $P < .01$ and $FDR < .05$ for all gene sets except for SNU-5 oxidative phosphorylation.

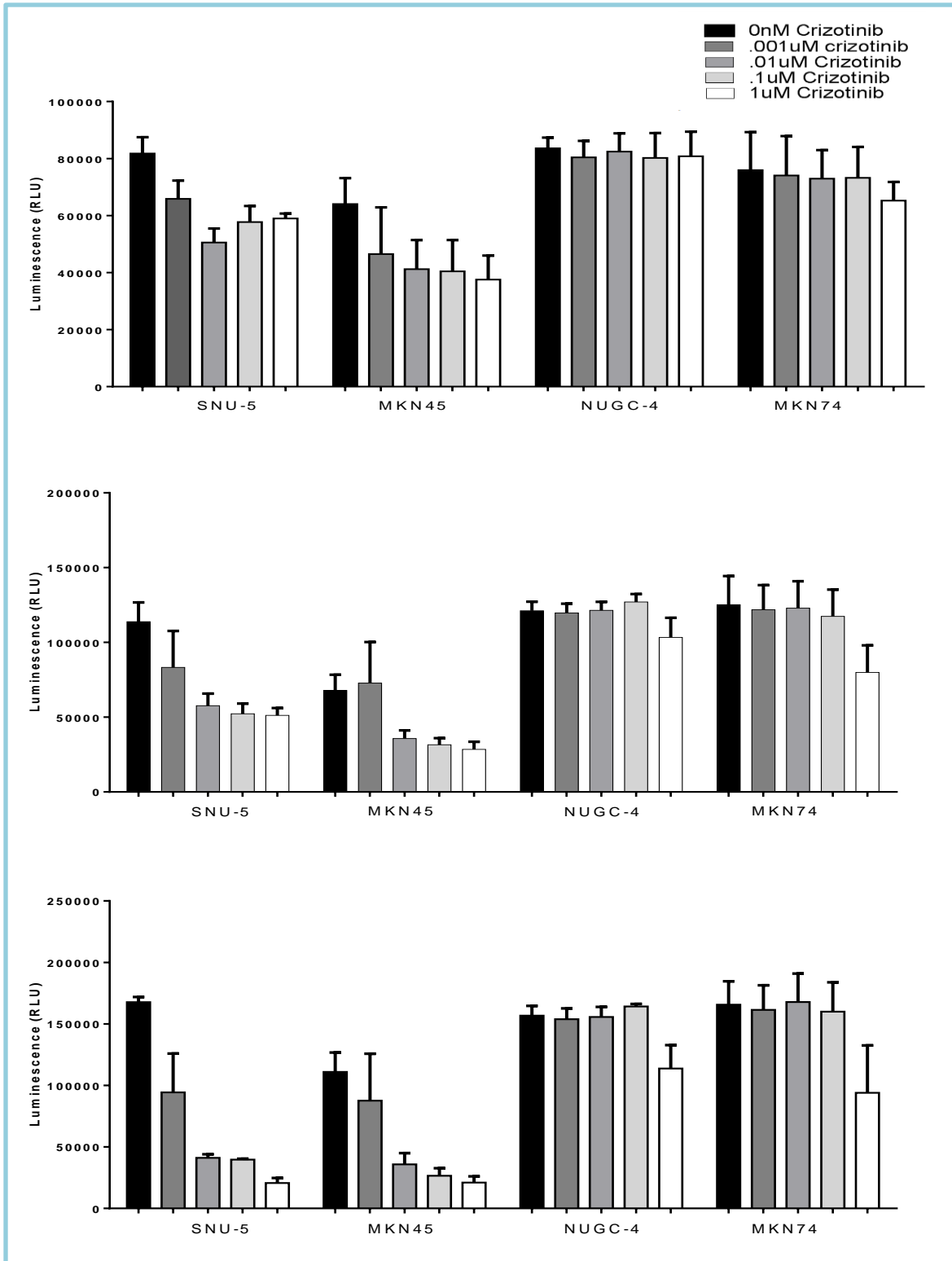


Figure 5.9 MET inhibition lowers ATP levels. A dose response and time course experiment for (A) 24hours (B) 48 hours and (C) 72 hours with increasing concentrations of crizotinib to measure ATP levels within the cells.

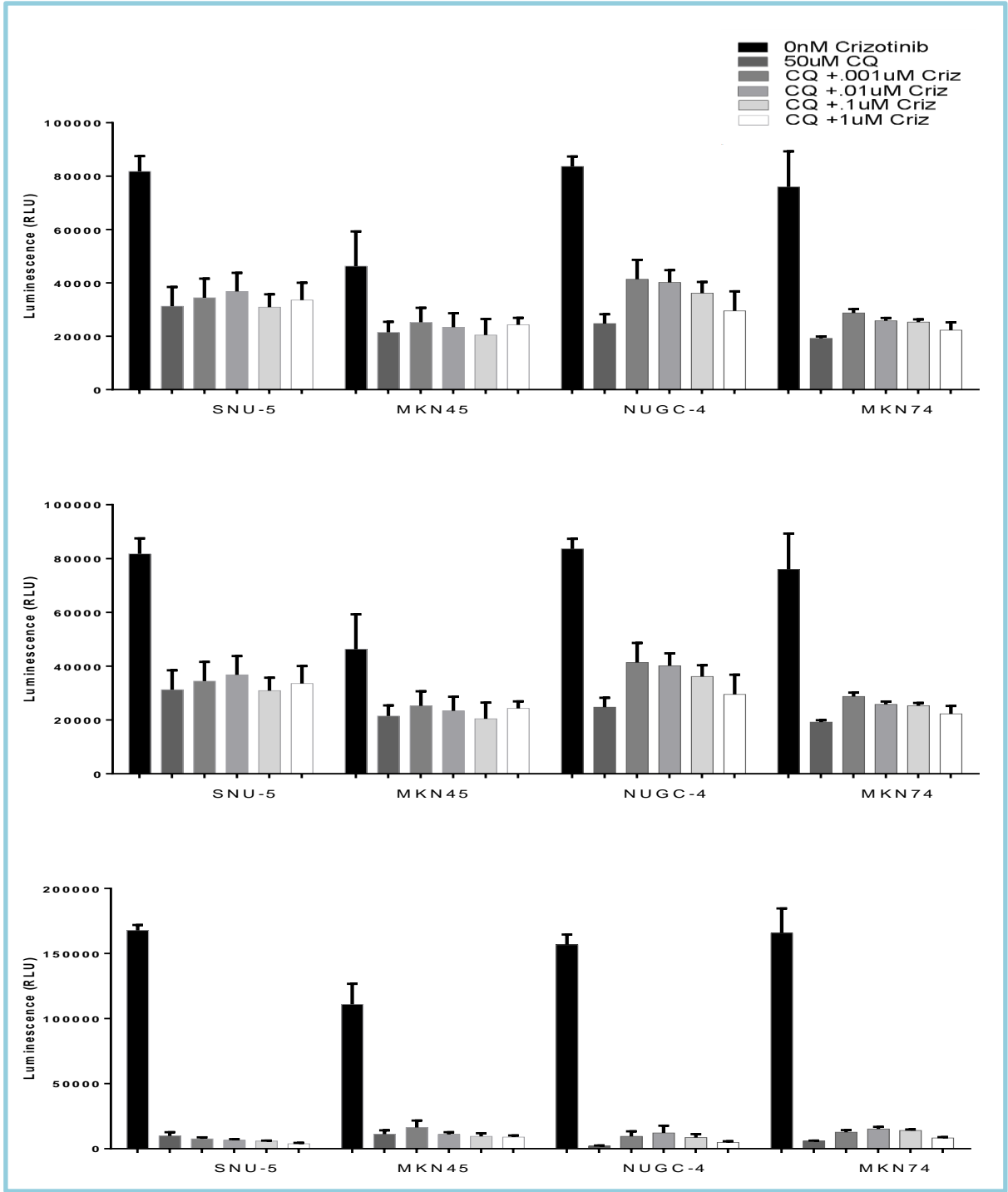


Figure 5.10 MET and autophagy antagonist lower ATP levels. A dose response and time course experiment for (A) 24hours (B) 48 hours and (C) 72 hours with increasing concentrations of crizotinib in combination with 50uM chloroquine to measure ATP levels within the cells.

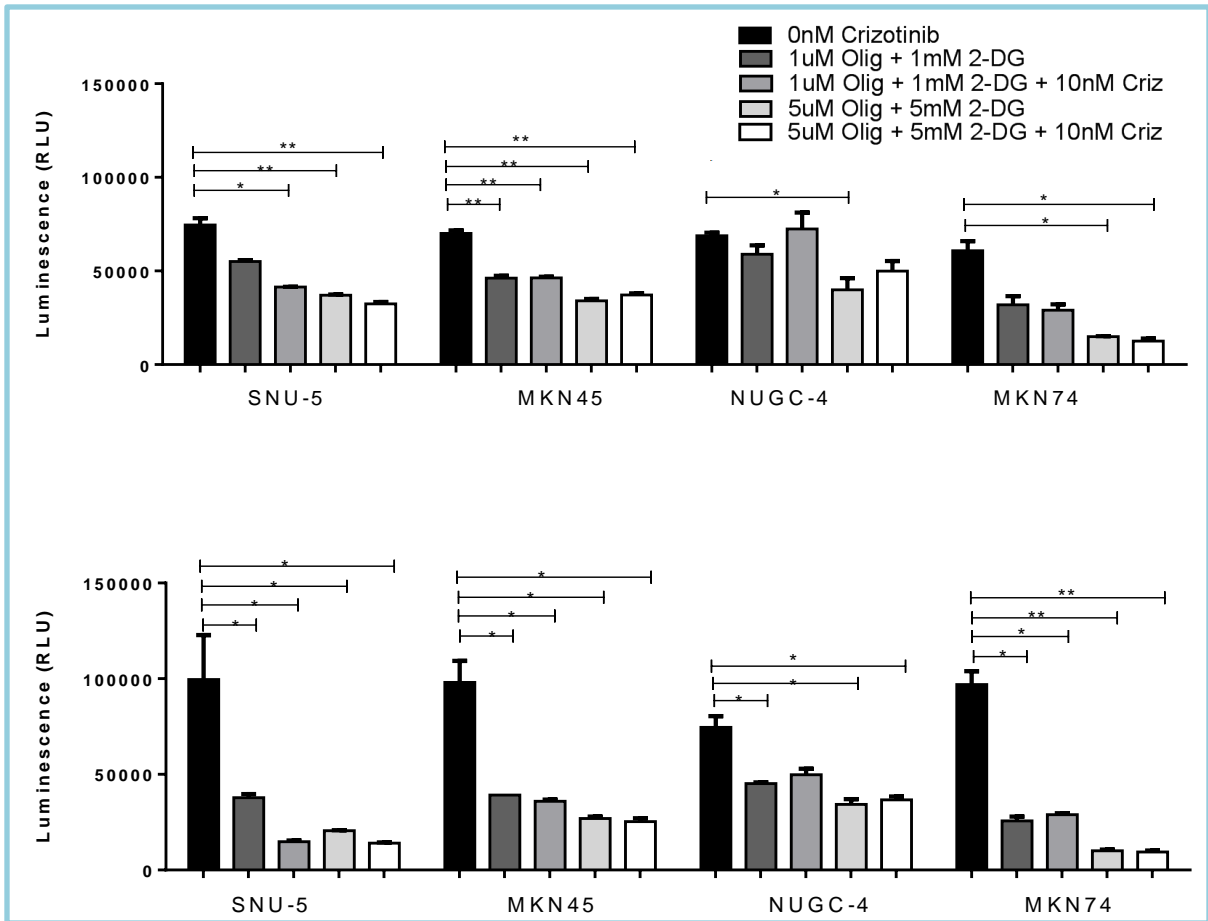


Figure 5.11 MET and metabolic antagonist lower ATP levels. A dose response and time course experiment for 24hours (top panel) and 48 hours (bottom panel) with increasing concentrations of Oligomycin A and 2-DG with or without 100nM crizotinib in combination to measure ATP levels within the cells.

5.2.4 Metabolic antagonists do not confer resistance to MET inhibitors.

To determine if decreased ATP levels could cause inhibition of crizotinib-induced apoptosis, as we observed following autophagy inhibition via chemical and molecular mechanisms, we inhibited ATP production by blocking oxidative phosphorylation and glycolysis using the chemical inhibitors oligomycin A and 2-deoxy-D-glucose (2-DG), respectively (158) [Figure 5.11]. Chemical reduction of ATP levels had no significant effect on apoptosis in the MKN45 or SNU-5 cells [Figure 5.12]. Because chloroquine or chemical ATP inhibition reduced ATP levels to a similar extent in both the SNU-5 and MKN45 cells, the results demonstrate that MET-amplified gastric cancer cells are not dependent on autophagy-mediated ATP production for apoptosis. Therefore, the anti-apoptotic effects of autophagy antagonist are due to another mechanism not related to the energetic requirements of apoptosis.

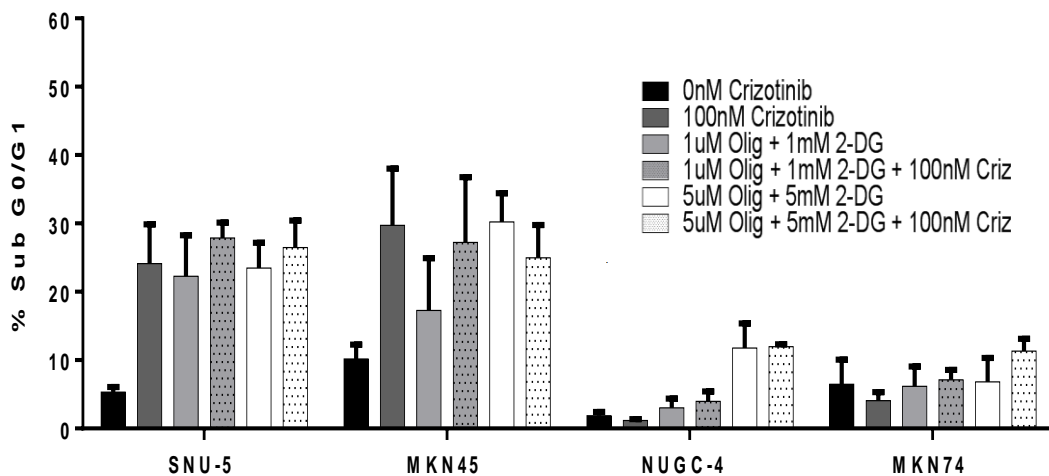


Figure 5.12 Metabolic antagonists do not confer resistance to MET inhibition.

Gastric cancer cells were exposed to oligomycin A and 2-DG with or without 100nM crizotinib and PI-FACS was used to measure apoptosis at 48hours.

5.2.5 Molecular mechanism behind anti-apoptotic effects of autophagy inhibition

Our ATP depletion results suggest a lack of involvement of a general apoptosis-related mechanism, such as ATP-dependent apoptosome formation. Therefore a crizotinib-specific mechanism of resistance is more plausible, and further interrogation was necessary. Cytochrome c release from mitochondria is a central commitment point for apoptotic cell death. We, therefore, wondered whether autophagy inhibition might attenuate apoptosis by preventing crizotinib-induced cytochrome c release [Figure 5.13]. To test this hypothesis, we incubated the SNU-5 or MKN45 cells with crizotinib with or without chloroquine for 6 hours and measured cytosolic cytochrome c levels by immunoblotting as described previously (75). Crizotinib caused statistically significant inhibition of cytochrome c release in both cell lines (representative western blots are displayed in Figure 5.13.a, and the results of 3 independent experiments are quantified in Figure 5.13.b). The results support our hypothesis that a resistance mechanism specific to crizotinib-induced apoptosis is occurring since cytochrome c release is initiated by BH3-only members of the BCL-2 family that are activated by specific upstream stimuli. Therefore, the localization of the defect to some point upstream of cytochrome c release is more consistent with the available data.

5.2.3 Autophagy inhibition does not confer resistance to other therapeutic agents

Finally, we wondered if the requirement for autophagy to allow cells to undergo apoptosis was specific for crizotinib, as suggested by the identification of a crizotinib-specific defect in the apoptotic cascades, or if it might also be observed with other stimuli since the mechanism of activation could be similar for other therapeutic agents.

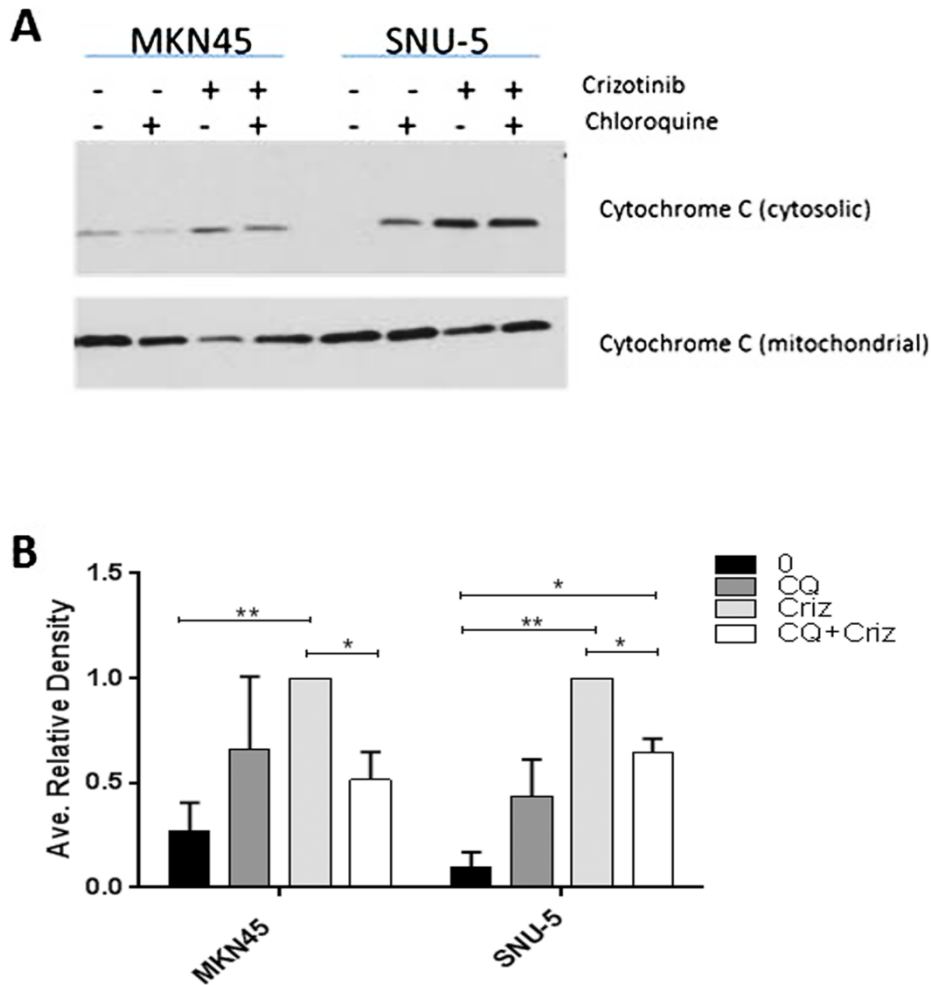


Figure 5.13 Autophagy is required for crizotinib-induced cytochrome c release.

(A) Measurement of cytochrome c release by immunoblotting. The MET-amplified, crizotinib-sensitive gastric cancer cell lines (SNU-, MKN45) were incubated with or without 100nM crizotinib, 50uM chloroquine (CQ) and 100nM crizotinib + 50uM chloroquine for 6 hours and western blot analysis was used to quantify cytochrome c levels in the cytosol and mitochondria. (B) Quantitative densitometry of the protein expression of the cytosolic fraction versus the mitochondrial fraction of cytochrome c. Data are means \pm SEM from three independent biological replicates. Student t test, * $p \leq 0.05$ ** $p \leq 0.005$.

To address this question, first we examined the effects of chloroquine on apoptosis induced by two alternative therapeutic agents (cisplatin and bortezomib) [Figure 5.14]. Bortezomib is an anti-cancer drug that works by inhibiting the proteasome from breaking down pro-apoptotic proteins thus allowing cell death to occur (159). Bortezomib is commonly used as a single-agent therapy and in combination with chemotherapeutic agents in advance stage (metastatic and/or unresectable) gastric cancers (160). Clinically achievable concentrations of bortezomib-induced significant increases in apoptosis in three of the four cell lines (MKN45, MKN74, and NUGC-4) [Figure 5.14]. Chloroquine caused a modest but statistically significant decrease in bortezomib-induced apoptosis only in the MKN45 cells at the highest concentration of bortezomib (100nM, $p=0.04$) [Figure 5.14.A].

Cisplatin is a chemotherapy agent commonly used in the treatment of advanced stage gastric cancer (161, 162). The cytotoxic mechanism employed by cisplatin involves damaging DNA and inhibiting DNA synthesis along with inducing apoptosis (163). In our panel of gastric cancer cell lines, we observed that cisplatin increased apoptosis in all four of the cell lines [Figure 5.14.B]. Again, as we observed in the bortezomib treated cells, chloroquine caused modest (and not statistically significant) decreases in cisplatin-induced apoptosis only in the MKN45 cells [Figure 5.14.B]. Together, the results of the bortezomib and cisplatin apoptosis experiments support the conclusion that autophagy plays a particularly important role in regulating crizotinib-induced apoptosis but is not relevant for other therapeutic agents.

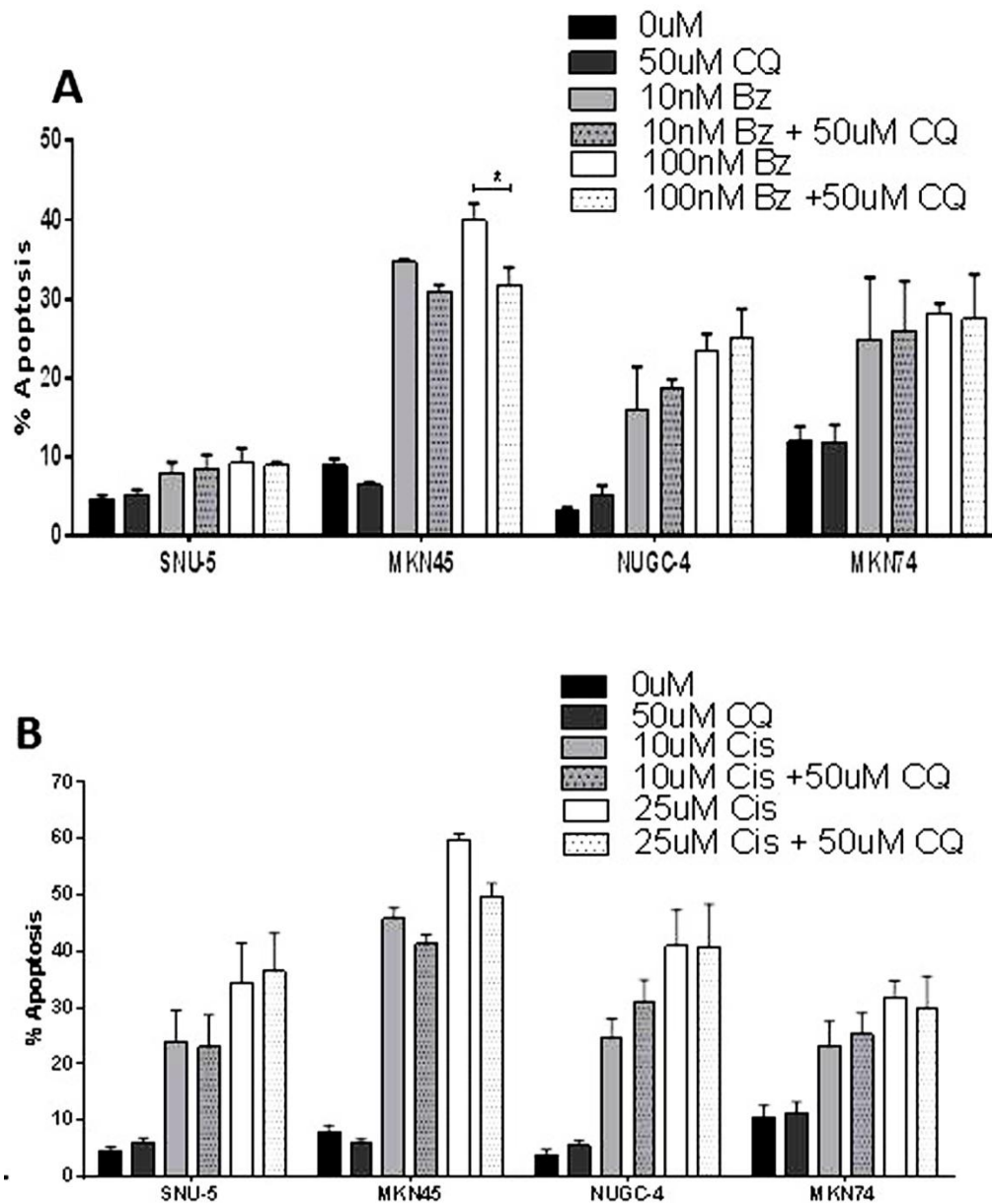


Figure 5.14 Autophagy is not required for apoptosis induced by other agents.

(A) Effects of chloroquine on bortezomib-induced apoptosis. Gastric cancer cell lines (SNU-, MKN45, MKN74, and NUGC-4) were incubated with 0, 10 or 100nM bortezomib with or without 50uM chloroquine (CQ) for 48hrs hours, and PI/FACS was used to quantify apoptosis. (B) Effects of chloroquine on cisplatin-induced apoptosis. Gastric cancer cell lines (SNU-, MKN45, MKN74, and NUGC-4) were incubated with 0, 10 or 25uM cisplatin with or without 50uM chloroquine (CQ) for 48hrs hours, and PI/FACS was used to quantify apoptosis. Data are means \pm SEM from three independent experiments. Student t-test, * $p < 0.05$.

5.3 Discussion

The functional consequences of activation of an autophagy associated gene signature, as observed using IPA and GSEA analysis, correlated with dose-dependent increases in autophagy in response to MET antagonist in both MET amplified cell lines. Autophagy levels were quantified using three independent assays (acridine orange staining, LC3 conversion, and CYTO-ID autophagy assay). Since autophagy activation plays many roles within the cells, it was important to define its role within our cells and determine the effects of modulating autophagy in combination with MET inhibition.

Our original hypothesis following the discovery that autophagy is activated by MET inhibition was that autophagy inhibition would act as a synergistic mechanism to intensify MET-induced apoptosis. What we observed was that in both of the drug-sensitive cell lines (MKN45 and SNU-5), autophagy inhibition caused statistically significant decreases in MET inhibitor-induced apoptosis regardless of the approach utilized (i.e. direct siRNA-mediated knockdown or chemical inhibition). And deeper analysis of the effects of autophagy inhibition on alternate cell death mechanisms (i.e. necrosis) and cell proliferation showed negligible effects that did not contribute to the anti-apoptotic effects of autophagy inhibition.

Further analysis of the GSEA results identified the decrease in metabolic pathways in both drug-sensitive cell lines. Since autophagy is known to be an alternative mechanism for cancer cells to generate cellular energy and apoptosis is an energy dependent form of programmed cell death we investigated whether the pro-apoptotic effects of autophagy

could be due to the generation of ATP. We use “chemical hypoxia” experiments to deplete ATP from the cells and measure crizotinib-induced apoptosis. We saw no effect on apoptosis following ATP depletion leading us to the conclusion that the defect in apoptosis is a crizotinib-specific mechanism and not a more generalized defect in the apoptotic cascade (i.e. apoptosome formation, deregulation of the balance of pro- and anti-apoptotic proteins, and disruption of P53 signaling). Because in apoptosis mitochondria are the central control point with cytochrome c release from the mitochondria being considered the proximal commitment point we investigated the effects of autophagy inhibition on crizotinib induced apoptosis (164, 165). Preliminary analyses of the molecular mechanisms demonstrated that autophagy was required for crizotinib-induced cytochrome c release. We then explored the effects of autophagy inhibition on apoptosis induced by other therapeutic agents (cisplatin and bortezomib) commonly used in advanced gastric cancers. Neither agent had pronounced levels of apoptosis modulation following the addition of chloroquine. The very modest effects of chloroquine on apoptosis induced by either bortezomib or cisplatin support the idea that the effects of chloroquine on apoptosis are unique to crizotinib. The results argue against the involvement of a general apoptosis-related mechanism and further indicate that a defect some point upstream of cytochrome c release is more consistent with the available data. Although these results were surprising to us, they are not unprecedented. Past studies also demonstrated that autophagy was essential for apoptosis (63, 136, 166), and another group concluded that autophagy was required for cytochrome c release (167), but these effects are highly cell type-dependent and additional mechanistic studies are needed to elucidate the exact point of defect.

**Chapter 6. DISCUSSION,
CONCLUSIONS AND FUTURE
DIRECTIONS**

6.1 Conclusions

The components of this thesis describe key new findings that expand upon the current body of knowledge with respect to the consequences of autophagy and MET inhibition in gastric cancer. In this section, the central conclusions from chapters 3-5 are outlined, and future strategies by which to expand these discoveries are discussed.

6.1.1 Chapter 3 Conclusions: *Sensitivity to crizotinib in gastric cancer cells is associated with met amplification.*

The data from this chapter expanded on the current knowledge in the field by confirming that MET amplification is critical mediator of sensitivity for gastric cancer cells in response to MET antagonists and correlating this mediator of sensitivity to high-level MET phosphorylation. Here we demonstrate that MET-amplified gastric cancer cells exhibited growth arrest and cell death in response to incubation with the MET inhibitor crizotinib, whereas MET inhibition had no significant effects in cells without MET amplification, irrespective of whether they had high MET mRNA expression or contained activating MET mutations.

Our results are consistent with previous preclinical observations (42, 43) and recent clinical experience where MET has been validated as a therapeutic target in gastric cancer (77, 91). Although, MET inhibitors have had success in the clinic, some potential drawbacks exist and additional investigation into these pitfalls is necessary. These potential downsides and future directions are outlined and thoroughly discussed in the next section.

6.1.2 Chapter 4 Conclusions: *Evaluation of the effects of crizotinib on global gene expression in MET amplified gastric cancer cells*

Recent failures in MET targeted clinical trials with novel MET inhibitors onartuzumab, tivantinib, and foretinib combined with our previous observations that crizotinib has both cytotoxic and cytostatic effects, resulted in the immediate need to identify strategies that increase MET inhibitor sensitivity that can overcome the development of the acquired resistance that is likely to emerge following prolonged MET inhibition (168-170). This therefore became a top priority for our studies. Using whole-genome mRNA expression profiling, we observed genes related to cell death and growth arrest were significantly modulated following MET inhibition in both MET amplified cell lines. These results support the MTT and PI-FACS data presented in Chapter 3 by confirming both growth inhibitory and cell death mechanisms are modulated by MET antagonists. The gene expression changes in each of the cell lines extensively overlapped showing that the effects of MET inhibition are more generalized and not cell line specific. This is of great importance when trying to identify and streamline targeted therapy options for wide-ranging classes of patients (i.e. patients with MET amplified tumors) as opposed to being focused on individual tumors and patients.

Additionally, we identified that gene modulation associated with autophagy was among the top modulated genes, gene sets, and biologic processes when we performed both pathway (IPA) and gene set (GSEA) analysis. As previously detailed in chapter 4, GSEA analysis yielded multiple results implicating autophagy related genes as significantly

enriched in group exposed to crizotinib. Additionally using IPA, GATA1 was among the top six transcriptional regulators activated in both cell lines. GATA1 is the master regulator of hematopoiesis and we observed in the GSEA hallmarks gene sets heme metabolism is one of the six significantly enriched gene sets shared between the two cell lines (171). This is interesting because GATA1 has been directly implicated in activating autophagy transcription factors encoding for LC3 as well as employing FOXO3 to activate autophagy genes (171). This serves as further evidence that autophagy modulation plays a significant role in response to MET inhibition in gastric cancer.

Because autophagy has been implicated as both a tumor suppressive and tumor promoting process and multiple clinically approved autophagy inhibitors are available, autophagy was an ideal target for the next phase of our research looking at possible synergistic and resistance mechanisms in response to MET inhibition.

6.1.3 Chapter 5 Conclusions: *Involvement of autophagy in response to MET inhibition in MET amplified gastric cancer cells*

Here, we first directly measured autophagy levels using three distinct assays and identified that crizotinib induced concentration-dependent autophagy increases in both cell lines, consistent with previous reports (49, 135). Autophagy is a complex process that mediates a variety of different physiological functions, including degrading dysfunctional cellular components, protection of organelle function, promoting cell survival, decreasing metabolic stress, and executing apoptosis (50, 136). With regard to cell death, the effects of autophagy are context-dependent, resulting in cytoprotective or cytotoxic effects

depending on the specific physiological or pathological context (136-138). Because of this complexity and the interest in targeting autophagy to improve the effects of cancer therapies, it was important to understand what role autophagy activation played in apoptosis induced by MET inhibition in the MET-amplified gastric cancer cells (135, 138, 140). We used PI-FACS to measure apoptosis levels with and without autophagy inhibition in both of the drug-sensitive cell lines (MKN45 and SNU-5). This revealed that autophagy inhibition caused statistically significant decreases in MET inhibitor-induced apoptosis, regardless of the approach utilized (i.e. direct siRNA-mediated knockdown or chemical inhibition).

We then sought to gain a deeper mechanistic understating of why autophagy in our cells is a pro-apoptotic process and where the potential defect in the apoptosis process occurred in response to autophagy inhibition. Because the gene expression profiling data had been such a valuable resource in identifying biologic processes and molecular mechanisms modulated by crizotinib, we mined the top down regulated processes for each cell line using the hallmarks gene sets and identified that the metabolic processes, oxidative phosphorylation and glycolysis, were down regulated following crizotinib exposure. Since apoptosis is an energy dependent process and autophagy is known to provide energy for the cell during times of metabolic stress we hypothesized that ATP depletion was the deficiency in the apoptotic process. We measured ATP levels following exposure to crizotinib +/- chloroquine and observed a decrease with crizotinib alone and further decrease with the addition of chloroquine. We performed “chemical hypoxia” experiments by depleting cellular ATP through exposure to oxidative phosphorylation and glycolysis

antagonists and measured ATP levels and crizotinib-induced apoptosis. We saw no effect on apoptosis in either drug-sensitive cell line even though ATP levels were decreased levels similar to was observed following chloroquine exposure. Because the mechanism did not appear to be a generalized defect in apoptosis (i.e. ATP dependent apoptosome formation) we looked at mechanisms that would be more specific to crizotinib-induced apoptosis. Our preliminary analyses of the molecular mechanisms involved demonstrated that autophagy was required for crizotinib-induced cytochrome c release, considered the proximal commitment point for apoptosis in most examples of the response.

Additional mechanistic studies are required to determine precisely how autophagy promotes cytochrome c release in gastric cancer cells exposed to MET inhibitors. Overall, our results suggest that autophagy inhibitors will not potentiate MET inhibitor-induced apoptosis in gastric cancer cells. Clinically, our findings underscore the importance of understanding tumor biology prior to launching trials of combination therapies with autophagy modulators and growth factor receptor inhibitors in patients.

6.2 Future Directions:

6.2.1 Chapter 3 Future Directions

Our studies detailing the relationship between MET amplification and MET inhibitor sensitivity in gastric cancer provides an important discovery that upon further experimental validation could have significant impact on the way MET inhibitors are used clinically. The recent failures of advanced phase MET inhibitor clinical trials has been largely credited with a poor understanding of the most effective method for selecting the appropriate patient

populations. Several methods for measuring MET levels in patients are available and each has advantages and pitfalls that need to be addressed prior to initiating studies that require specific properties for response. Future studies evaluating the most common clinical methods for measuring MET amplification and MET phosphorylation and correlating these to determinates of sensitivity that are outlined in our study are of the utmost important. We speculate that the currently employed methods are not actually providing an accurate picture of these, leading to patient populations enriched with patient that have high mRNA MET levels. mRNA expression levels are a misleading surrogate marker for MET amplification that we have shown in chapter 3 does not correlate with response. Additional studies have shown that IHC staining for MET has conflicting outcomes on overall patient survival when comparing the two advanced IHC grades (+2 and +3); which is troubling because IHC grading is highly subjective and could lead to the selection of inappropriate treatment plans for patients as well as skewing patient populations selected for targeted therapies (25). Methods used for determining MET status commonly include immunohistochemistry (IHC), qPCR, RT-PCR, silver in-situ hybridization (SISH) and fluorescence in situ hybridization (FISH), and some preliminary evaluation of their abilities to predicate positive patient populations has been accessed (25, 172). To more carefully explore the correlation of each of these methods future experiments should include retrospective analysis of patient tumors treated with MET inhibitors that can then be correlated to clinical response, experiments evaluating the effects of adding HGF ligand to cells and gauging the effects of MET inhibition by measuring apoptosis to help discriminate between the effects of amplification vs. overexpression of MET, as well as the use of

patient-derived xenograft (PDX) models. These PDX models would allow use to test multiple different methods (IHC, RT-PCR, and FISH) that monitor MET amplification and MET phosphorylation levels of tumors prior to and throughout treatment with MET inhibitors.

Another question that merits additional investigation is the need to further characterize the cytostatic versus cytotoxic effects of MET inhibition. Our experiments have shown that both growth arrest and apoptosis occur in response to exposure to crizotinib but we have yet to quantify the ratios of each mechanism in order to evaluate the long term usefulness of MET inhibitors. This can be achieved by employing the use of multiple different techniques including the use of clonogenic assays to further describe the effects on cell proliferation and survival following treatment with a MET inhibitor and *in vivo* experiments to evaluate the long-term effects of MET antagonists in mouse models with orthotopically implanted luciferase-tagged human gastric cell lines.

6.2.2 Chapter 4 Future Directions

In chapter 4, the gene expression profiling experiments generated the data we used to more thoroughly explore the effects of autophagy inhibition. The gene expression profiling data also provides leads for additional molecular mechanisms and biologic processes that could help identify additional synergistic and resistance mechanisms in response to MET inhibition. One interesting target is KRAS signaling, because it was identified in both the upregulated and downregulated hallmarks gene sets for both inhibitor sensitive cell lines [Tables 4.2 and 4.2]. KRAS mutations have been identified as a resistance mechanism to MET antagonists in MET-driven tumors and further investigation into KRAS

modulation could provide valuable insight in the importance of the interaction between MET and KRAS (173). Another target, which I outline thoroughly in the chapter 4 discussion, is the decreased expression of DUSP6 which is a member of the MAPK family and its expression level is modulated by ERK and KRAS. KRAS and DUSP6 could serve to be a therapeutically viable due to the availability of therapeutic agents targeting the MAPK cascade (174). Additionally, work done by the TCGA has increased our understanding of molecular subtypes in gastric cancer (27). The TCGAs comprehensive mutation, copy-number and pathway analysis serves as an additional source of knowledge for future experiments profiling targetable therapeutic agents in combination with MET antagonists (27) [Figure 6.1].

6.2.3 Chapter 5 Future Directions

Chapter 5 focused on confirming the functional effects of autophagy activation in response to MET inhibition. We discovered a novel resistance mechanism, where autophagy is required for cells to undergo apoptosis and then narrowed the point of the apoptotic defect to the point of cytochrome c release. Additional mechanistic studies are required to determine the exact point of defect in the apoptotic cascade. Since we discovered that it is most likely a defect in apoptosis that is MET-inhibitor specific and not a generalized apoptotic mechanism such as apoptosome formation we can achieved this aim in several ways. First we can use western blotting to measure the effects of apoptosis related proteins that occur upstream of cytochrome c release. This will reveal the point at which apoptosis fails to occur. Then we can confirm these results by using knock-down and overexpression technology to inhibit or promote proteins related to this defect and

measure the functional consequences. Additionally, we would want to see if the effects on apoptosis occur *in vivo*. Although *in vitro* cell line analysis is a good preliminary tool, ultimately *in vivo* studies are more clinically relevant.

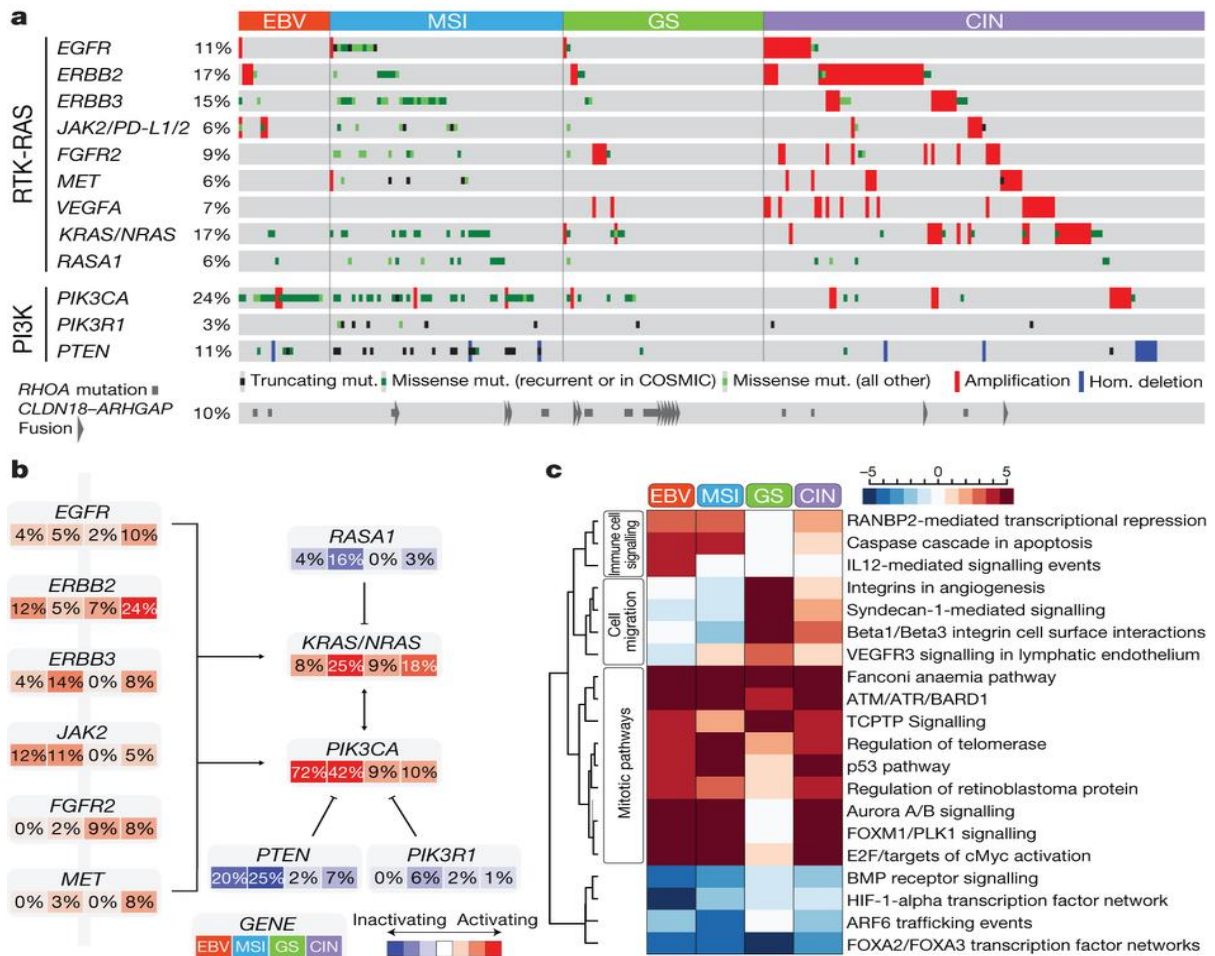


Figure 6.1 TCGA comprehensive gastric cancer molecular characterizations. “(A) Mutations, copy-number changes and translocations for select genes are shown across samples organized by molecular subtypes. (B) Alterations in RTK/RAS and RTK/PI3K signaling pathways across molecular subtypes. Red denotes predicted activation; blue denotes predicted inactivation. (C) The heatmap shows NCI-PID pathways that are significantly elevated (red) or decreased (blue) in each of the four subtypes as compared with non-malignant gastric mucosa.”(27)

*Reprinted with the permission of Nature Publishing Group. Comprehensive molecular characterization of gastric adenocarcinoma. (2014) The Cancer Genome Atlas Research Network (27).

6.3 Final Discussion:

In conclusion, I believe this thesis provides knowledgeable insight into the molecular mechanisms related to sensitivity and resistance to MET antagonists in gastric cancer. The advancements and setbacks within the field have only proven to make MET a more attractive target for research and the need for better biomarkers, patient selection, and MET targeted therapeutics is of the utmost importance.

While working on this project for the past several years one thing has become abundantly clear to me, the future successes of life science research will depend on a seamless integration of diverse disciplines. For years biologic researchers have been reluctant to collaborate with each other, even within their own institutions. It is my belief that collaboration inside our field and from many other fields of study is paramount to the future successes of life science advancements. Fortunately, we have seen advances in the way researchers collaborate through the design of large-scale multicenter collaboration networks. The Cancer Prevention and Control Research Network is one such network that has propelled the field of cancer prevention through its network of eleven distinct research institutions. Together these institutions have produced 249 multisite collaborative peer-reviewed scientific publications and contributed to the increase in cancer screening and decrease of cancer risk and cancer-related deaths (175). Other networks, such as The Cancer Genome Atlas (TCGA) Research Network have also been successful in driving the accelerated advancement of breakthroughs in understanding the molecular basis of cancer development in 33 cancer types. Through the collaboration of twenty institutions in the United States and Canada the TCGA has made breakthroughs in defining cancer sub-types

and the genomic foundations of cancer and then translating these results into valid therapeutic targets (176). Despite these advancements in large scale collaborative networks focused on cancer management, treatment, and prevention these intra-field collaborations are not enough to propel research into the next generation. We have to start utilizing the knowledge and fresh insights that other diverse disciplines can contribute. It is my belief that this multi-field collaboration will ultimately lead to break-through innovations we would not have otherwise achieved.

The time I have spent at this world-class cancer institution has given me the tools and understanding of how to conduct high quality research as well as the compassion and drive to understand how important every experiment is in the race to find the cure for cancer. The creation of the “moon shots” initiative has been a driving force in the advancement of cancer research worldwide. The parallels are not lost on me between MD Andersons initiative and the original “moon shot” program developed by NASA. Neil Armstrong was a pioneer of space exploration during a time that we were in our infancy of knowledge and understanding in the field, but he knew that “research is creating new knowledge” and because of this passion and understanding of the importance of scientific research and exploration he became the first man to ever walk on the moon. I can only hope that the drive and passion I have for cancer research will one day make a contribution towards fighting the greatest biomedical challenge of my generation.

Chapter 7. BIBLIOGRAPHY

1. Ferlay, J., I. Soerjomataram, R. Dikshit, S. Eser, C. Mathers, M. Rebelo, D. M. Parkin, D. Forman, and F. Bray. 2015. Cancer incidence and mortality worldwide: sources, methods and major patterns in GLOBOCAN 2012. *International journal of cancer. Journal international du cancer* 136: E359-386.
2. Ferlay, J., H. R. Shin, F. Bray, D. Forman, C. Mathers, and D. M. Parkin. 2010. Estimates of worldwide burden of cancer in 2008: GLOBOCAN 2008. *International journal of cancer. Journal international du cancer* 127: 2893-2917.
3. Parkin, D. M. 2001. Global cancer statistics in the year 2000. *The lancet oncology* 2: 533-543.
4. M. Ervik, F. L., J. Ferlay, L. Mery, I. Soerjomataram, F. Bray (2016). Cancer Today. Lyon, France: International Agency for Research on Cancer. Cancer Today. Available from: <http://gco.iarc.fr/today>, accessed [25/April/2017].
5. Torre, L. A., F. Bray, R. L. Siegel, J. Ferlay, J. Lortet-Tieulent, and A. Jemal. 2015. Global cancer statistics, 2012. *CA Cancer J Clin* 65: 87-108.
6. Zali, H., M. Rezaei-Tavirani, and M. Azodi. 2011. Gastric cancer: prevention, risk factors and treatment. *Gastroenterol Hepatol Bed Bench* 4: 175-185.
7. Hundahl, S. A., J. L. Phillips, and H. R. Menck. 2000. The National Cancer Data Base Report on poor survival of U.S. gastric carcinoma patients treated with gastrectomy: Fifth Edition American Joint Committee on Cancer staging, proximal disease, and the "different disease" hypothesis. *Cancer* 88: 921-932.

8. Sheh, A., Z. Ge, N. M. Parry, S. Muthupalani, J. E. Rager, A. R. Raczynski, M. W. Mobley, A. F. McCabe, R. C. Fry, T. C. Wang, and J. G. Fox. 2011. 17beta-estradiol and tamoxifen prevent gastric cancer by modulating leukocyte recruitment and oncogenic pathways in Helicobacter pylori-infected INS-GAS male mice. *Cancer Prev Res (Phila)* 4: 1426-1435.
9. Hu, B., N. El Hajj, S. Sittler, N. Lammert, R. Barnes, and A. Meloni-Ehrig. 2012. Gastric cancer: Classification, histology and application of molecular pathology. *J Gastrointest Oncol* 3: 251-261.
10. Wong, H., and T. Yau. 2013. Molecular targeted therapies in advanced gastric cancer: does tumor histology matter? *Therap Adv Gastroenterol* 6: 15-31.
11. Adachi, Y., K. Yasuda, M. Inomata, K. Sato, N. Shiraishi, and S. Kitano. 2000. Pathology and prognosis of gastric carcinoma: well versus poorly differentiated type. *Cancer* 89: 1418-1424.
12. Morishita, A., J. Gong, and T. Masaki. 2014. Targeting receptor tyrosine kinases in gastric cancer. *World journal of gastroenterology : WJG* 20: 4536-4545.
13. Dicken, B. J., D. L. Bigam, C. Cass, J. R. Mackey, A. A. Joy, and S. M. Hamilton. 2005. Gastric adenocarcinoma: review and considerations for future directions. *Annals of surgery* 241: 27-39.
14. Ajani, J. A., T. A. D'Amico, K. Almhanna, D. J. Bentrem, J. Chao, P. Das, C. S. Denlinger, P. Fanta, F. Farjah, C. S. Fuchs, H. Gerdes, M. Gibson, R. E. Glasgow, J. A. Hayman, S.

- Hochwald, W. L. Hofstetter, D. H. Ilson, D. Jaroszewski, K. L. Johung, R. N. Keswani, L. R. Kleinberg, W. M. Korn, S. Leong, C. Linn, A. C. Lockhart, Q. P. Ly, M. F. Mulcahy, M. B. Orringer, K. A. Perry, G. A. Poultsides, W. J. Scott, V. E. Strong, M. K. Washington, B. Weksler, C. G. Willett, C. D. Wright, D. Zelman, N. McMillian, and H. Sundar. 2016. Gastric Cancer, Version 3.2016, NCCN Clinical Practice Guidelines in Oncology. *J Natl Compr Canc Netw* 14: 1286-1312.
15. Shawver, L. K., D. Slamon, and A. Ullrich. 2002. Smart drugs: tyrosine kinase inhibitors in cancer therapy. *Cancer cell* 1: 117-123.
 16. Regad, T. 2015. Targeting RTK Signaling Pathways in Cancer. *Cancers* 7: 1758-1784.
 17. Sangwan, V., and M. Park. 2006. Receptor tyrosine kinases: role in cancer progression. *Curr Oncol* 13: 191-193.
 18. Deng, N., L. K. Goh, H. Wang, K. Das, J. Tao, I. B. Tan, S. Zhang, M. Lee, J. Wu, K. H. Lim, Z. Lei, G. Goh, Q. Y. Lim, A. L. Tan, D. Y. Sin Poh, S. Riahi, S. Bell, M. M. Shi, R. Linnartz, F. Zhu, K. G. Yeoh, H. C. Toh, W. P. Yong, H. C. Cheong, S. Y. Rha, A. Boussioutas, H. Grabsch, S. Rozen, and P. Tan. 2012. A comprehensive survey of genomic alterations in gastric cancer reveals systematic patterns of molecular exclusivity and co-occurrence among distinct therapeutic targets. *Gut* 61: 673-684.
 19. Organ, S. L., and M. S. Tsao. 2011. An overview of the c-MET signaling pathway. *Therapeutic advances in medical oncology* 3: S7-S19.

20. Birchmeier, C., W. Birchmeier, E. Gherardi, and G. F. Vande Woude. 2003. Met, metastasis, motility and more. *Nature reviews. Molecular cell biology* 4: 915-925.
21. Furge, K. A., Y. W. Zhang, and G. F. Vande Woude. 2000. Met receptor tyrosine kinase: enhanced signaling through adapter proteins. *Oncogene* 19: 5582-5589.
22. Granito, A., E. Guidetti, and L. Gramantieri. 2015. c-MET receptor tyrosine kinase as a molecular target in advanced hepatocellular carcinoma. *J Hepatocell Carcinoma* 2: 29-38.
23. Sierra, J. R., and M. S. Tsao. 2011. c-MET as a potential therapeutic target and biomarker in cancer. *Therapeutic advances in medical oncology* 3: S21-35.
24. An, X., F. Wang, Q. Shao, F. H. Wang, Z. Q. Wang, C. Chen, C. Li, H. Y. Luo, D. S. Zhang, R. H. Xu, and Y. H. Li. 2014. MET amplification is not rare and predicts unfavorable clinical outcomes in patients with recurrent/metastatic gastric cancer after chemotherapy. *Cancer* 120: 675-682.
25. Lee, H. E., M. A. Kim, H. S. Lee, E. J. Jung, H. K. Yang, B. L. Lee, Y. J. Bang, and W. H. Kim. 2012. MET in gastric carcinomas: comparison between protein expression and gene copy number and impact on clinical outcome. *British journal of cancer* 107: 325-333.
26. Shi, J., D. Yao, W. Liu, N. Wang, H. Lv, N. He, B. Shi, P. Hou, and M. Ji. 2012. Frequent gene amplification predicts poor prognosis in gastric cancer. *International journal of molecular sciences* 13: 4714-4726.

27. 2014. Comprehensive molecular characterization of gastric adenocarcinoma. *Nature* 513: 202-209.
28. Lee, J., J. W. Seo, H. J. Jun, C. S. Ki, S. H. Park, Y. S. Park, H. Y. Lim, M. G. Choi, J. M. Bae, T. S. Sohn, J. H. Noh, S. Kim, H. L. Jang, J. Y. Kim, K. M. Kim, W. K. Kang, and J. O. Park. 2011. Impact of MET amplification on gastric cancer: possible roles as a novel prognostic marker and a potential therapeutic target. *Oncology reports* 25: 1517-1524.
29. Wang, X., M. C. DeFrances, Y. Dai, P. Pediaditakis, C. Johnson, A. Bell, G. K. Michalopoulos, and R. Zarnegar. 2002. A mechanism of cell survival: sequestration of Fas by the HGF receptor Met. *Molecular cell* 9: 411-421.
30. Lee, D., E. S. Sung, J. H. Ahn, S. An, J. Huh, and W. K. You. 2015. Development of antibody-based c-Met inhibitors for targeted cancer therapy. *Immunotargets Ther* 4: 35-44.
31. Lennerz, J. K., E. L. Kwak, A. Ackerman, M. Michael, S. B. Fox, K. Bergethon, G. Y. Lauwers, J. G. Christensen, K. D. Wilner, D. A. Haber, R. Salgia, Y. J. Bang, J. W. Clark, B. J. Solomon, and A. J. Iafrate. 2011. MET amplification identifies a small and aggressive subgroup of esophagogastric adenocarcinoma with evidence of responsiveness to crizotinib. *Journal of clinical oncology : official journal of the American Society of Clinical Oncology* 29: 4803-4810.

32. Graziano, F., N. Galluccio, P. Lorenzini, A. Ruzzo, E. Canestrari, S. D'Emidio, V. Catalano, V. Sisti, C. Ligorio, F. Andreoni, E. Rulli, E. Di Oto, G. Fiorentini, C. Zingaretti, M. De Nictolis, F. Cappuzzo, and M. Magnani. 2011. Genetic activation of the MET pathway and prognosis of patients with high-risk, radically resected gastric cancer. *Journal of clinical oncology : official journal of the American Society of Clinical Oncology* 29: 4789-4795.
33. Teng, L., and J. Lu. 2013. cMET as a potential therapeutic target in gastric cancer (Review). *International journal of molecular medicine* 32: 1247-1254.
34. Bradley, C. A., M. Salto-Tellez, P. Laurent-Puig, A. Bardelli, C. Rolfo, J. Tabernero, H. A. Khawaja, M. Lawler, P. G. Johnston, S. Van Schaeybroeck, and M. E. consortium. 2017. Targeting c-MET in gastrointestinal tumours: rationale, opportunities and challenges. *Nature reviews. Clinical oncology*.
35. Inokuchi, M., S. Otsuki, Y. Fujimori, Y. Sato, M. Nakagawa, and K. Kojima. 2015. Clinical significance of MET in gastric cancer. *World J Gastrointest Oncol* 7: 317-327.
36. Okamoto, W., I. Okamoto, K. Tanaka, E. Hatashita, Y. Yamada, K. Kuwata, H. Yamaguchi, T. Arao, K. Nishio, M. Fukuoka, P. A. Janne, and K. Nakagawa. 2010. TAK-701, a humanized monoclonal antibody to hepatocyte growth factor, reverses gefitinib resistance induced by tumor-derived HGF in non-small cell lung cancer with an EGFR mutation. *Molecular cancer therapeutics* 9: 2785-2792.

37. Kang, Y. K., K. Muro, M. H. Ryu, H. Yasui, T. Nishina, B. Y. Ryoo, Y. Kamiya, S. Akinaga, and N. Boku. 2014. A phase II trial of a selective c-Met inhibitor tivantinib (ARQ 197) monotherapy as a second- or third-line therapy in the patients with metastatic gastric cancer. *Investigational new drugs* 32: 355-361.
38. Garajova, I., E. Giovannetti, G. Biasco, and G. J. Peters. 2015. c-Met as a Target for Personalized Therapy. *Transl Oncogenomics* 7: 13-31.
39. Finley, R. S. 2003. Overview of targeted therapies for cancer. *Am J Health Syst Pharm* 60: S4-10.
40. Arora, A., and E. M. Scholar. 2005. Role of tyrosine kinase inhibitors in cancer therapy. *J Pharmacol Exp Ther* 315: 971-979.
41. Ludwig, D. L., D. S. Pereira, Z. Zhu, D. J. Hicklin, and P. Bohlen. 2003. Monoclonal antibody therapeutics and apoptosis. *Oncogene* 22: 9097-9106.
42. Smolen, G. A., R. Sordella, B. Muir, G. Mohapatra, A. Barmettler, H. Archibald, W. J. Kim, R. A. Okimoto, D. W. Bell, D. C. Sgroi, J. G. Christensen, J. Settleman, and D. A. Haber. 2006. Amplification of MET may identify a subset of cancers with extreme sensitivity to the selective tyrosine kinase inhibitor PHA-665752. *Proceedings of the National Academy of Sciences of the United States of America* 103: 2316-2321.
43. Okamoto, W., I. Okamoto, T. Arao, K. Kuwata, E. Hatashita, H. Yamaguchi, K. Sakai, K. Yanagihara, K. Nishio, and K. Nakagawa. 2012. Antitumor action of the MET tyrosine

- kinase inhibitor crizotinib (PF-02341066) in gastric cancer positive for MET amplification. *Molecular cancer therapeutics* 11: 1557-1564.
44. Elmore, S. 2007. Apoptosis: a review of programmed cell death. *Toxicologic pathology* 35: 495-516.
 45. Ichim, G., and S. W. Tait. 2016. A fate worse than death: apoptosis as an oncogenic process. *Nature reviews. Cancer* 16: 539-548.
 46. McIlwain, D. R., T. Berger, and T. W. Mak. 2015. Caspase functions in cell death and disease. *Cold Spring Harbor perspectives in biology* 7.
 47. Fulda, S., and K. M. Debatin. 2006. Extrinsic versus intrinsic apoptosis pathways in anticancer chemotherapy. *Oncogene* 25: 4798-4811.
 48. Beesoo, R., V. Neergheen-Bhujun, R. Bhagooli, and T. Bahorun. 2014. Apoptosis inducing lead compounds isolated from marine organisms of potential relevance in cancer treatment. *Mutat Res* 768: 84-97.
 49. Lai, A. Z., S. Cory, H. Zhao, M. Gigoux, A. Monast, M. C. Guiot, S. Huang, A. Tofigh, C. Thompson, M. Naujokas, V. A. Marcus, N. Bertos, B. Sehat, R. M. Perera, E. S. Bell, B. D. Page, P. T. Gunning, L. E. Ferri, M. Hallett, and M. Park. 2014. Dynamic reprogramming of signaling upon met inhibition reveals a mechanism of drug resistance in gastric cancer. *Science signaling* 7: ra38.

50. White, E. 2015. The role for autophagy in cancer. *The Journal of clinical investigation* 125: 42-46.
51. White, E. 2012. Q&A: Eileen White on understanding autophagy. *Cancer discovery* 2: 863.
52. White, E., and R. S. DiPaola. 2009. The double-edged sword of autophagy modulation in cancer. *Clinical cancer research : an official journal of the American Association for Cancer Research* 15: 5308-5316.
53. Alers, S., A. S. Loffler, S. Wesselborg, and B. Stork. 2012. Role of AMPK-mTOR-Ulk1/2 in the regulation of autophagy: cross talk, shortcuts, and feedbacks. *Molecular and cellular biology* 32: 2-11.
54. Heras-Sandoval, D., J. M. Perez-Rojas, J. Hernandez-Damian, and J. Pedraza-Chaverri. 2014. The role of PI3K/AKT/mTOR pathway in the modulation of autophagy and the clearance of protein aggregates in neurodegeneration. *Cellular signalling* 26: 2694-2701.
55. Bhaskar, P. T., and N. Hay. 2007. The two TORCs and Akt. *Developmental cell* 12: 487-502.
56. Kim, J., M. Kundu, B. Viollet, and K. L. Guan. 2011. AMPK and mTOR regulate autophagy through direct phosphorylation of Ulk1. *Nature cell biology* 13: 132-141.

57. Sarkar, S. 2013. Regulation of autophagy by mTOR-dependent and mTOR-independent pathways: autophagy dysfunction in neurodegenerative diseases and therapeutic application of autophagy enhancers. *Biochem Soc Trans* 41: 1103-1130.
58. Mizushima, N. 2007. Autophagy: process and function. *Genes & development* 21: 2861-2873.
59. Tanida, I., T. Ueno, and E. Kominami. 2008. LC3 and Autophagy. *Methods Mol Biol* 445: 77-88.
60. Tian, Y., L. Wang, and J. H. Ou. 2015. Autophagy, a double-edged sword in hepatocarcinogenesis. *Mol Cell Oncol* 2: e1004968.
61. Cicchini, M., V. Karantza, and B. Xia. 2015. Molecular pathways: autophagy in cancer--a matter of timing and context. *Clinical cancer research : an official journal of the American Association for Cancer Research* 21: 498-504.
62. Marino, G., M. Niso-Santano, E. H. Baehrecke, and G. Kroemer. 2014. Self-consumption: the interplay of autophagy and apoptosis. *Nature reviews. Molecular cell biology* 15: 81-94.
63. Nishida, K., O. Yamaguchi, and K. Otsu. 2008. Crosstalk between autophagy and apoptosis in heart disease. *Circ Res* 103: 343-351.
64. Glick, D., S. Barth, and K. F. Macleod. 2010. Autophagy: cellular and molecular mechanisms. *The Journal of pathology* 221: 3-12.

65. Barretina, J., G. Caponigro, N. Stransky, K. Venkatesan, A. A. Margolin, S. Kim, C. J. Wilson, J. Lehar, G. V. Kryukov, D. Sonkin, A. Reddy, M. Liu, L. Murray, M. F. Berger, J. E. Monahan, P. Morais, J. Meltzer, A. Korejwa, J. Jane-Valbuena, F. A. Mapa, J. Thibault, E. Bric-Furlong, P. Raman, A. Shipway, I. H. Engels, J. Cheng, G. K. Yu, J. Yu, P. Aspesi, Jr., M. de Silva, K. Jagtap, M. D. Jones, L. Wang, C. Hatton, E. Palesscandolo, S. Gupta, S. Mahan, C. Sougnez, R. C. Onofrio, T. Liefeld, L. MacConaill, W. Winckler, M. Reich, N. Li, J. P. Mesirov, S. B. Gabriel, G. Getz, K. Ardlie, V. Chan, V. E. Myer, B. L. Weber, J. Porter, M. Warmuth, P. Finan, J. L. Harris, M. Meyerson, T. R. Golub, M. P. Morrissey, W. R. Sellers, R. Schlegel, and L. A. Garraway. 2012. The Cancer Cell Line Encyclopedia enables predictive modelling of anticancer drug sensitivity. *Nature* 483: 603-607.
66. Kassouf, W., C. P. Dinney, G. Brown, D. J. McConkey, A. J. Diehl, M. Bar-Eli, and L. Adam. 2005. Uncoupling between epidermal growth factor receptor and downstream signals defines resistance to the antiproliferative effect of Gefitinib in bladder cancer cells. *Cancer research* 65: 10524-10535.
67. Kawakami, H., I. Okamoto, T. Arao, W. Okamoto, K. Matsumoto, H. Taniguchi, K. Kuwata, H. Yamaguchi, K. Nishio, K. Nakagawa, and Y. Yamada. 2013. MET amplification as a potential therapeutic target in gastric cancer. *Oncotarget* 4: 9-17.
68. Riccardi, C., and I. Nicoletti. 2006. Analysis of apoptosis by propidium iodide staining and flow cytometry. *Nat Protoc* 1: 1458-1461.

69. Cheng, T., B. Roth, W. Choi, P. C. Black, C. Dinney, and D. J. McConkey. 2013. Fibroblast growth factor receptors-1 and -3 play distinct roles in the regulation of bladder cancer growth and metastasis: implications for therapeutic targeting. *PLoS One* 8: e57284.
70. Choi, W., S. Porten, S. Kim, D. Willis, E. R. Plimack, J. Hoffman-Censits, B. Roth, T. Cheng, M. Tran, I. L. Lee, J. Melquist, J. Bondaruk, T. Majewski, S. Zhang, S. Pretzsch, K. Baggerly, A. Siefker-Radtke, B. Czerniak, C. P. Dinney, and D. J. McConkey. 2014. Identification of distinct basal and luminal subtypes of muscle-invasive bladder cancer with different sensitivities to frontline chemotherapy. *Cancer cell* 25: 152-165.
71. Tran, M. N., W. Choi, M. F. Wszolek, N. Navai, I. L. Lee, G. Nitti, S. Wen, E. R. Flores, A. Siefker-Radtke, B. Czerniak, C. Dinney, M. Barton, and D. J. McConkey. 2013. The p63 protein isoform DeltaNp63alpha inhibits epithelial-mesenchymal transition in human bladder cancer cells: role of MIR-205. *The Journal of biological chemistry* 288: 3275-3288.
72. Marx, V. 2015. Autophagy: eat thyself, sustain thyself. *Nat Methods* 12: 1121-1125.
73. Strober, W. 2015. Trypan Blue Exclusion Test of Cell Viability. *Curr Protoc Immunol* 111: A3 B 1-3.

74. Crouch, S. P., R. Kozlowski, K. J. Slater, and J. Fletcher. 1993. The use of ATP bioluminescence as a measure of cell proliferation and cytotoxicity. *Journal of immunological methods* 160: 81-88.
75. Chandra, J., I. Niemer, J. Gilbreath, K. O. Kliche, M. Andreeff, E. J. Freireich, M. Keating, and D. J. McConkey. 1998. Proteasome inhibitors induce apoptosis in glucocorticoid-resistant chronic lymphocytic leukemic lymphocytes. *Blood* 92: 4220-4229.
76. Hughes, P. E., K. Rex, S. Caenepeel, Y. Yang, Y. Zhang, M. A. Broome, H. T. Kha, T. L. Burgess, B. Amore, P. J. Kaplan-Lefko, J. Moriguchi, J. Werner, M. A. Damore, D. Baker, D. M. Choquette, J. C. Harmange, R. Radinsky, R. Kendall, I. Dussault, and A. Coxon. 2016. In Vitro and In Vivo Activity of AMG 337, a Potent and Selective MET Kinase Inhibitor, in MET-Dependent Cancer Models. *Molecular cancer therapeutics* 15: 1568-1579.
77. Hong, D. S., P. LoRusso, O. Hamid, D. M. Beaupre, F. Janku, R. Khan, M. Kittaneh, R. D. Loberg, B. Amore, I. Caudillo, Y. C. Hwang, R. Rui Tang, G. Ngarmchamnanrith, and E. L. Kwak. First-in-human study of AMG 337, a highly selective oral inhibitor of MET, in adult patients (pts) with advanced solid tumors. *J Clin Oncol* 32:5s, 2014 (suppl; abstr 2508).
78. Sahu, A., K. Prabhash, V. Noronha, A. Joshi, and S. Desai. 2013. Crizotinib: A comprehensive review. *South Asian J Cancer* 2: 91-97.

79. Camidge, D. R., Y. J. Bang, E. L. Kwak, A. J. Iafrate, M. Varella-Garcia, S. B. Fox, G. J. Riely, B. Solomon, S. H. Ou, D. W. Kim, R. Salgia, P. Fidias, J. A. Engelman, L. Gandhi, P. A. Janne, D. B. Costa, G. I. Shapiro, P. Lorusso, K. Ruffner, P. Stephenson, Y. Tang, K. Wilner, J. W. Clark, and A. T. Shaw. 2012. Activity and safety of crizotinib in patients with ALK-positive non-small-cell lung cancer: updated results from a phase 1 study. *The lancet oncology* 13: 1011-1019.
80. Cui, J. J., M. Tran-Dube, H. Shen, M. Nambu, P. P. Kung, M. Pairish, L. Jia, J. Meng, L. Funk, I. Botrous, M. McTigue, N. Grodsky, K. Ryan, E. Padrique, G. Alton, S. Timofeevski, S. Yamazaki, Q. Li, H. Zou, J. Christensen, B. Mroczkowski, S. Bender, R. S. Kania, and M. P. Edwards. 2011. Structure based drug design of crizotinib (PF-02341066), a potent and selective dual inhibitor of mesenchymal-epithelial transition factor (c-MET) kinase and anaplastic lymphoma kinase (ALK). *Journal of medicinal chemistry* 54: 6342-6363.
81. National Center for Biotechnology Information. PubChem Compound Database; CID=11626560, h. p. n. n. n. g. c. a. J., 2017).
82. Yang, W., J. Soares, P. Greninger, E. J. Edelman, H. Lightfoot, S. Forbes, N. Bindal, D. Beare, J. A. Smith, I. R. Thompson, S. Ramaswamy, P. A. Futreal, D. A. Haber, M. R. Stratton, C. Benes, U. McDermott, and M. J. Garnett. 2013. Genomics of Drug Sensitivity in Cancer (GDSC): a resource for therapeutic biomarker discovery in cancer cells. *Nucleic acids research* 41: D955-961.

83. Asaoka, Y., M. Tada, T. Ikenoue, M. Seto, M. Imai, K. Miyabayashi, K. Yamamoto, S. Yamamoto, Y. Kudo, D. Mohri, Y. Isomura, H. Ijichi, K. Tateishi, F. Kanai, S. Ogawa, M. Omata, and K. Koike. 2010. Gastric cancer cell line Hs746T harbors a splice site mutation of c-Met causing juxtamembrane domain deletion. *Biochemical and biophysical research communications* 394: 1042-1046.
84. Uyy, E., V. I. Suica, R. M. Boteanu, D. Manda, A. E. Baci, C. Badiu, and F. Antohe. 2016. Endoplasmic Reticulum Chaperones Are Potential Active Factors in Thyroid Tumorigenesis. *Journal of proteome research* 15: 3377-3387.
85. Matsubara, D., S. Ishikawa, S. Oguni, H. Aburatani, M. Fukayama, and T. Niki. 2010. Molecular predictors of sensitivity to the MET inhibitor PHA665752 in lung carcinoma cells. *Journal of thoracic oncology : official publication of the International Association for the Study of Lung Cancer* 5: 1317-1324.
86. Koenig, M. N., E. Naik, L. Rohrbeck, M. J. Herold, E. Trounson, P. Bouillet, T. Thomas, A. K. Voss, A. Strasser, and L. Coultas. 2014. Pro-apoptotic BIM is an essential initiator of physiological endothelial cell death independent of regulation by FOXO3. *Cell death and differentiation* 21: 1687-1695.
87. Corbitt, A. J., N. Bennion, and S. J. Forsythe. 2000. Adenylate kinase amplification of ATP bioluminescence for hygiene monitoring in the food and beverage industry. *Lett Appl Microbiol* 30: 443-447.

88. Deveraux, Q. L., R. Takahashi, G. S. Salvesen, and J. C. Reed. 1997. X-linked IAP is a direct inhibitor of cell-death proteases. *Nature* 388: 300-304.
89. Galban, S., and C. S. Duckett. 2010. XIAP as a ubiquitin ligase in cellular signaling. *Cell death and differentiation* 17: 54-60.
90. O'Connor, L., A. Strasser, L. A. O'Reilly, G. Hausmann, J. M. Adams, S. Cory, and D. C. Huang. 1998. Bim: a novel member of the Bcl-2 family that promotes apoptosis. *EMBO J* 17: 384-395.
91. Aprile, G., F. Leone, R. Giampieri, M. Casagrande, D. Marino, L. Faloppi, S. Cascinu, G. Fasola, and M. Scartozzi. 2015. Tracking the 2015 Gastrointestinal Cancers Symposium: bridging cancer biology to clinical gastrointestinal oncology. *Onco Targets Ther* 8: 1149-1156.
92. Janjigian, Y. Y., L. H. Tang, D. G. Coit, D. P. Kelsen, T. D. Francone, M. R. Weiser, S. C. Jhanwar, and M. A. Shah. 2011. MET expression and amplification in patients with localized gastric cancer. *Cancer epidemiology, biomarkers & prevention : a publication of the American Association for Cancer Research, cosponsored by the American Society of Preventive Oncology* 20: 1021-1027.
93. Yap, T. A., D. Olmos, A. T. Brunetto, N. Tunariu, J. Barriuso, R. Riisnaes, L. Pope, J. Clark, A. Futreal, M. Germuska, D. Collins, N. M. deSouza, M. O. Leach, R. E. Savage, C. Waghorne, F. Chai, E. Garmey, B. Schwartz, S. B. Kaye, and J. S. de Bono. 2011. Phase I trial of a selective c-MET inhibitor ARQ 197 incorporating proof of

- mechanism pharmacodynamic studies. *Journal of clinical oncology : official journal of the American Society of Clinical Oncology* 29: 1271-1279.
94. Smith, H. S. 1979. In vitro properties of epithelial cell lines established from human carcinomas and nonmalignant tissue. *Journal of the National Cancer Institute* 62: 225-230.
95. Liu, X., Y. Jia, M. B. Stoopler, Y. Shen, H. Cheng, J. Chen, M. Mansukhani, S. Koul, B. Halmos, and A. C. Borczuk. 2016. Next-Generation Sequencing of Pulmonary Sarcomatoid Carcinoma Reveals High Frequency of Actionable MET Gene Mutations. *Journal of clinical oncology : official journal of the American Society of Clinical Oncology* 34: 794-802.
96. Segaliny, A. I., M. Tellez-Gabriel, M. F. Heymann, and D. Heymann. 2015. Receptor tyrosine kinases: Characterisation, mechanism of action and therapeutic interests for bone cancers. *J Bone Oncol* 4: 1-12.
97. Li, E., and K. Hristova. 2010. Receptor tyrosine kinase transmembrane domains: Function, dimer structure and dimerization energetics. *Cell adhesion & migration* 4: 249-254.
98. Shokat, K. M. 2014. Methods in Enzymology. Protein kinase inhibitors in research and medicine. Preface. *Methods in enzymology* 548: xi-xii.

99. Hedger, G., M. S. Sansom, and H. Koldso. 2015. The juxtamembrane regions of human receptor tyrosine kinases exhibit conserved interaction sites with anionic lipids. *Scientific reports* 5: 9198.
100. de Aguirre, I., A. Salvatierra, A. Font, J. L. Mate, M. Perez, M. Botia, M. Taron, and R. Rosell. 2006. c-Met Mutational Analysis in the Sema and Juxtamembrane Domains in Small-Cell-Lung-Cancer. *Transl Oncogenomics* 1: 11-18.
101. Kong-Beltran, M., S. Seshagiri, J. Zha, W. Zhu, K. Bhawe, N. Mendoza, T. Holcomb, K. Pujara, J. Stinson, L. Fu, C. Severin, L. Rangell, R. Schwall, L. Amler, D. Wickramasinghe, and R. Yauch. 2006. Somatic mutations lead to an oncogenic deletion of met in lung cancer. *Cancer research* 66: 283-289.
102. Aveic, S., and G. P. Tonini. 2016. Resistance to receptor tyrosine kinase inhibitors in solid tumors: can we improve the cancer fighting strategy by blocking autophagy? *Cancer cell international* 16: 62.
103. Weinstein, I. B., and A. Joe. 2008. Oncogene addiction. *Cancer research* 68: 3077-3080; discussion 3080.
104. Alexander, P. B., and X. F. Wang. 2015. Resistance to receptor tyrosine kinase inhibition in cancer: molecular mechanisms and therapeutic strategies. *Front Med* 9: 134-138.
105. Huang, L., and L. Fu. 2015. Mechanisms of resistance to EGFR tyrosine kinase inhibitors. *Acta Pharm Sin B* 5: 390-401.

106. Pohlmann, P. R., I. A. Mayer, and R. Mernaugh. 2009. Resistance to Trastuzumab in Breast Cancer. *Clinical cancer research : an official journal of the American Association for Cancer Research* 15: 7479-7491.
107. Engelman, J. A. 2009. Targeting PI3K signalling in cancer: opportunities, challenges and limitations. *Nature reviews. Cancer* 9: 550-562.
108. Chen, M., N. Rothman, Y. Ye, J. Gu, P. A. Scheet, M. Huang, D. W. Chang, C. P. Dinney, D. T. Silverman, J. D. Figueroa, S. J. Chanock, and X. Wu. 2016. Pathway analysis of bladder cancer genome-wide association study identifies novel pathways involved in bladder cancer development. *Genes Cancer* 7: 229-239.
109. Liberzon, A., C. Birger, H. Thorvaldsdottir, M. Ghandi, J. P. Mesirov, and P. Tamayo. 2015. The Molecular Signatures Database (MSigDB) hallmark gene set collection. *Cell Syst* 1: 417-425.
110. Kim, Y. C., and K. L. Guan. 2015. mTOR: a pharmacologic target for autophagy regulation. *The Journal of clinical investigation* 125: 25-32.
111. Martina, J. A., Y. Chen, M. Gucek, and R. Puertollano. 2012. MTORC1 functions as a transcriptional regulator of autophagy by preventing nuclear transport of TFEB. *Autophagy* 8: 903-914.
112. Ashburner, M., C. A. Ball, J. A. Blake, D. Botstein, H. Butler, J. M. Cherry, A. P. Davis, K. Dolinski, S. S. Dwight, J. T. Eppig, M. A. Harris, D. P. Hill, L. Issel-Tarver, A. Kasarskis, S. Lewis, J. C. Matese, J. E. Richardson, M. Ringwald, G. M. Rubin, and G.

- Sherlock. 2000. Gene ontology: tool for the unification of biology. The Gene Ontology Consortium. *Nature genetics* 25: 25-29.
113. Gene Ontology, C. 2015. Gene Ontology Consortium: going forward. *Nucleic acids research* 43: D1049-1056.
114. Zhang, H., Q. Guo, C. Wang, L. Yan, Y. Fu, M. Fan, X. Zhao, and M. Li. 2013. Dual-specificity phosphatase 6 (Dusp6), a negative regulator of FGF2/ERK1/2 signaling, enhances 17beta-estradiol-induced cell growth in endometrial adenocarcinoma cell. *Molecular and cellular endocrinology* 376: 60-69.
115. Zhang, Z., S. Kobayashi, A. C. Borczuk, R. S. Leidner, T. Laframboise, A. D. Levine, and B. Halmos. 2010. Dual specificity phosphatase 6 (DUSP6) is an ETS-regulated negative feedback mediator of oncogenic ERK signaling in lung cancer cells. *Carcinogenesis* 31: 577-586.
116. Kidger, A. M., and S. M. Keyse. 2016. The regulation of oncogenic Ras/ERK signalling by dual-specificity mitogen activated protein kinase phosphatases (MKPs). *Seminars in cell & developmental biology* 50: 125-132.
117. Nguyet Minh Hoang, O. R. P., Brian Danysh and Marie Claude Hofmann. 2011. ETV5, an Ets Family Transcription Factor, is a Marker for RAS-Dependent Papillary Thyroid Cancer. *The FASEB Journal* vol. 30 no. 1 Supplement 1119.1.
118. Akagi, T., S. Kuure, K. Uranishi, H. Koide, F. Costantini, and T. Yokota. 2015. ETS-related transcription factors ETV4 and ETV5 are involved in proliferation and

- induction of differentiation-associated genes in embryonic stem (ES) cells. *The Journal of biological chemistry* 290: 22460-22473.
119. Schmidt, E. V. 1999. The role of c-myc in cellular growth control. *Oncogene* 18: 2988-2996.
120. Dang, C. V. 2013. MYC, metabolism, cell growth, and tumorigenesis. *Cold Spring Harb Perspect Med* 3.
121. Kurita, K., M. Maeda, M. A. Mansour, T. Kokuryo, K. Uehara, Y. Yokoyama, M. Nagino, M. Hamaguchi, and T. Senga. 2016. TRIP13 is expressed in colorectal cancer and promotes cancer cell invasion. *Oncol Lett* 12: 5240-5246.
122. Zhou, K., W. Zhang, Q. Zhang, R. Gui, H. Zhao, X. Chai, Y. Li, X. Wei, and Y. Song. 2017. Loss of thyroid hormone receptor interactor 13 inhibits cell proliferation and survival in human chronic lymphocytic leukemia. *Oncotarget* 8: 25469-25481.
123. Bauerschmidt, C., S. Pollok, E. Kremmer, H. P. Nasheuer, and F. Grosse. 2007. Interactions of human Cdc45 with the Mcm2-7 complex, the GINS complex, and DNA polymerases delta and epsilon during S phase. *Genes Cells* 12: 745-758.
124. Pollok, S., C. Bauerschmidt, J. Sanger, H. P. Nasheuer, and F. Grosse. 2007. Human Cdc45 is a proliferation-associated antigen. *FEBS J* 274: 3669-3684.
125. Pollok, S., and F. Grosse. 2007. Cdc45 degradation during differentiation and apoptosis. *Biochemical and biophysical research communications* 362: 910-915.

126. Blum, W., L. Pecze, E. Felley-Bosco, and B. Schwaller. 2015. Overexpression or absence of calretinin in mouse primary mesothelial cells inversely affects proliferation and cell migration. *Respir Res* 16: 153.
127. Blum, W., and B. Schwaller. 2013. Calretinin is essential for mesothelioma cell growth/survival in vitro: a potential new target for malignant mesothelioma therapy? *International journal of cancer. Journal international du cancer* 133: 2077-2088.
128. He, X., Z. Zhu, C. Johnson, J. Stoops, A. E. Eaker, W. Bowen, and M. C. DeFrances. 2008. PIK3IP1, a negative regulator of PI3K, suppresses the development of hepatocellular carcinoma. *Cancer research* 68: 5591-5598.
129. Zhu, Z., X. He, C. Johnson, J. Stoops, A. E. Eaker, D. S. Stoffer, A. Bell, R. Zarnegar, and M. C. DeFrances. 2007. PI3K is negatively regulated by PIK3IP1, a novel p110 interacting protein. *Biochemical and biophysical research communications* 358: 66-72.
130. Nagy, D. T., B. Fulesdi, and J. Hallay. 2013. [The relationship between selenium and gastrointestinal inflammatory diseases]. *Orv Hetil* 154: 1636-1640.
131. Liu, K., C. Zhao, J. Chen, S. Wu, Y. Yao, C. Wu, G. Luo, and X. Zhang. 2016. [Overexpression of SEPP1 inhibits the proliferation and induces cell cycle G2/M arrest of 786-O and 769-P human renal carcinoma cells]. *Xi Bao Yu Fen Zi Mian Yi Xue Za Zhi* 32: 764-769.

132. Fond, A. M., C. S. Lee, I. G. Schulman, R. S. Kiss, and K. S. Ravichandran. 2015. Apoptotic cells trigger a membrane-initiated pathway to increase ABCA1. *The Journal of clinical investigation* 125: 2748-2758.
133. Hamon, Y., O. Chambenoit, and G. Chimini. 2002. ABCA1 and the engulfment of apoptotic cells. *Biochimica et biophysica acta* 1585: 64-71.
134. Singh, R., A. Mortazavi, K. H. Telu, P. Nagarajan, D. M. Lucas, J. M. Thomas-Ahner, S. K. Clinton, J. C. Byrd, M. A. Freitas, and M. R. Parthun. 2013. Increasing the complexity of chromatin: functionally distinct roles for replication-dependent histone H2A isoforms in cell proliferation and carcinogenesis. *Nucleic acids research* 41: 9284-9295.
135. Humbert, M., M. Medova, D. M. Aebersold, A. Blaukat, F. Bladt, M. F. Fey, Y. Zimmer, and M. P. Tschan. 2013. Protective autophagy is involved in resistance towards MET inhibitors in human gastric adenocarcinoma cells. *Biochemical and biophysical research communications* 431: 264-269.
136. Gozuacik, D., and A. Kimchi. 2004. Autophagy as a cell death and tumor suppressor mechanism. *Oncogene* 23: 2891-2906.
137. Yonekawa, T., and A. Thorburn. 2013. Autophagy and cell death. *Essays in biochemistry* 55: 105-117.
138. Boya, P., R. A. Gonzalez-Polo, N. Casares, J. L. Perfettini, P. Dessen, N. Larochette, D. Metivier, D. Meley, S. Souquere, T. Yoshimori, G. Pierron, P. Codogno, and G.

- Kroemer. 2005. Inhibition of macroautophagy triggers apoptosis. *Molecular and cellular biology* 25: 1025-1040.
139. Wirawan, E., T. Vanden Berghe, S. Lippens, P. Agostinis, and P. Vandenabeele. 2012. Autophagy: for better or for worse. *Cell Res* 22: 43-61.
140. Inguscio, V., E. Panzarini, and L. Dini. 2012. Autophagy Contributes to the Death/Survival Balance in Cancer PhotoDynamic Therapy. *Cells* 1: 464-491.
141. Dang, S., Z. M. Yu, C. Y. Zhang, J. Zheng, K. L. Li, Y. Wu, L. L. Qian, Z. Y. Yang, X. R. Li, Y. Zhang, and R. X. Wang. 2015. Autophagy promotes apoptosis of mesenchymal stem cells under inflammatory microenvironment. *Stem Cell Res Ther* 6: 247.
142. Liao, A., R. Hu, Q. Zhao, J. Li, Y. Li, K. Yao, R. Zhang, H. Wang, W. Yang, and Z. Liu. 2012. Autophagy induced by FTY720 promotes apoptosis in U266 cells. *Eur J Pharm Sci* 45: 600-605.
143. Cui, Q., S. Tashiro, S. Onodera, M. Minami, and T. Ikejima. 2007. Autophagy preceded apoptosis in oridonin-treated human breast cancer MCF-7 cells. *Biol Pharm Bull* 30: 859-864.
144. Grimaldi, A., D. Santini, S. Zappavigna, A. Lombardi, G. Misso, M. Boccellino, V. Desiderio, P. P. Vitiello, G. Di Lorenzo, A. Zoccoli, F. Pantano, and M. Caraglia. 2015. Antagonistic effects of chloroquine on autophagy occurrence potentiate the anticancer effects of everolimus on renal cancer cells. *Cancer biology & therapy* 16: 567-579.

145. Paglin, S., T. Hollister, T. Delohery, N. Hackett, M. McMahonill, E. Sphicas, D. Domingo, and J. Yahalom. 2001. A novel response of cancer cells to radiation involves autophagy and formation of acidic vesicles. *Cancer research* 61: 439-444.
146. Traganos, F., and Z. Darzynkiewicz. 1994. Lysosomal proton pump activity: supravital cell staining with acridine orange differentiates leukocyte subpopulations. *Methods in cell biology* 41: 185-194.
147. Honscheid, P., K. Datta, and M. H. Muders. 2014. Autophagy: detection, regulation and its role in cancer and therapy response. *International journal of radiation biology* 90: 628-635.
148. White, E. 2012. Deconvoluting the context-dependent role for autophagy in cancer. *Nature reviews. Cancer* 12: 401-410.
149. Amaravadi, R. K., J. Lippincott-Schwartz, X. M. Yin, W. A. Weiss, N. Takebe, W. Timmer, R. S. DiPaola, M. T. Lotze, and E. White. 2011. Principles and current strategies for targeting autophagy for cancer treatment. *Clinical cancer research : an official journal of the American Association for Cancer Research* 17: 654-666.
150. Long, L., X. Yang, M. Southwood, J. Lu, S. J. Marciniak, B. J. Dunmore, and N. W. Morrell. 2013. Chloroquine prevents progression of experimental pulmonary hypertension via inhibition of autophagy and lysosomal bone morphogenetic protein type II receptor degradation. *Circ Res* 112: 1159-1170.

151. Shintani, T., and D. J. Klionsky. 2004. Autophagy in health and disease: a double-edged sword. *Science* 306: 990-995.
152. Li, P., D. Nijhawan, I. Budihardjo, S. M. Srinivasula, M. Ahmad, E. S. Alnemri, and X. Wang. 1997. Cytochrome c and dATP-dependent formation of Apaf-1/caspase-9 complex initiates an apoptotic protease cascade. *Cell* 91: 479-489.
153. Liu, X., C. N. Kim, J. Yang, R. Jemmerson, and X. Wang. 1996. Induction of apoptotic program in cell-free extracts: requirement for dATP and cytochrome c. *Cell* 86: 147-157.
154. Leist, M., B. Single, A. F. Castoldi, S. Kuhnle, and P. Nicotera. 1997. Intracellular adenosine triphosphate (ATP) concentration: a switch in the decision between apoptosis and necrosis. *The Journal of experimental medicine* 185: 1481-1486.
155. Rabinowitz, J. D., and E. White. 2010. Autophagy and metabolism. *Science* 330: 1344-1348.
156. Riss, T. L., R. A. Moravec, A. L. Niles, H. A. Benink, T. J. Worzella, and L. Minor. 2004. Cell Viability Assays. In *Assay Guidance Manual*. G. S. Sittampalam, N. Gal-Edd, M. Arkin, D. Auld, C. Austin, B. Bejcek, M. Glicksman, J. Inglese, V. Lemmon, Z. Li, J. McGee, O. McManus, L. Minor, A. Napper, T. Riss, O. J. Trask, and J. Weidner, eds, Bethesda (MD).

157. Chen, E. I., J. Hewel, J. S. Krueger, C. Tiraby, M. R. Weber, A. Kralli, K. Becker, J. R. Yates, 3rd, and B. Felding-Habermann. 2007. Adaptation of energy metabolism in breast cancer brain metastases. *Cancer research* 67: 1472-1486.
158. Imamura, H., K. P. Nhat, H. Togawa, K. Saito, R. Iino, Y. Kato-Yamada, T. Nagai, and H. Noji. 2009. Visualization of ATP levels inside single living cells with fluorescence resonance energy transfer-based genetically encoded indicators. *Proceedings of the National Academy of Sciences of the United States of America* 106: 15651-15656.
159. Adams, J., and M. Kauffman. 2004. Development of the proteasome inhibitor Velcade (Bortezomib). *Cancer investigation* 22: 304-311.
160. Bae, S. H., H. M. Ryoo, M. K. Kim, K. H. Lee, J. I. Sin, and M. S. Hyun. 2008. Effects of the proteasome inhibitor bortezomib alone and in combination with chemotherapeutic agents in gastric cancer cell lines. *Oncology reports* 19: 1027-1032.
161. Petrelli, F., S. Barni, S. Cascinu, and A. Zaniboni. 2014. Gastric cancer: toward a cisplatin-free disease? *J Gastrointest Oncol* 5: 318-322.
162. Petrelli, F., A. Zaniboni, A. Coiu, M. Cabiddu, M. Ghilardi, G. Sgroi, and S. Barni. 2013. Cisplatin or not in advanced gastric cancer: a systematic review and meta-analysis. *PLoS One* 8: e83022.
163. Basu, A., and S. Krishnamurthy. 2010. Cellular responses to Cisplatin-induced DNA damage. *J Nucleic Acids* 2010.

164. Desagher, S., and J. C. Martinou. 2000. Mitochondria as the central control point of apoptosis. *Trends in cell biology* 10: 369-377.
165. Martinou, J. C., S. Desagher, and B. Antonsson. 2000. Cytochrome c release from mitochondria: all or nothing. *Nature cell biology* 2: E41-43.
166. Jia, L., R. R. Dourmashkin, P. D. Allen, A. B. Gray, A. C. Newland, and S. M. Kelsey. 1997. Inhibition of autophagy abrogates tumour necrosis factor alpha induced apoptosis in human T-lymphoblastic leukaemic cells. *British journal of haematology* 98: 673-685.
167. Yee, K. S., S. Wilkinson, J. James, K. M. Ryan, and K. H. Vousden. 2009. PUMA- and Bax-induced autophagy contributes to apoptosis. *Cell death and differentiation* 16: 1135-1145.
168. Rolfo, C., N. Van Der Steen, P. Pauwels, and F. Cappuzzo. 2015. Onartuzumab in lung cancer: the fall of Icarus? *Expert Rev Anticancer Ther* 15: 487-489.
169. Brower, V. 2017. Onartuzumab ineffective in non-small-cell lung cancer. *The lancet oncology* 18: e66.
170. Garber, K. 2014. MET inhibitors start on road to recovery. *Nat Rev Drug Discov* 13: 563-565.

171. Kang, Y. A., R. Sanalkumar, H. O'Geen, A. K. Linnemann, C. J. Chang, E. E. Bouhassira, P. J. Farnham, S. Keles, and E. H. Bresnick. 2012. Autophagy driven by a master regulator of hematopoiesis. *Molecular and cellular biology* 32: 226-239.
172. Peng, Z., Y. Zhu, Q. Wang, J. Gao, Y. Li, S. Ge, and L. Shen. 2014. Prognostic significance of MET amplification and expression in gastric cancer: a systematic review with meta-analysis. *PLoS ONE* 9: e84502.
173. Leiser, D., M. Medova, K. Mikami, L. Nisa, D. Stroka, A. Blaukat, F. Bladt, D. M. Aebersold, and Y. Zimmer. 2015. KRAS and HRAS mutations confer resistance to MET targeting in preclinical models of MET-expressing tumor cells. *Mol Oncol* 9: 1434-1446.
174. Burkhard, K., and P. Shapiro. 2010. Use of inhibitors in the study of MAP kinases. *Methods Mol Biol* 661: 107-122.
175. Anreddy, N., P. Gupta, R. J. Kathawala, A. Patel, J. N. Wurpel, and Z. S. Chen. 2014. Tyrosine kinase inhibitors as reversal agents for ABC transporter mediated drug resistance. *Molecules* 19: 13848-13877.
176. Tomczak, K., P. Czerwinska, and M. Wiznerowicz. 2015. The Cancer Genome Atlas (TCGA): an immeasurable source of knowledge. *Contemp Oncol (Pozn)* 19: A68-77.

VITA

Rebecca Lynette Dunbar Schroeder was born in El Campo, Texas on April 24, 1986, the daughter of Lydia Ann Dunbar and Henry Leonard Dunbar, and sister of Ashley Morris. After graduating from Victoria Memorial High School, (Victoria, Texas) in 2004, she entered Texas A&M University in College Station, Texas. There she earned a Bachelor of Science degree with a major in Biomedical Science from Texas A&M University in May, 2008. For the next three years, she worked as a clinical research assistant in the Department of Investigational Cancer Therapeutics and married her husband, Joshua Schroeder. In August of 2011 she began had doctorate work at The University of Texas MD Anderson Cancer Center UTHealth Graduate School of Biomedical Sciences. During this time she became a mother to her beautiful daughter, Abigail Lynette Schroeder. Following completion of her Ph.D. she will pursue a career in clinical research.